An Investigation of Methods to Attenuate Soft Tissue Artifact of the Thigh in High Knee Flexion

by

Jessa Buchman-Pearle

A thesis

presented to the University of Waterloo

in fulfillment of the

thesis requirement for the degree of

Master of Science

in

Kinesiology

Waterloo, Ontario, Canada, 2020

Authors Declaration

I hereby declare that I am the sole author of this thesis. This is a true copy of the thesis, including any required final revisions, as accepted by my examiners. I understand that my thesis may be made electronically available to the public.

Abstract

Soft tissue artifact during optical motion capture, or the movement of skin markers relative to bone, is widely accepted as a significant source of error in estimations of angles and moments. In some cases, the error associated with soft tissue movement exceeds that of the physiological motion of the joint, thereby calling into question the accuracy of the data obtained and casting doubt on the ability to determine mechanical demands of a given task. While previous studies have attempted to quantify soft tissue artifact, the variability in error with placement of skin markers (i.e. location specificity), the subject investigated (i.e. subject specificity), and the requirements of the task examined (i.e. task specificity), severely compromises the ability to develop methods which minimize and compensate for soft tissue artifact. Thus, the global objective of this thesis was to investigate soft tissue artifact of the thigh in high knee flexion movements and develop recommendations to standardize data collection and processing techniques. High knee flexion was examined because knee flexion beyond approximately 100° lacks investigation despite the unique deformation of soft tissue that occurs in this range (i.e. thigh-calf contact). Additionally, the repetitive adoption of high knee flexion is associated with knee joint injury and disease; thus, to more clearly elucidate mechanisms for these injuries and disease, improvements in the accuracy and reliability of collection and processing procedures is required.

Fifty participants performed squatting and kneeling movements while motion of the pelvis and lower limb was recorded with optical motion capture and force data was synchronously recorded from four embedded force plates. Six identical rigid marker clusters were distributed on the distal and middle third of the thighs, and on the anterior, lateral, and anterolateral aspect of the thighs, while one marker cluster was adhered to the

pelvis, shanks, and feet. Anthropometric measures were also taken for each subject including sex, height, mass, waist circumference, thigh length, thigh proximal, middle, and distal circumference, and thigh skinfold thickness. Data processing was divided into two studies.

The first study developed a non-invasive method to estimate soft tissue artifact for each thigh marker cluster which consisted of measuring the mean of the peak difference in the hip joint center position when tracked with the pelvis cluster (i.e. the gold standard) versus each of the six thigh marker clusters. Bland-Altman methods were then utilized to compare agreement between the pelvis and thigh marker clusters for each task during maximal knee flexion. Across the tasks, the mean difference ranged from -4.93 to 0.03 cm while the lower and upper limits of agreement ranged from -11.86 to -3.27 cm and -0.87 to 5.33 cm, respectively. The mid-anterolateral cluster tended to be least susceptible to soft tissue artifact across the tasks and thus would be recommended, while the lateral clusters were most susceptible and should be avoided.

Utilizing the anthropometric measures for each subject, regression models were also developed to determine the association between subject anthropometry and the mean difference in hip joint center position for each marker cluster. Ten of eighteen regression models significantly predicted soft tissue artifact with poor to moderate fit (R = 0.37 to 0.63) and explained between 14 and 40% of variation in the sample. These results suggest that while soft tissue artifact is somewhat associated with measures of anthropometry, marker placement should not be adjusted based on anthropometry alone. Additionally, negative unstandardized beta coefficients and partial correlations for thigh skinfold

thickness and proximal thigh circumference revealed that adipose tissue may act to dampen artifact resulting from muscular contractions.

The second study evaluated the difference in peak knee joint angles and moments between the thigh marker clusters and assessed the ability of global optimization, implemented in Visual3D utilizing IK constraints, to increase precision and reliability between marker clusters. Without global optimization, there were significant differences in estimated angles and moments between the marker clusters, wherein the mean difference was up to 8.9° and 0.6 %BW*H for flexion, 5.2° and 1.0 %BW*H for abduction, 4.9° and 0.7 %BW*H for adduction, 7.5° and 0.1 %BW*H external rotation, and 9.5° and 0.1 %BW*H for internal rotation. Global optimization was partially effective in compensating for differences between marker clusters in the sagittal plane (peak mean difference decreased 2.7° and 0.4 %BW*H) but less so in the frontal and transverse plane. Additionally, while global optimization decreased the partial eta squared (i.e. measure of effect of marker cluster location) for 12 of 30 outcome measures, intraclass correlation coefficients (i.e. measure of marker cluster reliability) only increased for 2 of 30 outcome measures. These findings highlight the importance of consistent marker placement for a given subject (i.e. between legs and laboratory sessions) and between subjects, as well as the need for researchers to report marker placement and all processing methods.

Acknowledgements

I would like to thank all of those who have supported me throughout this process, and who without, this thesis would not have been possible. First, to my supervisor, Dr. Stacey Acker, I am extremely grateful for your guidance and encouragement. As well, to my supervisory committee, Dr. Andrew Laing and Dr. Steven Fischer, your input in this project was invaluable and your contributions truly challenged me to 'dig deeper' into this thesis. I would also like to thank Dr. Jack Callaghan for your 'mentoring moments;' you continually challenged me to see the bigger picture and consider what's next.

I would also like to thank my lab mates and colleagues who helped me with data collection, troubleshooting, and general support throughout this process. Special thanks to David Kingston, I am forever appreciative of your patience, mentorship, and advice both inside and outside of academics. As well, to Annemarie Laudanski and Natasha Ivanochko, I cannot thank you enough for your patience and willingness to bounce ideas around.

Finally, I would like to thank my friends and family. To my parents and grandparents, thank you for your unconditional support and advice. As well, to Justin Davidson, I cannot imagine having gone through this experience without you. For the countless hours you have patiently helped me troubleshoot, made me laugh when I wanted to cry, and reminded me to take a break; I am so grateful for all your love and support.

Table of Contents

List of Figures

List of Tables

List of Abbreviations

Marker Clusters

DA	Distal-anterior
DAL	Distal-anterolateral
DL	Distal-lateral
MA	Mid-anterior
MAL	Mid-anterolateral
ML	Mid-lateral

Movements

FS	Flat-foot Squat
HS	Heels-up Squat
DK	Dorsiflexed Kneel
PK	Plantarflexed Kneel
-S	Symmetrical
-L	Lead leg
-T	Trail leg

Other

ANOVA	Analysis of Variance
CT	Computerized Tomography
IK	Inverse Kinematics
MRI	Magnetic Resonance Imaging
RMS	Root Mean Square
3D	Three Dimensional
%BW	Percent Body Weight
%BW*H	Percent Body Weight Multiplied by Height

Chapter 1 - General Introduction

1.1 Introduction

Motion capture remains one of the most widely used techniques for collecting kinematic data as it is non-invasive, minimally time consuming, and it is relatively non-constraining for individuals to complete a range of tasks. It is utilized in clinical settings for injury and disease diagnosis and treatment planning, entertainment settings for production of movies and games, and laboratory settings for evaluating kinematic demands of a given task, for input and validation of musculoskeletal models, and for designing *in vitro* testing protocols. During motion capture data collections, it is assumed that well-placed markers on the skin are rigidly coupled to the underlying bone; and therefore, skin marker position is representative of bone motion. Although this method provides a feasible method for quantifying whole-body kinematics; the accuracy of the data is vulnerable to soft tissue artifact.

Soft tissue artifact is the movement of skin markers relative to underlying bone that results during human movement as skin slides, muscles contract and relax, and muscle and adipose tissue oscillate due to inertial effects (Leardini et al., 2005). Soft tissue artifact results in inaccurate and unreliable segment and joint kinematics and kinetics (Akbarshahi et al., 2010; Barré et al., 2013; Benoit et al., 2006; Cappozzo et al., 1996; Kuo et al., 2011; Miranda et al., 2013; Stagni et al., 2006; Tsai et al., 2011), which is problematic when estimating task mechanical demands, defining occupational safety thresholds and guidelines, and hypothesizing mechanisms of injury and disease.

It is known that soft tissue artifact is location, subject, and task specific (Leardini et al., 2005). Soft tissue quantity, composition, and distribution varies throughout the body,

and as such, soft tissue artifact is not uniform within or between body segments (location specificity), or between individuals (subject specificity). Additionally, soft tissue deformation and displacement is not constant throughout motion, variation in movement velocity, segment orientation, and joint range of motion, result in different magnitudes and patterns of soft tissue artifact (task specificity). During tasks which require large changes in joint range of motion, significant skin sliding, and muscle and adipose deformation occurs; thus, the accuracy of the data obtained becomes increasingly vulnerable to soft tissue artifact.

High knee flexion, where the knee flexion angle exceeds 120°, is commonly adopted in activities of daily living and occupational tasks where kneeling or squatting is required; however, repetitive or sustained adoption of high knee flexion is a known risk factor for knee joint tissue injury and disease (Baker et al., 2003; Canetti et al., 2020; Felson, 2013; Henriksen et al., 2014). Standard motion tracking design includes adhering marker clusters to areas of the segment with the least expected soft tissue deformation (Cappozzo et al., 1995), while maintaining marker visibility. With this goal in mind, markers are typically placed on the distal-lateral thigh due to the decreased volume of muscle and adipose tissue. Although the decreased volume of soft tissue may act to reduce inertial effects, at approximately 125° of knee flexion, intersegmental contact between the shank and thigh occurs (thigh-calf contact) (Kingston & Acker, 2018), thereby resulting in significant deformation of shank and thigh topography, specifically in the posterior and medial-lateral aspect of the segment. Despite the large magnitude of error in estimated kinematics and kinetics that result due to soft tissue artifact in a range of similar tasks [e.g. step-up, stair ascent and descent, or sit-to-stand (Akbarshahi et al., 2010; Kuo et al., 2011;

Stagni et al., 2005; Tsai et al., 2011)], soft tissue artifact in high knee flexion has been minimally investigated.

1.2 Rationale

The first goal of this research was to investigate the location, subject, and task specificity of soft tissue artifact of the thigh in high knee flexion. Location specificity was examined by distributing six rigid marker clusters on different areas of the thighs. Subject specificity was investigated by evaluating the correlation between multiple measures of subject anthropometry and soft tissue artifact. Task specificity was examined by investigating soft tissue artifact of the thigh that occurs throughout the knees full range of flexion, including both squatting and kneeling movements which elicit high knee flexion. By examining these factors, recommendations for data collection techniques (i.e. marker placement) which attenuate soft tissue artifact could be made.

The second goal of this thesis was to examine the effects of marker cluster location on meaningful biomechanical outcomes, specifically peak knee joint angles and moments. Consequently, this research demonstrated the power of varying marker placement and the need for consistency. Additionally, to examine if data processing techniques could partially compensate for soft tissue artifact in high knee flexion, the ability of global optimization to attenuate differences in knee joint angles and moments between the different marker clusters on the thigh was investigated. Briefly, global optimization has been proposed to attenuate soft tissue artifact by constraining the degrees of freedom of two adjacent segments, thereby preventing unphysiological joint motion (Lu & O'Connor, 1999).

This research not only contributes to the collection of more accurate data, through both collection and processing techniques, but it facilitates standardization across

laboratories, collections, equipment, protocols, and subjects. In turn, this enables stronger comparisons and greater reproducibility between studies and provides stronger justification of similarities and differences in results and conclusions. While scientists are challenged to formulate new ideas and tools, hypotheses cannot be considered fact without reproducible and repeatable results.

1.3 Objectives

The global objective of this thesis was to investigate soft tissue artifact of the thigh in high knee flexion movements and develop recommendations to standardize data collection and processing techniques which minimize and compensate for soft tissue artifact. The specific objectives were:

1. To investigate the effect of thigh marker cluster location (i.e. placement of the marker cluster on the thigh) on soft tissue artifact during high knee flexion tasks (Chapter 3).
2. To assess the accuracy in which measures of anthropometry could predict soft tissue artifact for marker clusters localized to different areas of the thigh (Chapter 3).
3. To compare peak knee joint angles and moments between the thigh marker clusters during high knee flexion tasks with and without global optimization (Chapter 4).

Chapter 2 - Literature Review

2.1 Overview of High Knee Flexion

2.1.1 Defining high knee flexion

The knee joint has adapted to loading in activities of daily living, such as walking, stair ascent and descent, sit-to-stand, and squatting, where knee joint angles range from full extension to 120° (Kutzner et al., 2010; Mündermann et al., 2008). However, during high knee flexion, which is defined as a pose where knee flexion exceeds 120° (Hemmerich et al., 2006), unique loads are placed on less-conditioned structures of the knee joint. High knee flexion is most commonly observed during activities of daily living (e.g. gardening, prayer, and toileting) and occupational tasks (e.g. childcare, roofing, and flooring) which require kneeling, squatting, or cross-legged sitting. Understanding the mechanics of high flexion is important because exposures to high knee flexion have been implicated in the onset and progression of bursitis (Thun et al., 1987), meniscal injuries (Baker et al., 2003), and knee osteoarthritis at the tibiofemoral and patellofemoral joints (Canetti et al., 2020; Jensen, 2008; Rytter et al., 2009). For individuals who habitually adopt these postures, such as those in specific occupations or ethnic populations, there is an increased prevalence of knee joint injuries and diseases (Coggon et al., 2000; Jensen, 2005); thereby suggesting a causal relationship.

As the knee flexes to 120°, there is an approximate linear increase in lateral femoral condyle posterior translation relative to the tibia (Johal et al., 2005); however as knee flexion increases past 120°, rapid posterior translation of the medial and lateral femoral condyles occurs (Johal et al., 2005; Leszko et al., 2011; Nakagawa et al., 2000) (Figure 2-1). Below 120° of knee flexion, the medial and lateral femoral condyles were found to

translate 3.6 ± 2.0 and 21.1 ± 4.7 mm posteriorly; however, when flexing to 140° knee flexion, the condyles translated an additional 8.4 ± 2.1 and 9.8 ± 2.1 mm, respectively (Johal et al., 2005). Similarly, from 90 to 133° of active knee flexion, the medial and lateral condyle, translated posteriorly 2 ± 2 mm and 13 ± 6 mm then from 133 to 162° of passive knee flexion, the condyles translated an additional 5 ± 2 mm and 15 ± 4 mm, respectively (Nakagawa et al., 2000). As this posterior translation of the femoral condyles occurs in high knee flexion, anatomical changes in tibiofemoral contact result, whereby there is decreased tibiofemoral contact area. For example, an MRI imaging study on ten subjects found that contact area significantly decreased from 6.3 ± 1.4 mm^2 to 4.7 ± 0.9 mm^2 for the lateral femoral condyle, and 5.4 ± 0.7 mm^2 to 3.3 ± 0.7 mm^2 for the medial femoral condyle, at 139 ± 3° compared to full extension (Yao et al., 2008). Ultimately, decreases in contact area result in concentrated application of joint forces to unconditioned tissue, thereby cumulating to tissue damage and loss of tissue integrity (Andriacchi et al., 2004).

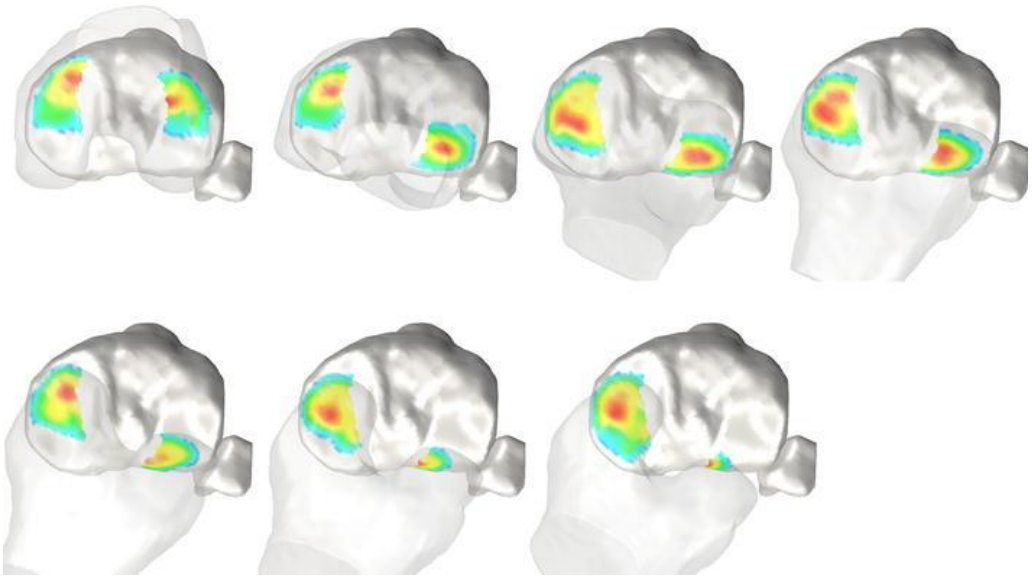

Figure 2-1: Tibiofemoral contact point location throughout progressive knee flexion [adapted from Leszko et al. (2011)]. The distance between the surface of tibial plateau and center of the femoral condyles, represented by the red colour, was used to determine contact point location.

2.1.2 Knee joint loading during high knee flexion

To understand injury and disease mechanisms in high knee flexion, quantification of joint loading, and partitioning of this load to individual structures is required. This can be accomplished by *in vivo* collections with an instrumented knee prosthesis, *in vitro* testing, or musculoskeletal modelling. The gold standard for directly measuring knee joint contact forces is using an instrumented knee prosthesis, with force transducers embedded into the prosthesis tibial tray (D'Lima et al., 2006; Fregly et al., 2012; Zhao et al., 2007). Studies utilizing a knee prosthesis have found that knee joint loading is highly activity dependent, where peak compressive load was approximately 2.0, 2.5, and 3.5 percent body weight (%BW) for squatting to 90º, walking, and stair ascent and descent, respectively (Kutzner et al., 2010; Mündermann et al., 2008). In one study that investigated two subjects transitioning into and out of kneeling, peak compressive load was 24.2 N/kg at 78.2° of knee flexion and 31.1 N/kg at 63.5° of knee flexion (Acker et al., 2018).

Since utilizing an instrumented knee prosthesis is often not feasible, *in vitro* testing is a useful alternative for investigating knee joint loading under simulated *in vivo* conditions. Cadaveric studies that have investigated high knee flexion most commonly describe the relative movement between the tibial and femoral condyles. Similar to the *in vivo* investigations described previously, the femur posteriorly translates and externally rotates during transition into high knee flexion (Hofer et al., 2011; Iwaki et al., 2000). Some studies have attempted to simulate *in vivo* loading of the knee joint during squatting and kneeling (Hofer et al., 2011; Thambyah et al., 2005), however these studies are largely quasi-static and have difficultly reproducing six degrees-of-freedom motion of the knee joint and realistic partitioning of muscular forces.

To determine forces and moments at the knee during high knee flexion, inverse dynamics is the most commonly used musculoskeletal modeling technique. In nineteen subjects transitioning into and out of kneeling (90 to 150°), net flexion moments ranged from 6.9 to 13.5 percent body weight times height (%BW*H) and net posterior force ranged from 58.3 to 67.8 %BW, approximately twice as high as those typically occurring during gait (Nagura et al., 2002). Similarly, in fifteen males performing kneeling transitions, the peak flexion moment ranged from 3.3 to 12.6 %BW*H, while the peak adduction moment (1.0 to 2.0 %BW*H) did not exceed values reported in gait (Chong et al., 2017). Furthermore, axial joint contact forces during squatting have been reported as high as 3.7 times body weight, at 138.7 ± 8.1° knee flexion (Smith et al., 2008), and 7.3 ± 1.9 times body weight, at 146.3° knee flexion (Nagura et al., 2006). However, these forces and moments may be overestimated as models did not account for thigh-calf or heel-gluteal contact. Inclusion of thigh-calf and heel-gluteal contact in inverse-dynamics-based models has resulted in a 48% decrease in the net flexion moment (Pollard et al., 2011) and a decrease in joint compressive and shear force from 4.37 to 3.07 and 1.31 to 0.72 times body weight, respectively (Zelle et al., 2007, 2009).

In vitro testing and musculoskeletal modeling rely on accurate *in vivo* data. For *in vitro* testing protocols to accurately simulate *in vivo* loading conditions, the load at a given joint position, or vice versa, must be known. Additionally, musculoskeletal models utilize *in vivo* kinematics and kinetics for input, in the case of an optimization or finite element model, or for validation, like in an EMG-driven model. Therefore, to ensure joint mechanics determined by *in vitro* tests and musculoskeletal models reflect reality, accurate *in vivo* kinematics and kinetics must be obtained. As well, *in vivo* data must be reliable, or

demonstrate consistency across studies investigating similar mechanics. Without repeatable and reproducible results, the scientific process of inductive reasoning cannot progress.

In high knee flexion, the coupling of high loads – determined by instrumented knee prostheses and musculoskeletal models – and minimal contact area – estimated by imaging techniques or cadaveric studies – may lead to knee joint tissue injury and disease onset and progression. Specifically, high knee flexion has been implicated in the initiation and progression of bursitis (Thun et al., 1987), meniscal injuries (Baker et al., 2003), and knee osteoarthritis at the tibiofemoral and patellofemoral joints (Canetti et al., 2020; Jensen, 2008; Rytter et al., 2009). However, to truly understand the underlying mechanics of high knee flexion that lead to tissue damage and degeneration, the *in vivo* kinematics and kinetics of high knee flexion must be accurately and precisely quantified.

2.2 Soft Tissue Artifact in Optical Motion Capture

Optical motion capture is a fundamental tool in biomechanical data acquisition as it enables three-dimensional (3D) digital representation of human movement. To accomplish this, cameras track the instantaneous position of markers on the skin surface, which are then used to define coordinate systems associated with each body segment. The coordinate systems are three orthogonal axes (Cartesian) methodically constructed to model the human body as a series of linked segments, for which segment and joint kinematics can be calculated. The coordinate systems are referred to here as the laboratory coordinate system, marker cluster coordinate system, and anatomical coordinate system. The laboratory coordinate system is the global coordinate system defined relative to gravity during the calibration of laboratory cameras' field of view (Wu & Cavanagh, 1995). The marker cluster coordinate system is the local coordinate system defined by the position of at least

three non-collinear markers on a segment (Wu & Cavanagh, 1995). If the markers are adhered to a rigid object which is then adhered to the segment, the cluster is called a rigid cluster or body; alternatively, if the cluster is constructed from markers individually adhered to the segment, it is termed a non-rigid cluster. The anatomical coordinate system is the local coordinate system defined by the position of anatomical landmarks; it is typically physiologically meaningful or clinically relevant to segment and joint kinematics (Grood & Suntay, 1983; Wu et al., 2002).

Although the purpose of this thesis was to investigate error in motion capture due to soft tissue artifact; it is recognized that other sources of error are present, largely instrumental error (Chiari et al., 2005) and anatomical landmark misplacement (Della Croce et al., 2005). Instrumental error and anatomical landmark misplacement will be briefly discussed below, prior to focusing on soft tissue artifact.

Instrumental error is the systematic or random error that results from collection equipment or processing techniques. In motion capture, systematic error is the optical distortion in marker coordinates due to inaccuracies, or non-linearities, in system calibration (Cappozzo, 1991); thus proper calibration procedures are essential for attenuation (Chiari et al., 2005). Conversely, random error is caused by electrical noise, imprecision in the analog to digital conversion process, and distortion of marker shape due to marker velocity, partial marker obstruction, or merging of marker signals (Furnee, 1997). Random error is mitigated by implementing appropriate filtering and smoothing techniques during data processing (Chiari et al., 2005).

High accuracy is imperative in anatomical landmark identification, as landmarks are used to construct anatomical coordinate systems. Anatomical landmark misplacement

may result from palpation errors as subcutaneous landmarks are not simply points, but large and/or irregularly shaped surfaces. When identifying landmarks of the lower extremity, intra-examiner variability ranged from 5.7 to 21.0 mm, while inter-examiner variability ranged from 11.5 to 24.8 mm (Della Croce et al., 1999). To increase anatomical landmark reliability, the same trained examiner should perform identification, and landmarks with poor identification reliability should be avoided in anatomical frame construction. Misplacement error may also occur when locating internal anatomical landmarks, such as a joint center, which can then propagate to errors in joint kinetic outcomes (Stagni et al., 2000). Multiple techniques for determining a joint center have been investigated, including prediction algorithms (Bell et al., 1990; Davis et al., 1991; Harrington et al., 2007) and functional methods (Camomilla et al., 2006; Gamage & Lasenby, 2002); however, functional methods are typically more accurate (Ehrig et al., 2006). Although instrumental error and anatomical landmark misplacement introduce inaccuracies, soft tissue artifact is recognized as one of the largest sources of error in motion capture marker coordinates (Andriacchi & Alexander, 2000; Cappozzo, 1991).

During dynamic tasks, the human body does not behave as rigid segments. The skin deforms and slides over bony landmarks, particularly at areas close to joints. Additionally, volumetric deformation of segments, or changes in shape and size, occurs as muscles contract and relax, and due to gravitational effects. As well, muscle and adipose tissue oscillate, or ‘wobble’, due to inertial effects. This movement of active and passive soft tissue propagates to skin markers; thus, marker trajectory is not solely the result of skeletal movement. Soft tissue artifact refers to the movement of skin markers relative to underlying bone. Multiple studies have quantified soft tissue artifact by synchronously

collecting and comparing skin marker position, determined by motion capture, and bone position, determined by bone fixation or imaging techniques, and through mathematical procedures using only optical motion capture (section 2.2.1). Ultimately, studies have found that soft tissue artifact results in less accurate marker position data which propagates to error in subsequent biomechanical outcomes (section 2.2.2). Additionally, the magnitude and pattern of soft tissue artifact has been shown to be modified by specific factors (section 2.2.3).

2.2.1 Methods for quantifying soft tissue artifact

The gold standard for quantifying soft tissue artifact requires skin marker position and bone position to be synchronously collected and compared. Although skin marker position is efficiently and effectively measured with a motion capture system, determination of error-free bone position can be cumbersome, expensive, and time-consuming, as it requires invasive techniques, such as bone fixated markers or radiation-based imaging techniques (Cereatti et al., 2017; Leardini et al., 2005; Peters et al., 2010).

Early attempts to quantify soft tissue artifact utilized bone fixation techniques, which requires fixing metal pins directly to bone (Benoit et al., 2006; Dal Maso et al., 2014; Fuller et al., 1997; Reinschmidt, van den Bogert, Lundberg, et al., 1997). Bone fixation requires surgical implantation of metal which is affixed to an externally visible marker cluster. Then, in a reference posture, typically supine or upright standing, anatomical landmarks are calibrated to the bone pin marker cluster either by a radiographic image (Benoit et al., 2006; Reinschmidt, van den Bogert, Lundberg, et al., 1997; Reinschmidt, van den Bogert, Nigg, et al., 1997) or manual palpation (Cappozzo et al., 1996; Holden et al., 1997; Manal et al., 2003; Rozumalski et al., 2007). The subject then

executes the protocol while skin marker and bone marker position are simultaneously collected by the motion capture system. Three types of bone fixation modalities have been previously used. Intra-cortical bone pins which involve surgical implantation of metal pins into cortical bone (Benoit et al., 2006; Dal Maso et al., 2014; Fuller et al., 1997; Reinschmidt, van den Bogert, Lundberg, et al., 1997; Reinschmidt, van den Bogert, Nigg, et al., 1997; Rozumalski et al., 2007). Percutaneous skeletal trackers which are comprised of two pins connected by a rigid link, that are inserted into opposite sides of the bone's periosteum (Holden et al., 1997; Manal et al., 2003). External fixation devices, which are fixated to bone for the treatment of fractures, and subsequently motion capture markers are mounted to the device frame (Cappozzo et al., 1996; Ryu et al., 2009).

While bone-fixated marker tracking can overcome some soft tissue artifact challenges, there are some limitations. During dynamic movements, intra-cortical pins and percutaneous skeletal trackers may bend or loosen, thereby disrupting anatomical frame calibration and the data must be excluded (Benoit et al., 2006; Holden et al., 1997). Additionally, implantation of pins is an invasive procedure with known risks to the subject; thus, they are not suitable for regular laboratory use. While the pins are inserted, the participants may experience pain or discomfort, which may result in compensatory locomotion during the collection (Fuller et al., 1997). This is especially problematic for percutaneous skeletal trackers and external fixators, as the devices are encumbering and may promote further alteration of movement patterns (Leardini et al., 2005). There is also concern that bone fixations may restrict or impede soft tissue deformation, specifically at insertion sites where skin and subcutaneous tissue displacement may be disrupted by local incisions (Leardini et al., 2005; Reinschmidt, van den Bogert, Lundberg, et al., 1997).

Additionally, since bone fixations increase the risk of infection and damage to bone (Fuller et al., 1997), they may have lasting health effects.

Although bone fixations pose ethical challenges, they are advantageous in acquiring bone position, as they utilize a motion capture system for data collection. Consequently, when quantifying soft tissue artifact through comparison with skin marker position, additional motion tracking equipment is not required to obtain synchronized data, which is collected at an acceptable sampling rate. This facilitates decreased data processing time, as similar filtering, smoothing, and kinematic calculation techniques can be used.

From 1996 to 2006, studies have largely utilized bone pins and fixation devices; however, from 2005 onwards, there has been a shift in focus to imaging techniques (Peters et al., 2010). Imaging techniques are advantageous as no physical incision or insertion of foreign material into the subject is required. X-ray is the most frequently used method of visualizing underlying bone; however, computerized tomography (CT) scans, MRI, and ultrasound have also been used. CT scans produce highly detailed cross-sectional images of internal structures, by taking a series of low-dose radiation x-rays from different perspectives and combining them computationally (Mehta et al., 1997). MRIs use a strong magnetic field to obtain even more detailed images of anatomical structures than a CT scan (Mehta et al., 1997). Ultrasound utilizes high frequency sound waves to view underlying structures, but in less detail than CT scans or MRI (Mehta et al., 1997). CT scans, MRI, and ultrasound are useful because the subject is not exposed to radiation, or a low dose in the case of CT scans. However, high-quality images are best obtained when the subject is stationary (Mehta et al., 1997). Although static images enable visualization of underlying soft tissue relative to bone when segments are in different postures, the images are not

indicative of instantaneous changes that occur. For example, muscle contraction and soft tissue oscillation during locomotion cannot be captured. Recently, coupling of motion capture and ultrasound have been investigated to track bony landmark trajectory during treadmill gait (Jia et al., 2017) and ultrasound has been used to determine spinal unit axial rotation (McKinnon & Callaghan, 2019); however, fluoroscopy and videoradiography, which make use of x-rays, are more universally employed and validated *in vivo*, particularly when examining the knee joint.

Fluoroscopy, or videoradiography, involve a series of radiographs, taken at an acceptable sampling frequency, to produce an x-ray movie. To track bone motion with videoradiography, a bone-embedded coordinate system is constructed and tracked with the radiographs at each time frame. The bone-embedded coordinate systems can be marker-based or markerless. Marker-based tracking requires invasive techniques to insert radio-opaque objects, such as joint replacements (Barré et al., 2013; Kuo et al., 2011; Stagni et al., 2005) or tantalum beads (Tashman et al., 2007; Tashman & Anderst, 2003), thereby limiting their applicability to human movement analysis. Alternatively, markerless tracking utilizes algorithms which match 3D subject-specific bone models, produced from MRI or CT scans, to x-ray motion data (Akbarshahi et al., 2010; Li et al., 2012; Miranda et al., 2013; Tsai et al., 2011), thereby providing information on bone morphology and bone motion, simultaneously, without error from soft tissue. Unfortunately, methods which utilize x-ray expose participants to radiation which can have lasting health effects.

Recently, methods for estimating soft tissue artifact which rely only on motion capture, have been investigated. Estimating soft tissue artifact with motion capture markers involves tracking individual marker displacement relative to different marker cluster

coordinate systems located on the same (Camomilla et al., 2009) or adjacent segments (Lucchetti et al., 1998; Ryu, 2012; Ryu et al., 2009). The multiple independent observer method was developed to quantify soft tissue artifact of markers located on the same segment (Camomilla et al., 2009). In the multiple independent observer method, independent observers (of individual marker displacement) are determined under the assumption that non-rigid clusters, which display uncorrelated deformation (i.e. size and shape changes), will estimate uncorrelated marker positions (Camomilla et al., 2009). Independent observers are identified by constructing all possible non-rigid clusters from a marker array of individual markers on a segment and comparing deformation of the clusters. If deformation is uncorrelated between the marker clusters, the clusters are considered independent observers of a marker which was not used in the construction of the independent clusters. Once independent observers are identified, marker displacement due to soft tissue artifact (soft tissue artifact vector) is estimated as the coherent average of displacement vectors reconstructed from the coordinate systems of the independent observers (Camomilla et al., 2009). This method was validated by comparing the estimated soft tissue artifact vector with fluoroscopy data of two subjects during a step-up task (Camomilla et al., 2009; Stagni et al., 2005). The magnitude of the soft tissue artifact vectors were consistent, with root mean square (RMS) values ranging from 2.5 to 23.0 mm, and demonstrated similar time-histories with a correlation of 0.83 ± 0.13 (Camomilla et al., 2009). The multiple independent observer method is limited in that it does not consider marker cluster rigid translation or rotation, which is likely correlated between clusters, despite uncorrelated deformation. As well, although the method estimates the magnitude and pattern of cluster deformation, no information is provided on the phase of

the signal (i.e. whether the non-rigid cluster shrinks or enlarges during deformation), and the soft tissue artifact vector estimate is affected by 180° of phase indeterminacy. However, upon consistent performance during the validation procedure, the multiple independent observer method has been deemed valuable for quantifying localized segment deformation (Camomilla et al., 2009).

Another method to estimate soft tissue artifact is the dynamic calibration method, which was originally used as a method to estimate and compensate for soft tissue artifact of a specific marker (Lucchetti et al., 1998; Ryu, 2012; Ryu et al., 2009). For dynamic calibration, the position of a marker is tracked by two marker clusters, one located on the same segment as the marker being tracked, and one located on the adjacent segment. The difference between the marker estimated position from the two clusters is assumed to be representative of soft tissue artifact. This method has been utilized to quantify soft tissue artifact of a given marker as a function of time (Lucchetti et al., 1998), joint angle (Lucchetti et al., 1998; Ryu, 2012), or offset between markers in the same marker cluster coordinate system (Ryu, 2012; Ryu et al., 2009). Typically, this method has been utilized during a hip flexion-extension task with the knee extended, where soft tissue artifact of the thigh is assumed to be correlated with hip rotation, and the shank is considered an artifact-free observer of this artifact on the thigh (Lucchetti et al., 1998; Ryu, 2012; Ryu et al., 2009). Soft tissue artifact is then calculated as the difference between the marker position vectors in the thigh and shank anatomical coordinate system. Two limitations are acknowledged in this method. First, errors may be amplified for thigh markers which are further away from the shank marker cluster (Cappozzo et al., 1997). This limitation was addressed by using a coordinate system constructed from both the thigh and shank markers

instead of solely the shank cluster (Lucchetti et al., 1998); however, it is unclear if this method would affect the accuracy of the initial estimation of soft tissue artifact. Additionally, the aforementioned method is limited as no segment can truly be artifact-free, in this case largely due to inertial effects and skin sliding on the shank. However, when the soft tissue artifact vector estimated during the hip flexion-extension was subtracted from marker position during gait, soft tissue artifact was shown to be partially compensated for, where RMS errors in knee joint rotation and translation were reduced from 6 to 3° and 14 to 4 mm (Lucchetti et al., 1998), and error in marker displacement was reduced between 30 and 60% while error in joint kinematics was reduced between 25 and 40% (Ryu, 2012). Although dynamic calibration does not appear to encompass all artifact, it is effective when utilizing the shank to estimate soft tissue artifact on the thigh during gait and may be useful for evaluation of other segments and tasks.

Methods which utilize only motion capture to estimate soft tissue artifact are a promising avenue for evaluating soft tissue artifact. Although they may not be as accurate as bone fixation and imaging techniques for quantifying absolute soft tissue artifact, they may be useful for comparing relative soft tissue artifact on a segment. For instance, these methods may be useful for comparing local soft tissue artifact between marker sets on the same segment.

2.2.2 Quantification of soft tissue artifact

Multiple studies have quantified soft tissue artifact, however varying results have been obtained due to inconsistency in equipment, motor tasks, subject characteristics, and marker quantity and location, as well as the metrics used to represent the data. Although it is recognized that soft tissue artifact occurs on all body segments (Cereatti et al., 2017;

Leardini et al., 2005; Peters et al., 2010); the scope of this thesis will be limited to soft tissue artifact at the thigh. This is because when examining the lower extremity, soft tissue artifact is greatest for thigh markers, due to the large volume of soft tissue that oscillates, slides, and deforms during movement. Consequently, errors in knee joint kinematics and kinetics are largely attributable to error at the thigh, as opposed to the shank (Kuo et al., 2011; Reinschmidt, van den Bogert, Lundberg, et al., 1997; Tsai et al., 2011).

Experimentally, soft tissue artifact is quantified in two ways: individual marker displacement within a bone-embedded coordinate system, determined by bone fixation or imaging techniques, or differences in skin marker estimated versus bone marker estimated thigh and knee kinematics. Although individual marker displacement is useful for determining soft tissue deformation at specific areas of a segment (location-specificity), and thus contributes to knowledge of optimal marker placement, marker displacement provides no indication of how soft tissue artifact will propagate to error in segment and joint kinematics. Some studies have also quantified differences in thigh and knee kinematics determined by skin markers versus known bone position. Studies examining the differences in thigh marker displacement and thigh and knee kinematics are summarized in Table 2-1 and Table 2-2, respectively, and will be discussed throughout this section. All values are presented in accordance with ISB standards, where the X axis is anterior-posterior, Y is proximal-distal, and Z is medial-lateral (Wu & Cavanagh, 1995).

To synthesize results of studies investigating soft tissue artifact, Cereatti et al. (2017) proposed a set of eight standardized metrics for describing soft tissue artifact in terms of marker displacement within a bone-embedded anatomical coordinate system: RMS error, which describes the mean displacement of the marker from its mean position

throughout the movement trial (total, along X, Y, and Z), and peak-to-peak amplitude, which represents the maximum displacement of the marker within the bone-embedded coordinate system (i.e. difference in the minimum and maximum position of the marker) (total, along X, Y, and Z). Although RMS error and peak-to-peak amplitude for X, Y, and Z depend on anatomical coordinate system definition, the total RMS error and peak-to-peak amplitude do not (Grimpampi et al., 2014). Furthermore, Cereatti et al. (2017) conducted a secondary analysis on a single participant and trial from multiple studies to facilitate soft tissue artifact comparison (Table 2-1). Across tasks and markers, soft tissue artifact on the thigh ranged from a mean RMS error of 0.41 to 2.53 mm, and a mean peak-to-peak error of 1.64 to 7.23 cm (Table 2-1).

Table 2-1: Thigh marker displacement relative to femur-embedded anatomical coordinate system [modified from Cereatti et al. (2017)].

Task	Study	Mean RMS Difference (cm)	Mean Peak-to-Peak Amplitude (cm)
Knee flexion-extension	Akbarashi et al. (2010)	0.74	2.55
Hip flexion-extension	Bonci et al. (2014)	0.61	1.64
Functional hip	Cereatti et al. (2009) Camomilla et al. (2013)	0.59	2.16
	Akbarashi et al. (2010)	0.67	1.77
Overground walking	Benoit et al. (2006)	0.76	2.40
Treadmill walking	Akbarashi et al. (2010)	1.37	4.12
	Barre et al. (2013)	0.85	2.84
Running	Rendschmidt et al. (1997)	0.69	2.11
Lateral cutting maneuver	Benoit et al. (2006)	0.73	2.22
Step-up	Stagni et al. (2005)	1.49	4.18
	Akbarashi et al. (2010)	1.24	3.48
	Tsai et al. (2011)	1.51	4.65
Sit-to-stand	Stagni et al. (2005)	2.53	7.23
	Kuo et al. (2011)	0.80	2.22

When artifact affects the position of anatomical landmarks, anatomical axis misalignment will result when constructing anatomical coordinate systems. Misalignment will lead to under or overestimation of segment and joint kinematics, with or without kinematic crosstalk (when the rotation about one axis is interpreted as rotation about another). Additionally, when soft tissue artifact affects markers which are utilized to determine joint centers, kinetic outcomes, such as net joint moments and joint reaction forces, will be affected (Cappozzo, 1991; Kuo et al., 2011; Stagni et al., 2000; Tsai et al., 2011). Ultimately, error in joint kinematics and kinetics will lead to error in joint loads estimated by musculoskeletal models and cadaveric studies. This may be problematic when determining mechanisms of a specific injury or disease, evaluating demands of occupational tasks, or from a clinical perspective during diagnosis or treatment.

While no study to date has quantified soft tissue artifact in high knee flexion, studies which have quantified error in thigh and knee rotation and translation in low to mid-range flexion activities are presented in Table 2-2. Peak rotation errors about each axis ranged from X = 2.7° to 18.2°, Y = 4.4° to 10.2°, and Z = 2.2° to 15.8°, while RMS rotation error was X = 2.0° to 8.6°, Y = 2.5° to 8.4°, and Z = 2.1° to 9.1° (Table 2-2). Although less studies have quantified translation error, peak and RMS translation error has ranged from 0.30 to 3.37 cm and 0.07 to 1.23 cm, respectively (Table 2-2). When examining kinematics, it is important to evaluate error as it pertains to motion in a specific plane, for a specific joint. For example, 5º of error at 100º of knee flexion results in error that is 5% of the physiological motion, while 5º of error at 10º of knee internal rotation is equivalent to 50% of the range of motion. Additionally, since translation values at the knee joint are so small (within mm), optical motion capture cannot confidently be used.

Compared to kinematics, the effect of soft tissue artifact on kinetic calculations has been minimally investigated. Two studies have investigated changes in knee joint moments, calculated with inverse dynamics, as a result of soft tissue artifact during sit-to-stand (Kuo et al., 2011) and stair ascent (Tsai et al., 2011) using single plane fluoroscopy. Throughout the stance phase of stair ascent, knee flexion-extension moments were significantly underestimated as a result of soft tissue artifact; however there was no difference in abduction-adduction or external-internal rotation moments (Tsai et al., 2011). As well, knee flexion-extension and abduction-adduction moments were significantly underestimated due to soft tissue artifact in a sit-to-stand, but there was no difference in external-internal rotation moments (Kuo et al., 2011). Although the results of the aforementioned studies suggest that kinetic outcomes may be less susceptible to soft tissue artifact, investigation into additional tasks, kinetic variables of interest, and metrics for describing variables (e.g. peaks versus mean) is warranted. This is especially true given that soft tissue artifact appears to result in underestimation of knee joint moments, which may have implications in the definition of thresholds for injury and disease.

Table 2-2: Kinematic error in femur and knee rotation and translation attributed to soft tissue artifact. Brackets indicate standard deviations. Commas separate subject-specific values. † indicates values for the femur, all other values are reported for the knee. Stdev of angle is the standard deviation of the orientation of the distal thigh cluster coordinate system relative to the femur anatomical coordinate system. Root mean square error is RMS and range of motion is RoM.

Task	Error	Rotation (°)			Translation (cm)		
		Z Flex-Ext	X Abd-Add	Y Int-Ext	Z Med-Lat	X Ant-Post	Y Comp-Dist
Walking	*Reinschmidt et al. (1997)*						
	Peak	4.3	4.4	8.4	-	-	-
	RMS	2.1	2.4	3.9	-	-	-
	Benoit et al. (2006)						
	RMS	2.6	3.3	2.5	0.62	0.90	0.44
	Barre et al. (2013)						

Treadmill Walking	RMS	8.2 (2.8)	0.2 (0.1)	7.7 (4.5)	0.09 (0.05)	0.14 (0.09)	0.07 (0.40)
	Akbarashi et al. (2010)						
	RMS	4.5	4.5	5.9	-	-	-
	RMS/Joint RoM (%)	8.9	93.5	82.6	-	-	-
Running	*Reinschmidt et al. (1997)*						
	Peak	7.9	4.1	4.4	-	-	-
	RMS	5.3	6.6	9.0	-	-	-
Treadmill Running	*Li et al. (2012)*						
	Peak	15.8	2.7	9.0	0.30	1.12	1.23
	RMS	9.1	2.0	6.5	0.19	0.71	0.88
Lateral Cutting	*Benoit et al. (2006)*						
	Peak	4.0	8.6	4.7	0.90	0.95	0.67
	Miranda et al. (2013)						
	Peak †	8.88	18.18	10.23		3.37	
	Median†	3.67	11.97	5.07		2.49	
	Peak	2.21	5.52	5.04	0.86	0.67	1.87
	Median	0.51	0.02	0.06	0.17	0.12	0.07
Hip External Rotation	*Akbarashi et al. (2010)*						
	RMS	2.4	2.7	6.1	-	-	-
	RMS/Joint RoM (%)	47.3	29.3	102.3	-	-	-
Knee Flexion-Extension	*Akbarashi et al. (2010)*						
	RMS	8.3	7.2	6.4	-	-	-
	RMS/Joint RoM (%)	7.3	69.0	46.7	-	-	-
	Stagni et al. (2005)						
	Stdev of angle†	9.3, 3.1	10.5, 3.7	8.8, 3.2	-	-	-
	RMS/Joint RoM (%)	10.1, 12.3	22.7, 66.2	26.2, 43.2	-	-	-
Stair Ascent	*Stagni et al. (2005)*						
	Stdev of angle†	18.3, 3.9	20.4, 4.1	17.2, 3.9	-	-	-
	RMS/Joint RoM (%)	11.2, 7.0	49.1, 35.8	57.4, 36.8	-	-	-
	Li et al. (2012)						
	Peak	5.9	3.5	7.3	0.20	0.87	1.30
	RMS	3.3	2.5	5.1	0.15	0.61	1.10
Step-up	*Stagni et al. (2005)*						
	Stdev of angle†	18.2, 6.0	20.2, 6.1	17.1, 6.0	-	-	-
	RMS/Joint RoM (%)	10.4, 12.6	79.4, 60.6	31.0, 34.8	-	-	-
	Akbarashi et al. (2010)						
	RMS	4.3	7.2	4.9	-	-	-
	RMS/Joint RoM (%)	7.7	76.0	43.0	-	-	-

	Stagni et al. (2005)						
Sit-to-stand	Stdev of angle†	25.3, 4.5	28.3, 4.1	25.3, 4.1	-	-	-
	RMS/Joint RoM (%)	9.5, 15.3	80.9, 70.5	27.2, 23.4	-	-	-

2.2.3 Factors influencing soft tissue artifact

In the literature on soft tissue artifact, three main themes have emerged:

1) Soft tissue artifact is *location specific*. Soft tissue composition and quantity varies throughout the body, and as a result, soft tissue artifact is not uniform between or within body segments.
2) Soft tissue artifact is *subject specific*. Subject anthropometrics, largely soft tissue composition and distribution, will affect features of soft tissue artifact. As well, how an individual completes a task, or the individual's movement patterns, will modify soft tissue artifact. Factors such as joint mobility or range of motion, and muscle recruitment strategies, could potentially alter soft tissue artifact between individuals and between repetitions of a given task.
3) Soft tissue artifact is *task specific*. Variation in segment orientation and joint angle, and the speed of the movement performed, will result in different magnitudes and patterns of soft tissue deformation, and thus, error in marker trajectories.

Location Specificity

Although total RMS error and peak-to-peak amplitude (Table 2-1) are useful for examining soft tissue artifact of the thigh as a whole segment, artifact amplitude and direction is not constant within a segment. Karlsson & Tranberg (1999) found that displacement was greatest for the proximal thigh in the anterior-posterior direction.

Cappozzo et al. (1996) found similar results where the largest displacement occurred anterior-posteriorly for thigh markers. The greater trochanter marker displaced up to 30 mm anteriorly during hip flexion and 30 mm posteriorly during hip external rotation, and the lateral epicondyle marker displaced up to 40 mm posteriorly during knee flexion, while medial-lateral and axial displacement for these markers did not exceed 15 mm (Cappozzo et al., 1996). Tsai et al. (2011) and Kuo et al. (2011) also found large anterior-posterior displacement, during stair ascent and sit-to-stand respectively, where lateral thigh markers displaced proximal-posterior during knee flexion, and distal-anterior during knee extension. However, anterior thigh markers displacement was largely axial. Across tasks (stair ascent and descent, step-up/down, and sit-to-stand), Stagni et al. (2005) found anterior-posterior and axial displacement was largest around the posterior-proximal thigh, while medial-lateral displacement was largest around the posterior-lateral thigh. During active knee flexion, Sati et al. (1996) found the displacement of individual markers (3 mm diameter) on the femoral epicondyles varied up to 41.5 mm anterior-posteriorly and 38 mm axially, where markers closest to the joint line experienced the largest displacement (Sati et al., 1996). Although it appears that marker displacement is somewhat predictable with joint motion, the magnitude and direction will vary depending on the location on the segment.

By evaluating individual marker displacement relative to a bone-embedded coordinate system constructed and tracked via fluoroscopy, Stagni et al. (2005) and Barré et al. (2015) created subject-specific maps of soft tissue artifact (Figure 2-2). Stagni et al. (2005) found soft tissue artifact was generally highest at the posterior-proximal thigh and lowest at the anterior-distal thigh during activities of daily living (Figure 2-2). Similarly, Barré et al. (2015) found maximal and minimal soft tissue artifact occurred at the proximal

and lateral thigh across subjects, respectively, during gait (Figure 2-2). These results suggest that while a distal-lateral cluster placement may be optimal for tasks which elicit soft tissue oscillation but require minimal joint range of motion, such as gait or running, a more anterior cluster placement may be best for tasks which require greater changes in knee joint range of motion.

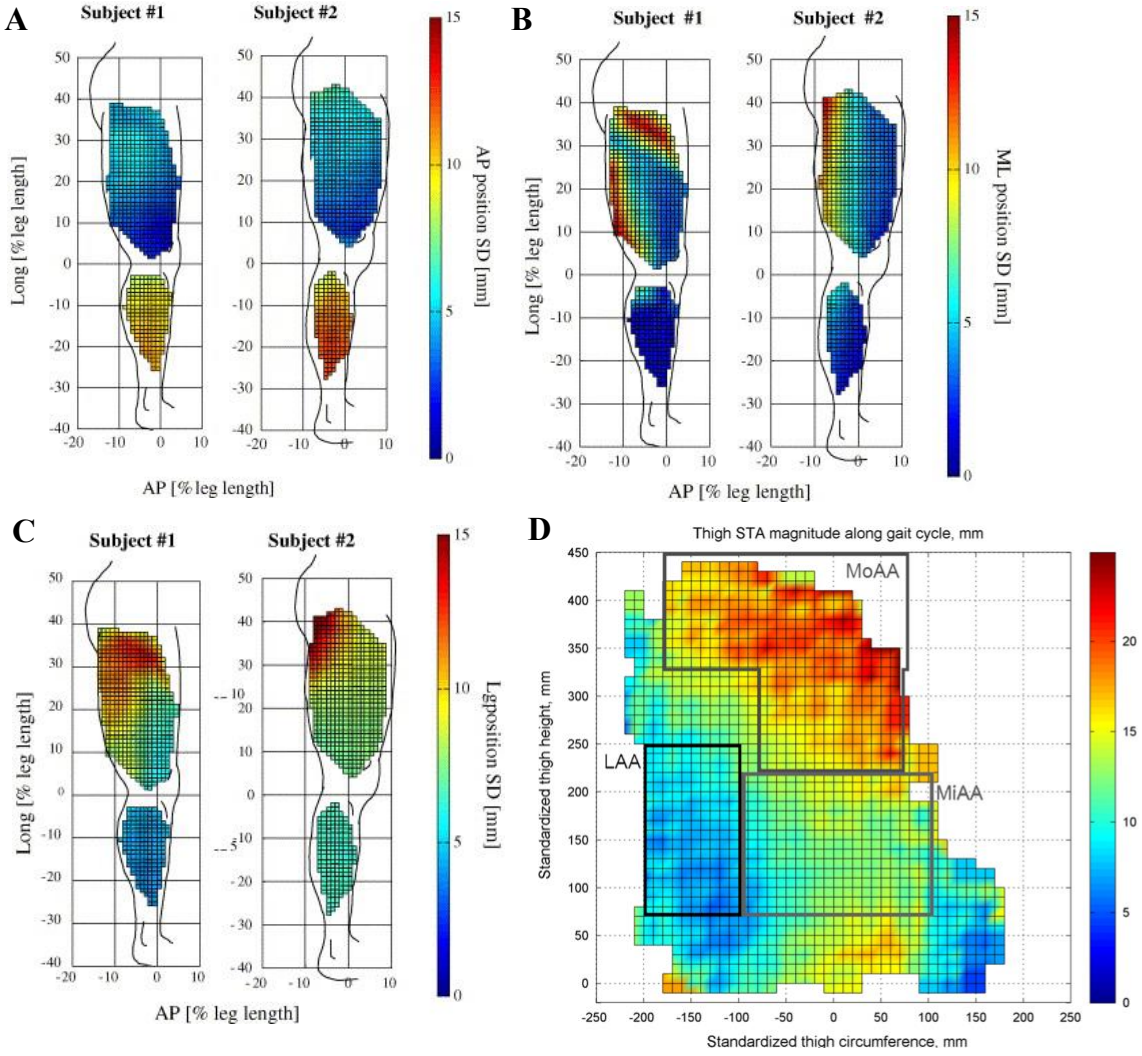

Figure 2-2: Soft tissue artifact topography of the right thigh. A) Anterior-posterior marker displacement during knee flexion-extension. B) Medial-lateral marker displacement during a step-up/down task. C) Axial displacement during sit-to-stand/stand-to-sit task [adapted from Stagni et al. (2005)]. D) Average total marker displacement across 19 subjects. Negative coordinates on the x-axis represent the lateral thigh. LAA is the least affected area, MoAA is most affected area, and MiAA is mid-affected area [adapted from Barre et al. (2015)].

Until now, soft tissue artifact has been discussed exclusively pertaining to the thigh segment; however, when constructing the femur anatomical coordinate system, the hip joint center is used as the proximal point for defining the longitudinal axis (Grood & Suntay, 1983). Without the use of imaging techniques, the hip joint center can be estimated by predictive methods, which involve regression equations based on distances between bony landmarks (Bell et al., 1990; Davis et al., 1991; Harrington et al., 2007), or functional methods, where the hip is circumducted in a star-arc pattern and the center of rotation between the pelvis and thigh is determined through optimization (Camomilla et al., 2006). When hip circumduction is not problematic, the functional method is preferred as it more accurately predicts hip joint center location (Ehrig et al., 2006). During upright standing, the hip joint center is coincident with the femoral head, and then throughout movement, it is tracked with the pelvis; thus, the thigh anatomical coordinate system is affected by pelvis soft tissue artifact. Although studies have quantified soft tissue artifact at pelvis bony landmarks during gait (Camomilla et al., 2017; Hara et al., 2014; Rozumalski et al., 2007), hip circumduction (Camomilla et al., 2017), and sit-to-stand tasks (Rozumalski et al., 2007), few studies have determined the effect of soft tissue artifact on hip joint center determination and trajectory during dynamic tasks.

To quantify the effect of soft tissue artifact on hip joint center determination, Cereatti et al. (2009) put four cadaveric specimens through the star-arc movement in a supine posture and compared bone pin and skin-marker determined hip joint center position. Error in determination was found to be independent of hip range of motion, ranging from 1.4 to 38.5 mm (Cereatti et al., 2009). However, these values may not be representative of true soft tissue artifact during the functional hip trial, due to the lack of

muscle activity, and because the functional trial is normally performed with subjects in upright standing.

To examine the effect of activity on the hip joint center trajectory, Fiorentino et al. (2016) compared position of the hip joint center, calculated by predictive and functional methods, and determined by dual fluoroscopy and motion capture, during six dynamic activities (level and incline walking, a functional hip trial, 45° of hip abduction, and end of range internal and external rotation). Soft tissue artifact was quantified as hip joint center deviation relative to the femoral head center position, which was determined with fluoroscopy and tracked with the thigh. Compared to the femoral head center, the functional method had lower absolute error in determining the hip joint center (fluoroscopy = 1.3 ± 0.5 mm, motion capture = 12.5 ± 4.8 mm) than the predictive methods (fluoroscopy = 18.6 ± 8.9 mm, motion capture = 19.4 ± 9.2 mm) (Fiorentino et al., 2016). Additionally, during motion, all calculated hip joint centers remained within the pelvis acetabulum, where RMS error was 2.8 ± 0.7 mm. Collectively, these results suggest that the functional method should be utilized to define hip joint center position and that the hip joint centre trajectory is relatively robust to pelvis soft tissue artifact.

Subject Specificity

Due to the specialized equipment required for quantifying soft tissue artifact, studies often consist of small sample sizes; however, this may be problematic since soft tissue artifact demonstrates high subject-dependency. A large part of this subject-dependency is likely due to variability in subject anthropometrics. Intuitively, it makes sense that individuals with greater volume of soft tissue, quantified by values such as body mass index (BMI), would have greater soft tissue artifact, yet, the relationship appears to

be more complex. Barré et al. (2013) investigated the correlation between soft tissue artifact during treadmill gait and subject BMI, where their sample consisted of nineteen subjects with BMI ranging from 23.0 to 37.8 kg/m2. For the femur and knee, no significant correlation was found for rotation about X or Z, while rotation about Y was inversely correlated with BMI (femur R = -0.53, knee R = -0.56) (Barré et al., 2013). When comparing to an exoskeleton, which clamped onto the femoral epicondyles, and biplanar videoradiography during a squat, Clément et al. (2018) found similar results, where there was greater soft tissue artifact in non-obese (BMI = 24.8 ± 2.3 kg/m2) compared to obese subjects (BMI = 34.3 ± 2.7 kg/m2). These results were believed to be a result of greater adipose tissue in obese subjects, which acted to attenuate soft tissue deformation that resulted from muscular contractions (Clément et al., 2018). Conversely, Garling et al. (2007) found no correlation between BMI (ranging from 26 to 34 kg/m2 across ten subjects) and error in knee joint angles. Camomilla et al. (2017) found soft tissue artifact of the pelvis increased with BMI when examining cadaveric specimens. The lack of consensus regarding the relationship between BMI and soft tissue artifact may be because BMI is too general a description of subject anthropometrics, without consideration of other factors such as, individual soft tissue distribution, segment soft tissue volume and composition, or variability in data collection modalities.

The subject specificity of soft tissue artifact complicates the ability to produce data collection methods for attenuation and models for compensation. However, it may be possible to identify subject specific characteristics, such as BMI, segment circumference, or joint mobility, which aid in the development of methods to reduce soft tissue artifact on a subject-by-subject basis (e.g. marker configurations for a specific population).

Task Specificity

Intra- and inter-subject variability in task execution, due to factors like joint range of motion or muscle recruitment strategies, may affect soft tissue artifact between subjects and trials. Soft tissue artifact varies across motor tasks, due to differences in the velocity of movement and orientation of segments or joints during movement execution. As movement velocity increases, during impact or upon rapid changes in direction, soft tissue artifact increases as a result of increased soft tissue oscillation. Oscillation occurs due to inertial effects, where soft tissue behaves as a second-order underdamped system and will oscillate in a dampened manner during dynamic activities (Gruber et al., 1998). In this way, activities such as running and cutting, will elicit greater oscillation than walking, as greater acceleration is required.

Increases in joint angle also tend to increase soft tissue artifact, as skin sliding, changes in muscular contractions, and compression of muscle and adipose tissue occurs. During cycling, Fuller et al. (1997), found displacement of markers on the greater trochanter and lateral femoral epicondyle cyclically varied with the movement. Cappozzo et al. (1996) found as the angle of the joint closest to the marker increased, marker displacement also tended to increase. Similarly, when evaluating stair ascent and sit-to-stand, respectively, Tsai et al. (2011) and Kuo et al. (2011) found significant differences in knee rotation and translation measured by skin markers and fluoroscopy when the knee was most flexed (Kuo et al., 2011; Tsai et al., 2011). However, the majority of studies which have determined this relationship between soft tissue artifact and joint angle, have examined gait and tasks which require low to moderate joint range of motion, typically less 100°.

Multiple processing techniques, which have been successful in partially attenuating soft tissue artifact, build on the assumption that there is a specific relationship between soft tissue artifact and joint(s) position or orientation. Briefly, as these methods are discussed in detail in section 2.3.2, double calibration methods assume that soft tissue artifact is linearly correlated with joint angle (Cappello et al., 1997; Stagni et al., 2005, 2009) while multiple calibration (Lucchetti et al., 1998; Ryu, 2012; Ryu et al., 2009) and kinematic-optimization methods (Bonci et al., 2014; Camomilla et al., 2013, 2015) assume the relationship depends on the specific task requirements. Through experimental *in vivo* studies which quantify soft tissue artifact throughout movement and construction of models which assume soft tissue artifact changes predictably throughout motion, it is concluded that, to some extent, soft tissue artifact demonstrates task specificity, typically resulting from changes in segment orientation and/or joint range of motion.

Implications of Soft Tissue Artifact

Although soft tissue artifact is a complex source of error affected by a number of factors, motion capture remains a feasible and widely used method for quantifying whole-body kinematics. Therefore, it is necessary that soft tissue artifact be quantified – in the context of marker location, subject characteristics, and throughout a given motor task – to facilitate the development of methods which minimize and compensate for soft tissue artifact.

2.3 Methods to Reduce Soft Tissue Artifact

Mathematically, soft tissue artifact has been described by four geometric parameters: marker rotation and translation, and marker cluster scaling and deformation (Grimpampi et al., 2014). Rotation and translation, at the level of individual markers or a

marker cluster, has been collectively defined as the rigid component of soft tissue artifact. Conversely, scaling and deformation of a non-rigid cluster formed by individual markers, has been defined as the non-rigid component of soft tissue artifact. The rigid component refers to changes in marker orientation and position, while the non-rigid component refers to changes in marker cluster size and shape. Rigid and non-rigid soft tissue artifact, for an individual marker or a marker cluster, are assumed to be independent and additive to result in total soft tissue artifact, where the rigid component tends to dominate soft tissue artifact (Dumas et al., 2014). This has been concluded by studies discerning rotation, translation, and deformation components relative to a reference pose (Barré et al., 2017; Benoit et al., 2015; De Rosario et al., 2012; Dumas et al., 2014), using principal component analysis (Andersen et al., 2012), and by comparing the performance of models which attenuate soft tissue artifact by accounting for different components of artifact (Dumas & Cheze, 2009).

In order to substantially reduce soft tissue artifact, methods should place emphasis on minimizing and compensating for the rigid component of soft tissue artifact. During data collection, this can be accomplished by varying marker cluster physical characteristics, method of attachment to the segment, and marker location on the segment (section 2.3.1). Additionally, mathematical procedures and models have been developed to partially compensate for soft tissue artifact in data processing applications (section 2.3.2).

2.3.1 Minimizing soft tissue artifact in data collection

Markers which are located on different areas of a segment will exhibit similar movement due to bone motion, and independent movement due to local deformations of the underlying soft tissue (Bonci et al., 2014). To reduce individual marker motion from local soft tissue deformation, real or digitized markers are calibrated to a non-rigid or rigid

cluster coordinate system in a reference pose, typically upright standing, and the marker coordinates are reconstructed relative to the coordinate system throughout the task (Cappozzo et al., 1995). In this way, all calibrated markers undergo uniform deformation due to soft tissue artifact, equivalent to the artifact affecting the marker cluster; however, there is no direct attenuation of the cluster soft tissue artifact.

While rigid clusters only experience rigid artifact, non-rigid clusters will experience non-rigid and rigid artifact. Non-rigid artifact modifies the relative distance between markers, thereby disrupting the marker cluster coordinate system calibrated during the reference pose. Ultimately, this results in unpredictable changes to marker cluster coordinate systems, which can vary at each time frame. Although a number of data processing techniques have been proposed to minimize non-rigid artifact in non-rigid marker clusters (section 2.3.2); rigid clusters are more commonly used, since non-rigid artifact is completely eliminated and decreased instrumentation is required on the subject (Angeloni et al., 1992; Manal et al., 2000).

Rigid cluster design criteria have been proposed to minimize error propagation, including the effects of soft tissue artifact, from marker coordinates to segment and joint kinematics. By simulating experimental error on marker coordinates and altering specific cluster characteristics, it was concluded that rigid clusters should consist of at least four non-collinear markers on an isotropic and quasi-planar surface, where cluster radius is at least ten times greater than the standard deviation of the system's instrumental error (Cappozzo et al., 1997). However, beyond this, recommendations for rigid cluster shape and size are complicated by the additional mass, and subsequent inertial effects (Benedetti et al., 1998). For example, markers often need to be projected on wands or fins to ensure

optimal camera visibility, yet this affects cluster mass distribution and resonant frequency (Karlsson & Tranberg, 1999). Since higher frequency noise is more distinguishable from the frequency of human movement (approximately 1 to 10 Hz), low-mass rigid clusters that oscillate at higher frequencies may be recommended. Additionally, studies which have examined reducing contact area between a rigid cluster and the skin, accomplished by elevating clusters or decreasing cluster size, have found a decrease in cluster stability, resulting in greater cluster oscillation during movement (Südhoff et al., 2007). While there are strict marker cluster design criteria to ensure successful data collections, characteristics of the marker cluster, such as mass and contact area on the subject's skin, may be altered to modify soft tissue artifact.

For motion capture data collections, specific marker attachment methods have been shown to attenuate soft tissue artifact. In general, markers should be adhered directly to the subject's skin (i.e. avoiding clothing) with double-sided tape, and for a rigid cluster, straps around the cluster and segment should be used to facilitate cluster movement with skeletal movement rather than local soft tissue displacement (Manal et al., 2000). These attachment recommendations were initially made in the context of gait; however, they are widely used for motion capture collections across a range of tasks.

Although varying rigid cluster physical characteristics and attachment method may assist in slightly attenuating soft tissue artifact, altering marker location on a segment has the potential to be more effective. Standard practice to maximize marker visibility, while minimizing marker distortion and soft tissue artifact, is to place markers on areas with the least expected soft tissue deformation and at angles perpendicular to the cameras. Since the largest changes in joint rotation typically occur in the sagittal plane, markers are commonly

placed on the lateral aspect of the thigh, where there is a smaller volume of muscle and adipose tissue, and away from joint lines (Cappozzo et al., 1995). Although the performance of rigid clusters localized to different areas of a segment has been minimally investigated; multiple studies have compared the performance of non-rigid marker clusters. For these studies, the non-rigid clusters have undergone a solidification procedure (Andriacchi et al., 1998; Chèze et al., 1995; Söderkvist & Wedin, 1993; Veldpaus et al., 1988) to minimize changes in the markers' relative position between time frames; thereby increasing rigidity. Cappozzo et al. (1996) evaluated different combinations of three-marker clusters formed from six different markers on the lateral thigh during cycling and hip external rotation in one subject. RMS error in femur rotation ranged from 1.0 to 7.0º, where no single marker cluster was superior across tasks or axes of rotation. Akbarshahi et al. (2010) compared different three-marker non-rigid clusters formed from combinations of six markers distributed over the anterior and lateral thigh, and one on the patella. For knee flexion to 90º and a step-up task, thigh clusters constructed from two anterior and one distal or mid-lateral marker performed best for knee flexion-extension and abduction-adduction, while a cluster formed from one anterior, one lateral, and the patella marker most accurately quantified knee internal-external rotation (Akbarshahi et al., 2010). In activities of daily living, Stagni et al. (2005) compared knee joint rotations from marker clusters formed by markers on the whole, or proximal, central, or distal third of the thigh, while the shank cluster remained constant. Across subjects and tasks, error in rotation was largest with the proximal thigh cluster (Stagni et al., 2005). For both subjects, knee flexion-extension was most artifact-free with a distal thigh cluster (Stagni et al., 2005). Abduction-adduction for subject 1 was also best with a distal cluster, but the total (for stair ascent and

descent, step-up/down, and knee extension) and proximal (for sit-to-stand) thigh cluster were best for subject 2 (Stagni et al., 2005). For internal-external rotation, results were highly variable as each thigh cluster performed best for at least one subject during one of the tasks (Stagni et al., 2005). Unfortunately, the number and specific location of the markers forming each cluster were not provided (Stagni et al., 2005). Barré et al. (2015) found similar results by creating a subject-specific soft tissue artifact map based on individual marker displacement, of the thigh during treadmill gait, and classifying areas of the thigh as least, mid, and most affected by soft tissue deformation. Non-rigid clusters were formed from markers on the different classified areas of the thigh, and femur transformations from the various clusters were compared. RMS differences were similar across all clusters, with two exceptions: 1) axial rotation was largest for clusters built from markers in least and most affected areas (least = 8.1 ± 3.9°, most = 7.3 ± 2.0°, mix = 5.7 ± 2.1°, mid = 5.2 ± 2.6°), and 2) translation along all axes was smallest for the least affected area cluster (anterior-posterior = 3.0 ± 1.6 mm, axial = 4.4 ± 1.7 mm, medial-lateral = 8.6 ± 3.2 mm). Additionally, mean coefficients of multiple correlation were excellent (> 0.90) for all clusters and transformations, except for rotation about the axial (0.35 to 0.52) and medial-lateral (0.59 to 0.77) axes. Evidently, soft tissue artifact within a segment is complex, whereby the placement of motion capture markers has been shown to affect kinematic outcomes. Thus, there is a need to assess which marker configuration results in the most accurate kinematics, in the context of specific outcome measures, such as joint rotation or translation within a specific plane, for a specific task.

2.3.2 Compensating for soft tissue artifact in data processing

The following section in no way provides an exhaustive list of the computational processing procedures tested and/or validated; however, some of the most common and relevant techniques for mitigating soft tissue artifact are discussed below.

Standard practice to reduce noise in a signal is to filter the data, where the goal is to maximize noise removal and signal retention. This is accomplished by utilizing an appropriate filter and cut-off frequency. Unfortunately, soft tissue artifact resonates at a range of frequency harmonics, some of which are indistinguishable from human movement (Fuller et al., 1997). For example, skin sliding will exhibit lower frequency content, approximately identical to the frequency of human movement, since they have identical sources – the movement of bone. Alternatively, muscle and adipose tissue will oscillate at higher frequencies, possibly at distinct frequency harmonics from human movement, thereby facilitating effective removal by digital filtering. To discern the contributions of skin sliding, muscular contractions, and soft tissue oscillation, Bonci et al. (2014) modelled thigh soft tissue artifact under the assumption that artifact increases linearly with skin sliding, due to changes in hip and knee angle, using *in vivo* (Reinschmidt, van den Bogert, Nigg, et al., 1997) and *in vitro* (Cereatti et al., 2009) data to calibrate the model. By comparing estimated soft tissue artifact outputted by the model, and measured soft tissue artifact from the data sets, they attempted to distinguish skin sliding contribution to total artifact (Bonci et al., 2014). The model-estimated soft tissue artifact had an average 89% of frequency content between 0 and 5 Hz, encompassing the majority of skin sliding and voluntary movement (Bonci et al., 2014). Frequency analysis of *in vivo* soft tissue artifact during running revealed that an average of 73% of frequency content also fell between 0

and 5 Hz (Bonci et al., 2014). Furthermore, the correlation between the time histories of the model-estimated and measured soft tissue artifact was excellent ($r > 0.93$) across markers, axes, and subjects (Bonci et al., 2014). The similarity between model-estimated and measured soft tissue artifact in the frequency and time domain suggests that oscillation may not be the primary source for soft tissue artifact. Additionally, since oscillation demonstrates higher frequency content (above ~5 Hz) (Bonci et al., 2014), it may be more easily mitigated through filtering techniques. Evidently, digital filtering will not be successful in eliminating all noise due to soft tissue artifact; thus, other data processing techniques must be implemented for further attenuation of noise resulting from soft tissue deformation.

Unlike a rigid cluster, formed from markers on an isotropic rigid body which exhibits no change in size or shape throughout movement; non-rigid clusters exhibit relative changes in marker displacement which can be partially compensated for by mathematical approaches. Least square methods compute optimal marker transformation by minimizing marker cluster deformation between two time points, typically relative to the marker arrangement during a reference pose (Chèze et al., 1995; Söderkvist & Wedin, 1993; Veldpaus et al., 1988). Inertial methods, such as the point cluster or interval deformation technique, utilize a marker cluster tensor of inertia to assign each individual marker a mass that minimizes segment cluster deformation between successive time points (Alexander & Andriacchi, 2001; Andriacchi et al., 1998). Although least square and inertial methods compensate for the non-rigid component of soft tissue artifact, they do not address rigid motion of the cluster relative the underlying bone; and thus, error in knee rotation (up to 5^{o}) and translation (up to 10 mm) persists (Cereatti et al., 2006).

Least square and inertial methods are commonly utilized to attenuate non-rigid soft tissue artifact at the level of the segment. However, segment error will propagate to joint error; often exhibited as motion about some degree-of-freedom which is larger than realistically probable. Global, or multi-body, optimization models attempt to limit this overestimated joint motion by imposing constraints on the degrees-of-freedom between two adjacent segments (Lu & O'Connor, 1999). Mathematically, marker position is calculated by minimizing the difference between measured and model-predicted marker coordinates, under these kinematic constraints (Lu & O'Connor, 1999). Most commonly, joint translation is constrained, thereby creating a chain of three degrees-of-freedom spherical joints. A global optimization model was first effective in preventing knee joint dislocation during gait analysis (Lu & O'Connor, 1999), and has since been tested and validated on a range of other tasks including, running (Bonnet et al., 2017; Gasparutto et al., 2015; Richard et al., 2017), hopping and cutting (Potvin et al., 2017; Richard et al., 2017), sit-to-stand and step-up (Richard et al., 2017; Stagni et al., 2009), squatting (Clément et al., 2015), and quasi-static knee flexion to 110° (Charbonnier et al., 2017).

Although global optimization has been effective in partially compensating for soft tissue artifact (Charbonnier et al., 2017; Clément et al., 2015; Gasparutto et al., 2015; Potvin et al., 2017; Reinbolt et al., 2005), it is not a consistently reliable method (Andersen et al., 2010; Bonnet et al., 2017; Richard et al., 2017; Stagni et al., 2009). In quasi-static knee flexion, RMS error in knee joint angles compared to bone orientation in an MRI system ranged from 6.8° to 8.7° without kinematic constraints and 7.1° to 9.8° with knee translation constrained and was largest for internal-external rotation, followed by abduction-adduction, then flexion-extension in the higher knee flexion ranges

(Charbonnier et al., 2017). Additionally, during squatting to 60°, Clément et al. (2015) demonstrated that spherical constraints on ankle, knee, and hip marginally reduced soft tissue artifact for knee abduction-adduction and internal-external rotation, typically between 1° and 3°, in healthy subjects and those with knee osteoarthritis, with minimal to no change in estimated knee flexion-extension. Translation constraints on the ankle, knee, and hip during a step-up and sit-to-stand task also minimally reduced soft tissue artifact, whereby the mean RMS error in knee joint angle compared to bone position measured by fluoroscopy, was approximately 10° but up to 25° (Stagni et al., 2009). Richard et al. (2017) found similar results when implementing six global optimization models, with varying joint constraints, in a step-up and sit-to-stand task, wherein no model substantially attenuated soft tissue artifact to within 2° or 2 mm of bone position and orientation.

Evidently, there are varying results on if global optimization is an effective tool for compensating for soft tissue artifact. Part of this dilemma extends from the fact that studies have implemented global optimization in a variety of different ways. For example, studies have evaluated different types of constraints on individual and multiple joints (Andersen et al., 2010; Clément et al., 2015; Gasparutto et al., 2015), applied two-step optimization procedures to increase subject specificity based on subject joint parameters and joint degrees of freedom (Reinbolt et al., 2005), and attempted to adjust constraints as a function of joint angle (Potvin et al., 2017). Nevertheless, global optimization presents itself as a feasible option for attenuating the effects of soft tissue artifact as it does not require any additional steps to be taken during data collection, and it can be easily implemented in biomechanical software. Furthermore, global optimization should be evaluated in its

effectiveness to partially compensate for soft tissue artifact in high knee flexion movements as dynamic flexion greater than approximately 90° has not been evaluated.

Multiple models which attempt to compensate for soft tissue artifact build upon the assumption that soft tissue artifact changes predictably or consistently over a joint's range of motion. In this way, a systematic pattern in marker trajectory, attributed to soft tissue artifact, is defined in relation to the motor task. Double calibration procedures define the pattern of soft tissue artifact in a given task by performing calibration procedures at the start and end of range of motion of the specific task, then interpolate between the two known anatomical landmark positions (Cappello et al., 1997, 2005). Double calibration has been effective in attenuating soft tissue artifact, wherein knee joint angles determined by motion capture are within approximately 3.5° and translations are within 4.5 mm (Cappello et al., 1997, 2005; Stagni et al., 2009). These findings support the claim that soft tissue artifact varies somewhat predictably with joint angle as assuming a relationship between knee joint angle and soft tissue artifact partially compensated for error in kinematics.

The largest criticism for double calibration procedures is that they impose a specific relationship, commonly through linear interpolation, on marker trajectories throughout the movement. To overcome this limitation, *ad hoc* task-specific movements can be used to calibrate marker artifact by determining the correlation between marker trajectory over time (Lucchetti et al., 1998), joint angle (Lucchetti et al., 1998; Ryu, 2012), or offset between markers in the same marker cluster coordinate system (Ryu, 2012; Ryu et al., 2009). Like double calibration procedures, dynamic calibration has also been effective in compensating for task-related soft tissue artifact of the lower extremity (Lucchetti et al.,

1998; Ryu, 2012; Ryu et al., 2009), providing further support to the presence of a relationship between soft tissue artifact and task demands.

Kinematic-driven optimization models, which like multiple calibration procedures, attempt to define the relationship between soft tissue artifact and the motor task performed, have been also proposed to compensate for soft tissue artifact. Specifically, these models assume there is a correlation between soft tissue artifact and joint angle, and an optimization model is then produced which minimizes the difference in measured and model-predicted and marker coordinates at each time frame (Bonci et al., 2014; Camomilla et al., 2013, 2015). During validation of these models against a gold standard, partial attenuation of soft tissue artifact occurs, whereby measured and model-predicted marker trajectories demonstrate similar time histories, but large residuals (Bonci et al., 2014; Camomilla et al., 2015). The large residuals are likely because models do not account for the effects of oscillation, resulting in only partial attenuation of soft tissue artifact (Bonci et al., 2014).

Although computational methods represent a feasible option for attenuating the effects of soft tissue artifact, these methods result in only partial compensation, and the models lack validation across a range of subjects and tasks. Therefore, models should be used in conjunction with data collection minimization techniques to facilitate a greater reduction in soft tissue artifact.

Chapter 3 - A Non-Invasive Assessment of Soft Tissue Artifact of the Thigh in High Knee Flexion

3.1 Introduction

Optical motion capture is used to quantify the motion of bones by measuring the position of markers that are adhered to the skin. However, as an individual moves, skin markers move relative to underlying bone due to the deformation and displacement of both active and passive tissue. This results in error in marker trajectories, known as soft tissue artifact, which can lead to kinematic and kinetic errors which are as large, or larger, than physiological joint angles and/or moments (Akbarshahi et al., 2010; Kuo et al., 2011; Reinschmidt, van den Bogert, Nigg, et al., 1997; Stagni et al., 2005; Tsai et al., 2011). Although multiple studies have quantified soft tissue artifact by synchronously collecting and comparing skin marker position, determined by motion capture, and bone position, determined by bone fixation (e.g. bone pins) or imaging techniques (e.g. x-ray or MRI), these methods are invasive, cumbersome, and expensive. Thus, recently, methods for estimating soft tissue artifact which rely only on motion capture have been investigated.

To quantify soft tissue artifact non-invasively, the position of a single marker is quantified by multiple coordinate systems, constructed from multiple marker clusters which are localized to the same (Camomilla et al., 2009) or adjacent segments (Lucchetti et al., 1998; Ryu, 2012; Ryu et al., 2009). The difference in the position of the marker reconstructed from the different marker clusters is considered to be an estimate of soft tissue artifact. For marker clusters located on the same segment, the multiple independent observer method has been proposed (Camomilla et al., 2009). This method requires a marker array of individual markers on a given segment [e.g. sixteen (Camomilla et al., 2009; Stagni et al., 2005)]. Non-rigid clusters are then formed from the individual markers

and the deformation of the different clusters throughout motion are compared. Non-rigid clusters that display uncorrelated deformation are considered ‘independent observers’ of a marker that is not used in the construction of the cluster (Camomilla et al., 2009). Each marker is then tracked throughout motion with each independent observer simultaneously, and soft tissue artifact of the specific marker is estimated as the average of the displacement vectors for each of the independent observers (Camomilla et al., 2009).

Alternatively, soft tissue artifact has been estimated by comparing the position of a digitized marker reconstructed from marker cluster coordinate systems on two adjacent segments (Lucchetti et al., 1998; Ryu, 2012; Ryu et al., 2009). For example, the location of the digitized marker on the thigh is tracked by both the thigh and shank coordinate system as the subject performs a hip flexion-extension task with the knee extended (Lucchetti et al., 1998; Ryu, 2012; Ryu et al., 2009). During this motion it is assumed that the reconstruction of the marker by the shank is artifact-free, and thus soft tissue artifact is equal to the difference between the thigh and shank estimated position of the marker as a function of time (Lucchetti et al., 1998), joint angle (Lucchetti et al., 1998; Ryu, 2012), or offset between markers in the same cluster coordinate system (Ryu, 2012; Ryu et al., 2009). The use of non-invasive methods for quantifying soft tissue artifact provide an alternative tool for examining soft tissue artifact on a task-by-task basis, without the need for overly specialized equipment or subsequent limitations on sample size.

Although these non-invasive methods may not quantify soft tissue artifact as accurately as bone fixation or imaging techniques, they may be useful for comparing local soft tissue artifact between marker clusters located on the same segment. Previous research has demonstrated that markers localized to different areas of the thigh experience different

soft tissue artifact (i.e. location specificity) (Akbarshahi et al., 2010; Barré et al., 2015; Cappozzo et al., 1996; Stagni et al., 2005); thus, it is theorized that placing markers on areas with the least soft tissue deformation and displacement may be optimal. That being said, defining an optimal marker placement is complicated by multiple factors, namely the subject and task (Leardini et al., 2005).

It is known that soft tissue artifact varies between individuals (i.e. subject specificity) (Barré et al., 2013; Clément et al., 2018; Garling et al., 2007; Stagni et al., 2005). Although previous studies have found a relationship between the magnitude of soft tissue artifact and subject BMI (Barré et al., 2013; Clément et al., 2018; Garling et al., 2007), there are conflicting results on if this is a positive or negative relationship and across the different planes of motion. It is likely that variability in soft tissue artifact would be partially explained by participant anthropometrics; however, no study to date has investigated the relationship between local (i.e. segment) measures of anthropometry and soft tissue artifact.

Soft tissue artifact has also been shown to vary with the task performed (i.e. task specificity). Specifically, soft tissue artifact is known to increase with joint angle (Cappozzo et al., 1996; Fuller et al., 1997; Kuo et al., 2011; Tsai et al., 2009); however, tasks which require large changes in joint angle have largely been unexplored. At the knee joint, high flexion, where the knee flexion angle exceeds 120°, may elicit different soft tissue artifact than low-to-moderate joint range of motion tasks, due to contact between the thigh and calf which begins at approximately 125° of knee flexion (Kingston & Acker, 2018). Consequently, a specific marker placement may be more optimal for use in high flexion. For example in gait, markers on the distal-lateral thigh have been shown to exhibit

the least soft tissue artifact (Barré et al., 2013); however, in a sit-to-stand task, which may elicit more similar soft tissue movement to thigh-calf contact, a distal-anterior cluster was more accurate (Stagni et al., 2005). Since repeated adoption of high knee flexion has been found to be associated with the development of knee joint injury and diseases (Baker et al., 2003; Canetti et al., 2020; Coggon et al., 2000; Jensen, 2005, 2008), recommendations for accurate and reproducible methods of data acquisition must be made for these tasks to more clearly discern mechanisms of injury.

3.1.1 Agreement between hip joint center and femoral head center as an estimate for soft tissue artifact

The first objective of this study was to investigate the effect of thigh marker cluster location on soft tissue artifact during high knee flexion tasks. Motion tracking for the thigh was collected from rigid marker clusters localized to the middle and distal third of the thigh, and on the anterior, lateral, and anterolateral aspect of the thigh while the participant completed different squatting and kneeling activities. As an estimate of local soft tissue artifact, the functional hip joint center, which was considered coincident with the femoral head center during upright standing (Camomilla et al., 2006; Fiorentino et al., 2016), was tracked with the pelvis cluster and each of the six thigh clusters through motion. Soft tissue artifact was defined as the difference in the position of the functional hip joint center estimated from the pelvis cluster (‘hip joint center’) and each of the thigh clusters (‘femoral head center’). Based on previous studies of tasks which require moderate changes in knee flexion (Akbarshahi et al., 2010; Stagni et al., 2005), it was hypothesized that soft tissue artifact would be smallest for the distal-anterior thigh cluster, as this cluster

would be least affected by posterior and medial-lateral topographic deformation of the thigh during thigh-calf contact.

3.1.2 Soft tissue artifact subject specificity

The second objective was to assess the accuracy in which global and local measures of anthropometry could predict soft tissue artifact for marker clusters localized to different areas of the thigh. Global measures included sex, height, mass, BMI, waist circumference while local measures were thigh length, thigh proximal, middle, and distal circumferences, and thigh skinfold thickness. Multiple linear regressions were performed, using backward stepwise procedures, between subject anthropometry (independent variables) and the mean of the peak difference in the estimated 3D position of the hip joint center and femoral head center (dependent variable) for each of the six thigh clusters independently. It was hypothesized that there would be a moderate fit between predicted soft tissue artifact and subject anthropometrics, thereby facilitating recommendations for marker placement (i.e. marker clusters which predict a larger difference in hip joint center and femoral head center position from subject anthropometry should be avoided for that subject). Additionally, based on previous findings which found soft tissue artifact was poorly correlated with global measures of anthropometry (Barré et al., 2013; Camomilla et al., 2017; Garling et al., 2007), it was hypothesized that local measures of the thigh anthropometry would have a stronger effect on soft tissue artifact than global measures of subject anthropometry, as indicated by the frequency of retention in the regression models and larger standardized beta coefficients and partial correlations.

3.2 Methods

3.2.1 Sample population

An *a-priori* analysis was completed, using G*Power 3.1, to determine the required sample size for the statistical methods presented in this thesis (Faul et al., 2007). The results were estimated using a power level (beta) of 0.80, an alpha level of 0.05, and a medium effect size of 0.06, which was estimated from data presented by Barré et al. (2015). The required sample size for the multiple linear regressions (chapter 3) when all ten independent variables were retained was seventy-five subjects. However, given that backward stepwise procedures were utilized and there was a high likelihood of collinearity in the regression models, it was considered unlikely that all independent variables would be retained in the final regression models. Thus, the same analysis was completed with five independent variables, and the required sample size was fifty-eight subjects. Alternatively, the three-way ANOVAs (chapter 4) indicated that a sample size of thirteen subjects would be sufficient. Given the large discrepancies in sample size requirements between the studies and the assumption of a modest medium effect size, fifty participants were collected for this thesis.

Fifty participants (Table 3-1) with no previous, or current, low back or lower extremity injury which required medical intervention or time off work for longer than three days within the past year were recruited from the University population. Subjects were required to have no difficulty or pain completing the squatting and kneeling protocol. All but three subjects were right leg dominant. Each subject read and signed an informed consent form approved by the university's research ethics board.

Table 3-1: Mean and standard deviation (in brackets) descriptive and anthropometric participant information. Prox is proximal, mid is middle, and dist is distal.

Parameter	Female (n = 28)	Male (n = 22)	Total (n = 50)
Age (years)	21.1 (3.0)	21.4 (2.6)	21.2 (2.9)
Height (m)	1.65 (0.09)	1.79 (0.06)	1.71 (0.10)
Mass (kg)	63.6 (11.6)	78.2 (10.2)	70.0 (13.1)
BMI (kg/m2)	23.2 (3.4)	24.3 (2.4)	23.7 (3.0)
Waist circumference (cm)	73.9 (8.2)	81.7 (6.4)	77.3 (8.4)
Thigh length (cm)	42.4 (3.1)	44.6 (2.0)	43.4 (2.8)
Prox thigh circumference (cm)	59.9 (5.40)	58.2 (7.5)	59.2 (6.4)
Middle thigh circumference (cm)	51.2 (4.7)	53.4 (4.0)	52.1 (4.5)
Dist thigh circumference (cm)	40.1 (3.6)	43.0 (7.2)	41.4 (5.6)
Thigh skinfold (mm)	28.0 (9.3)	15.0 (5.6)	22.3 (10.2)

3.2.2 Instrumentation

Kinematic data was collected using a six three-camera-bank optical motion capture system (Optotrak, Certus/3020, NDI, Waterloo, ON). Prior to participant arrival the collection space was calibrated, and a global coordinate system was defined using a rigid cube containing sixteen infrared diodes with known configuration. The global coordinate system was defined in conjunction with ISB standards, where Y was proximal(+)-distal, X was anterior(+)-posterior, and Z was medial-lateral (Wu & Cavanagh, 1995). Kinematic data was sampled at 50 Hz and kinetic data was synchronously recorded at 2000 Hz from four embedded force plates (OR6-7, AMTI, Watertown, MA), which were zeroed prior to each collection.

For instrumentation of each subject, rigid marker clusters of four non-collinear infrared diodes were placed on the sacrum of the pelvis, bilaterally on the thighs, shanks, and feet (Figure 3-1). A total of six marker clusters were localized to the middle and distal third of each thigh, with four clusters placed on the lateral and anterior aspect of the thigh

on one leg, and two clusters placed anterolateral aspect of the opposite thigh (Figure 3-2). Thigh cluster arrangement was randomized to the subject's right or left leg. Cluster placement was defined as: distal-anterior, distal-anterolateral, distal-lateral, mid-anterior, mid-anterolateral, and mid-lateral. The distal and middle third of the thighs were defined as 30-60% and 60-90% of the distance from the palpated greater trochanter to the lateral femoral condyle, respectively. The lateral clusters were placed such that the midline of the cluster was approximately in line with the greater trochanter and lateral femoral condyle, while the anterior clusters were placed such that the midline of the clusters were approximately in line with the anterior superior iliac spine and patella. The anterolateral clusters were placed such that the midline was approximately halfway between the lateral and anterior thigh clusters on the opposite leg. Marker clusters were attached to segments using double-sided carpet tape, and elastic Velcro straps which were wrapped through the cluster and around the respective segment for the shank, thigh, and pelvis. The straps were adjusted as needed prior to calibration trials to ensure that deformation of the segments did not occur during adoption of the high knee flexion postures (i.e. the straps were not too tight). The position of anatomical landmarks (Figure 3-1), tracked with each marker cluster, were identified while the participant stood in anatomical posture using a digitization probe (Cappozzo et al., 1995).

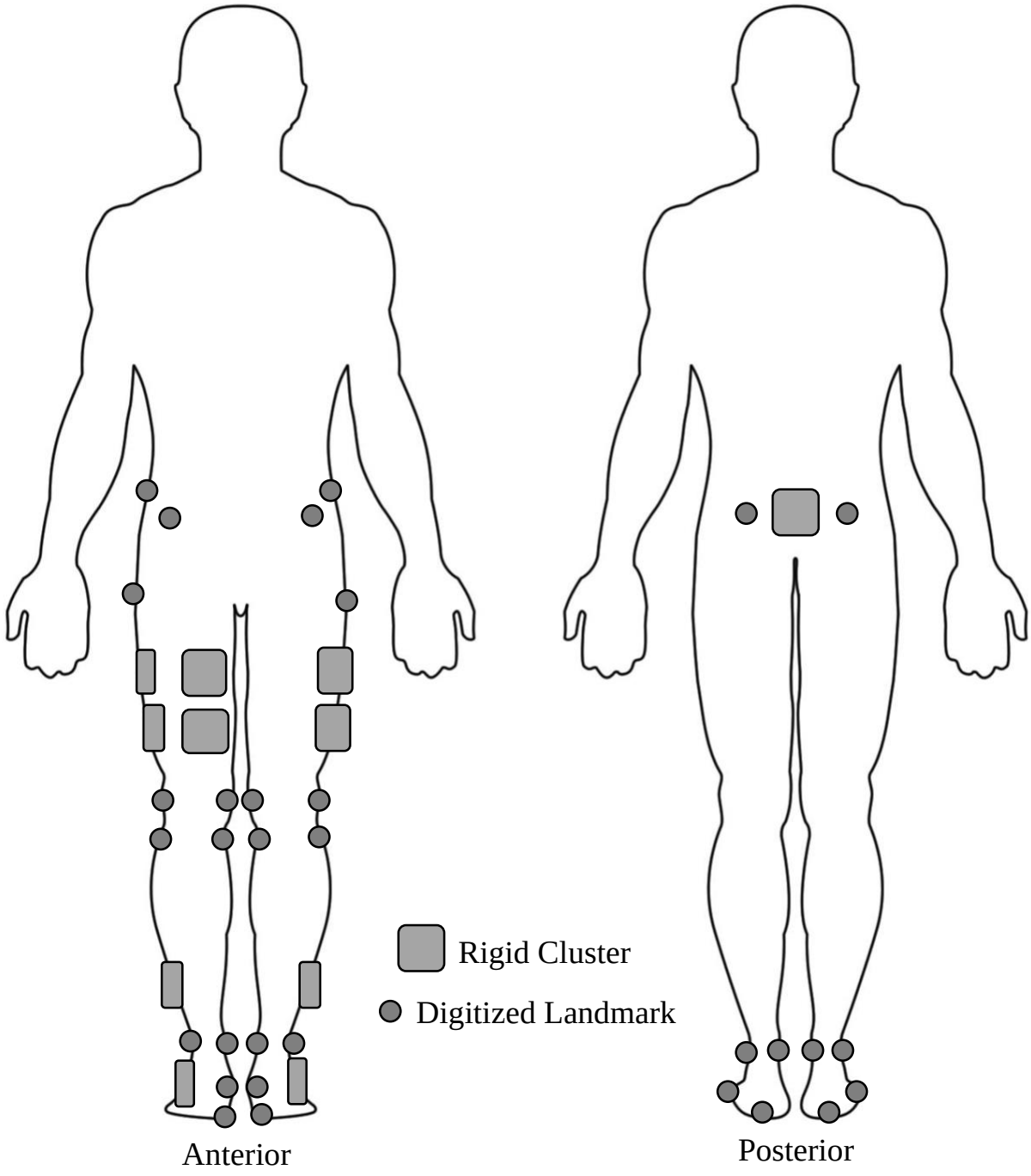

Figure 3-1: Optotrak marker placement and digitized landmarks for data collection.

Figure 3-2: Thigh cluster placement was defined as distal-anterior, distal-lateral, mid-anterior, and mid-lateral for one leg (left leg in this image), and distal-anterolateral and mid-anterolateral for the opposite leg.

3.2.3 Experimental protocol

Once participants read and provided informed consent, participants were given an overview of the experimental protocol and asked to change into athletic shorts and footwear. Demographic and anthropometric data for the dominant lower limb were then measured (Table 3-1). Thigh length was measured as the distance between the palpated greater trochanter and lateral femoral condyle. Thigh circumference measurements were taken at 30% (proximal), 60% (middle), and 90% (distal) of the thigh length as measured from the greater trochanter. Two thigh skinfold measurements were taken at the midpoint

between the inguinal fold and the anterior surface of the patella (Stewart & Marfell-Jones, 2011), wherein the average of the measurements was used as a gross representation of thigh adiposity.

Instrumentation then commenced by attaching rigid clusters to the pelvis, distal-lateral thighs, shanks, and feet. A functional hip joint center trial (star-arc pattern and hip circumduction) was performed (Camomilla et al., 2006) using the distal-lateral thigh clusters on the right and left legs, to ensure more symmetrical hip joint center localization. The participant was then instrumented with all the thigh rigid clusters for subsequent high knee flexion movement trials and anatomical landmarks were digitized (Figure 3-1 and 3-2). Following digitization, participants performed a quiet standing (static calibration) trial and a functional knee joint center trial (knee flexion-extension).

Participants then observed the high knee flexion movements performed by the researcher and were able to practice them until they could perform them comfortably. Participants completed the following four high knee flexion movements in a randomized order on the embedded force plates: flat-foot squat (FS), heels-up squat (HS), dorsiflexed kneel (DK), and plantarflexed kneel (PK) (Figure 3-3). Each trial consisted of the participant descending into maximal flexion, statically holding the posture for five seconds, then ascending to the starting posture in the same manner as the descent. Participants were instructed to maximize knee flexion and thigh-calf contact. Participants completed FS and HS with a symmetrical descent into the squat from upright standing, while DK and PK were completed with both asymmetrical and symmetrical transitions: asymmetrical – transition between upright standing and kneeling by moving through a lunging posture with the right or left leg, and symmetrical – beginning on knees, approximately 90° of knee

flexion with hips extended, and sitting back into kneel (Figure 3-4). For the asymmetrical kneeling transitions, the leg stepping forward into the lunge was defined as the lead leg and the other leg was defined as the trail leg (Figure 3-4). Five repetitions of each movement variation were completed. For analysis, eight tasks were defined: FS, HS, DK symmetrical (DK-S), PK symmetrical (PK-S), DK lead leg (DK-L), PK lead leg (PK-L), DK trail leg (DK-T), and PK trail leg (PK-T).

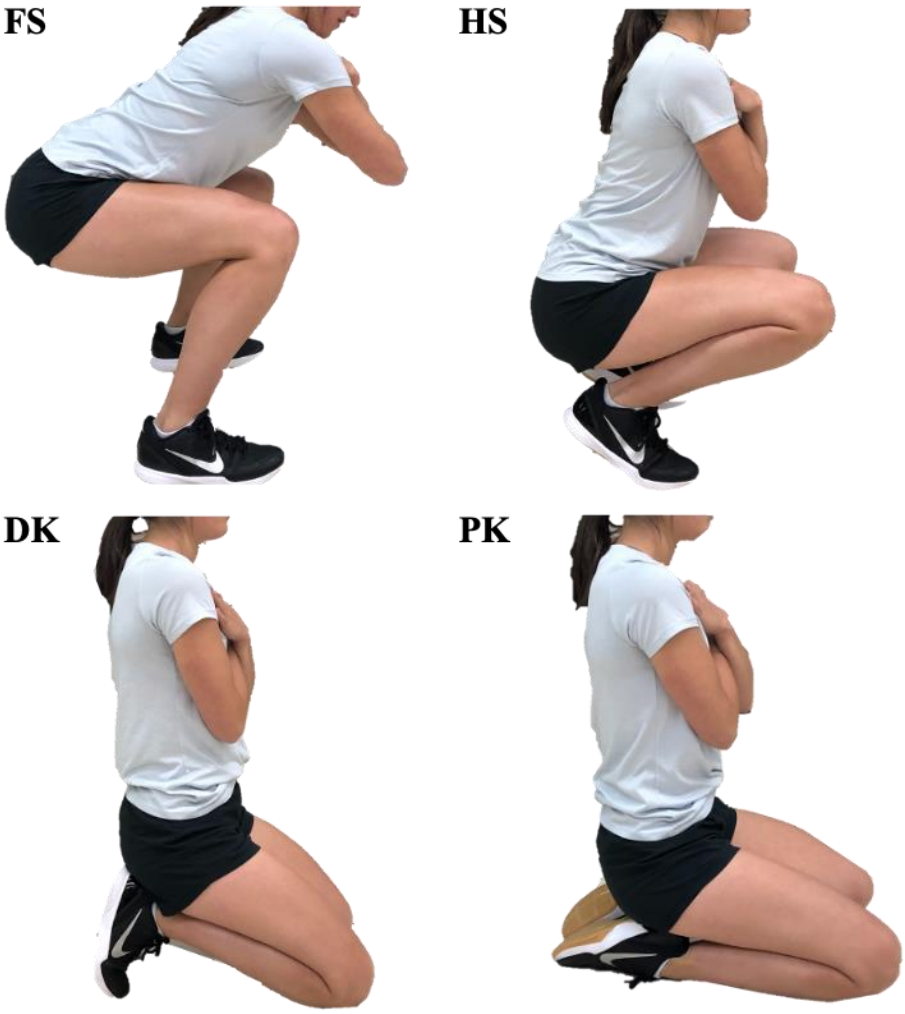

Figure 3-3: High knee flexion movements defined as the flat-foot squat (FS), heels-up squat (HS), dorsiflexed kneel (DK), and plantarflexed kneel (PK).

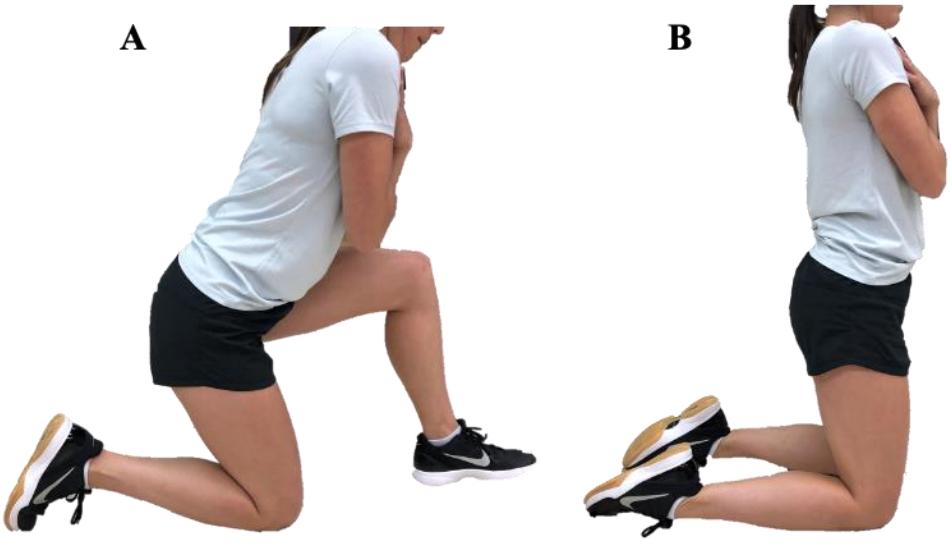

Figure 3-4: High knee flexion movement transitions. A) is the asymmetrical kneeling transition, where the left leg is the lead leg and the right leg is the trail leg, and B) is the symmetrical kneeling transition.

3.2.4 Data processing

Gaps in the position data that were less than 200 ms (10 frames of data) were filled with a cubic spline (Howarth & Callaghan, 2010) and kinematic and kinetic data were dual pass filtered using a second-order low pass Butterworth filter with a cut-off frequency of 6 Hz (Longpré et al., 2013; Winter, 2009) in Visual3D (C-Motion, Version 2.05, Germantown, USA). For padding prior to filtering, one second of data was reflected (Howarth & Callaghan, 2009). As well, the functional hip and knee joint centers were calculated from the functional trials (Schwartz & Rozumalski, 2005). The functional method has been shown to most accurately quantify the hip joint center (Camomilla et al., 2006; Ehrig et al., 2006; Fiorentino et al., 2016). The knee flexion angle throughout the movement trials was calculated using a Z-X-Y Cardan sequence (flexion-extension, abduction-adduction, internal-external rotation) for each thigh cluster, in conjunction with

the shank cluster. Thigh and shank anatomical coordinate system definitions are provided in Table 5-1 and 5-2.

The difference in the position of the hip joint center when tracked with the pelvis cluster ('hip joint center') versus when tracked with one of each of the six thigh clusters ('femoral head center') was calculated as an estimate of soft tissue artifact in a custom Matlab program (The Mathworks, Release R2019B, Natrick, MA). First, a local coordinate system, represented by a 3 x 3 rotation matrix, R, and origin, o, was constructed from the global coordinates of three non-collinear markers for the pelvis and each of the thigh marker clusters (Eq. 3.1 and 3.2) where the column vectors in Eq. 3.2 are the orthogonal unit vectors describing the cluster coordinate system.

$$o = \begin{bmatrix} o_x \\ o_y \\ o_z \end{bmatrix} \quad \textbf{Eq. 3.1}$$

$$R = [\vec{x} \quad \vec{y} \quad \vec{z}] \quad \textbf{Eq. 3.2}$$

During upright standing, the hip joint center was considered coincident with the femoral head center (Camomilla et al., 2006; Fiorentino et al., 2016); therefore, at the start of each movement trial, when the participant was in upright standing, or a similar posture for the hips in DK-S and PK-S, the hip joint center and the femoral head center were defined at the same global position. This was accomplished in the first frame of data, by defining a vector, $\overrightarrow{v_1}$ (Eq. 3.3) in the local coordinate system for the respective marker clusters, from the origin of the local coordinate system for the pelvis and each of the thigh marker clusters to the functional hip joint center, FHC, where o and FHC are point coordinates in the global coordinate system in Eq. 3.3.

$$\overrightarrow{v_1} = R' * (FHC - o) \quad \textbf{Eq. 3.3}$$

Throughout the movement trial, the position of the hip joint center was reconstructed relative to the pelvis cluster [i.e. gold standard (Camomilla et al., 2006)], while the position of the femoral head center was reconstructed relative to each thigh cluster. while the position of the femoral head center (FHC) was reconstructed relative to each thigh cluster ($T = 1{:}6$). The position of these two points was calculated by performing a local to global transformation at each frame of data, i (Eq. 3.4 shown for HJC).

$$HJC_i = R * \overrightarrow{v_1} + o \quad \textbf{Eq. 3.4}$$

Soft tissue artifact would theoretically cause these two points to diverge. The difference (D) between the hip joint center and femoral head center for each thigh cluster in the three orthogonal global directions, as well as the magnitude of the 3D difference, calculated by the vector norm, were then determined (Eq. 3.5).

$$D_i = HJC - FHC_{T=1:6} \quad \textbf{Eq. 3.5}$$

For each high knee flexion task, the mean of the peak difference across trials was calculated for each subject when knee flexion was greater than 120°, as determined by the distal-lateral and distal-anterolateral marker cluster for the respective legs. In FS, not all subjects achieved 120° of knee flexion; therefore, 80° of knee flexion was used. Additionally, for three subjects, the mid-lateral and/or mid-anterolateral marker clusters were used to define the high knee flexion range as the distal-lateral and/or distal-

anterolateral cluster had slid significantly from its calibrated location throughout the protocol.

In addition to determining peak soft tissue artifact in high knee flexion, soft tissue artifact was examined as a function of knee flexion angle. To accomplish this, the mean of the 3D difference across trials (equal to the Bland-Altman mean difference at each frame of data) and the mean knee flexion angle across the six thigh marker clusters, were first truncated and normalized to 101 frames of data. For the squats and symmetrical kneels, data was truncated based on pelvis marker vertical displacement decreasing 1 cm below mean height at the start and end of the trial and visually examined for consistency across subjects and trials. For the asymmetrical kneels, data was truncated when the vertical ground reaction force under the lead leg exceeded 20 N during descent and was less than 20 N during ascent. The mean difference and mean knee flexion angle were then plotted against each other and qualitatively examined to gain insight into the relationship between soft tissue artifact and joint angle.

3.2.5 Statistical analysis

To estimate soft tissue artifact of the thigh, agreement between the position of the hip joint center, tracked with the pelvis cluster, and femoral head center, tracked with each thigh cluster, was evaluated using methods described by Altman & Bland (1983) in a custom Matlab program. Bland-Altman methods graphically represent data by plotting the mean of two measurement methods (x-axis) versus the difference between the methods (y-axis); then, summarize the agreement between the methods with the calculated mean difference, also called the bias, and the limits of agreement (Altman & Bland, 1983). The limits of agreement are equal to the mean difference plus and minus two standard

deviations of the differences, thereby defining the upper and lower limit in which 95% of the differences between the two methods are expected to fall (Bland & Altman, 1986). The mean of the peak difference (position of hip joint center – femoral head center) for each subject in x, y, z, as well as the magnitude of this 3D difference, was input into the Bland-Altman analyses. Separate analyses were completed for each thigh cluster (six), high knee flexion movement (eight), and direction (four).

For interpretation of the Bland-Altman analysis, three questions were considered to compare agreement between the marker clusters. Firstly, was there a relationship between the mean position and difference in position between the hip joint center and femoral head center? This was accomplished by visually examining the Bland-Altman plots for an increasing or decreasing trend and changes in variability as the mean decreased or increased. Secondly, how large was the mean difference between the different marker clusters? This was accomplished by comparing the mean difference between the different marker clusters. Lastly, how wide were the limits of agreement between the different marker clusters? This was accomplished by visually examining the distance between the mean difference and limits of agreement in the Bland-Altman plots, which is equal to approximately two standard deviations of the differences. Marker clusters whose mean difference and limits of agreement were closer to zero – which would indicate no difference between the hip joint center and femoral head center – were concluded to demonstrate higher agreement; and thus, experience less soft tissue artifact. Of note, the difference between the hip joint center and femoral head center was calculated from the position in the global coordinate system and therefore, does not provide information on how each thigh coordinate system would be affected.

Multiple linear regressions were performed using a backward stepwise procedure (Babyak, 2004; Steyerberg et al., 2001) for each of the six thigh marker clusters in SPSS (IBM Corp., Version 26.0, Armonk, NY). Regressions were computed between the subjects' absolute mean of peak difference in the 3D position of the hip joint center and femoral head center (dependent variable), and ten independent variables (sex, height, mass, BMI, waist circumference, thigh length, thigh proximal, middle, and distal circumference, and thigh skinfold thickness) for each of the six thigh clusters separately. For evaluating sex, 0 was assigned to females and 1 was assigned to males; thus, a positive coefficient indicated a positive effect for males (Chehab et al., 2017; Schielzeth, 2010). Independent variable inclusion and exclusion criteria levels were set to $p < 0.05$ and > 0.10, respectively. Subjects were identified as outliers and removed if the mean peak difference was greater than the mean plus three standard deviations, their Mahalanobis' distance exceeded the critical value calculated from the degrees of freedom for the given model, and confirmed as an outlier by visually examining the data. This analysis was performed for both squatting and kneeling, using data from HS, the mean of DK-L and DK-T, collectively referred to as DK, and the mean of PK-L and PK-T, collectively referred to as PK. Each of the models was assessed by evaluating the correlation coefficient (R), the adjusted R square (R_2), and the level of significance with a Bonferroni corrected alpha level of 0.05/6 = 0.008, for each of the thigh marker clusters. Correlation coefficient strengths were defined using the following criteria: 0 to 0.3 is weak, 0.3 to 0.5 is low, 0.5 to 0.7 is moderate, and 0.7 to 1.0 is strong (Mukaka, 2012). All models were also examined for collinearity (tolerance < 0.1 and variance inflation factor > 5) (Babyak, 2004). If independent variables were found to be collinear, stepwise regression was performed with

suspect variables removed until all criteria were met (Legendre & Legendre, 2012). To interpret the relationship between independent and dependent variables, unstandardized and standardized beta coefficients, as well as partial correlations were compared (Schielzeth, 2010).

3.3 Results

3.3.1 Agreement between hip joint center and femoral head center

The mean difference in the hip joint center and femoral head center was greatest along the Y axis (vertical), followed by the X axis (anterior-posterior), then the Z axis (medial-lateral); however, agreement was similar across the different planes of motion (Table 5-4 to Table 5-6). Similar trends between the thigh marker clusters (i.e. the relative order of mean difference and limits of agreement) were found across the different planes of motion; therefore, the magnitude of the 3D difference (Table 5-3) will be discussed to summarize the differences between the marker clusters.

No increasing or decreasing trend between the mean and difference was observed in the Bland-Altman plots, and the data points were uniformly scattered around the horizontal axis (Figure 5-1 to 5-8). Together, this suggests there was no relationship in the mean and difference in the hip joint center and femoral head center position across the different movements or between different marker clusters.

The mean difference was largest for the distal-lateral cluster (-3.26 to -4.93 cm) and smallest for the mid-anterior cluster (0.03 to -1.00 cm) across all movements; however, the order of the other four marker clusters varied somewhat across movements (Figure 3-5; Table 5-3). The anterolateral and anterior clusters had a smaller mean difference than the mid-lateral cluster for all movements except DK-S (Figure 3-5; Table 5-3). The mid-

anterolateral cluster had a smaller mean difference than the distal-anterolateral cluster for all movements except FS, and the distal-anterior cluster for all movements (Figure 3-5; Table 5-3). The distal-anterior and distal-anterolateral cluster performed very similarly; however, the distal-anterolateral cluster typically demonstrated a smaller mean difference than the distal-anterior, and in cases where this was not true, the mean difference between the clusters was within 0.15 cm (Figure 3-5; Table 5-3).

Across the movements, the mid-lateral cluster had the narrowest limits of agreement (Figure 3-5; Table 5-3), with a peak lower and upper limit of -7.25 and 1.21 cm, respectively (Figure 3-5; Table 5-3). The distal-lateral cluster had the widest limits of agreement (peak lower = 11.86 cm; peak upper = 2.38 cm) in all movements except FS and DK-L (Figure 3-5; Table 5-3), where the distal-anterior had wider limits of agreement (peak lower = -8.92 cm; peak upper = 5.08 cm) (Figure 3-5; Table 5-3). The limits of agreement for the mid-anterior, mid-anterolateral, and distal-anterolateral clusters were similar across all movements (Figure 3-5; Table 5-3).

Although marker clusters with a smaller mean difference did not necessarily have narrower limits of agreement, the mean difference and limits of agreement were consistent between the high knee flexion tasks (Figure 3-5 and 3-6; Table 5-3). The mean difference was generally larger in the kneels than the squats. Additionally, the limits of agreements tended to be narrowest in the symmetrical kneels and widest in the asymmetrical kneels (Figure 3-5; Table 5-3).

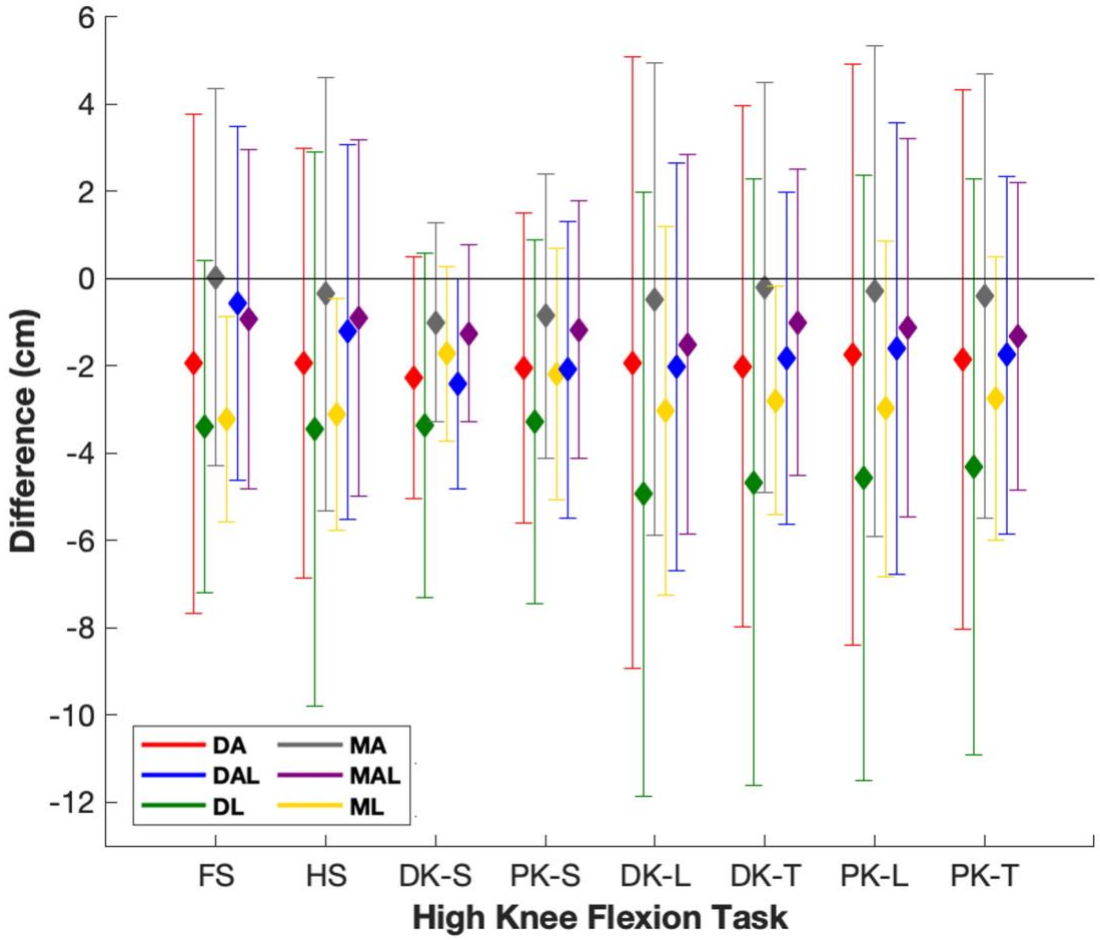

Figure 3-5: Summary of Bland-Altman mean of the peak difference (bias) and limits of agreement for each marker cluster [distal-anterior (DA), distal-anterolateral (DAL), distal-lateral (DL), mid-anterior (MA), mid-anterolateral (MAL), and mid-lateral (ML)] in each task. The solid black line indicates perfect agreement, the diamond markers are the mean difference, and the error bars are the upper and lower limits of agreement.

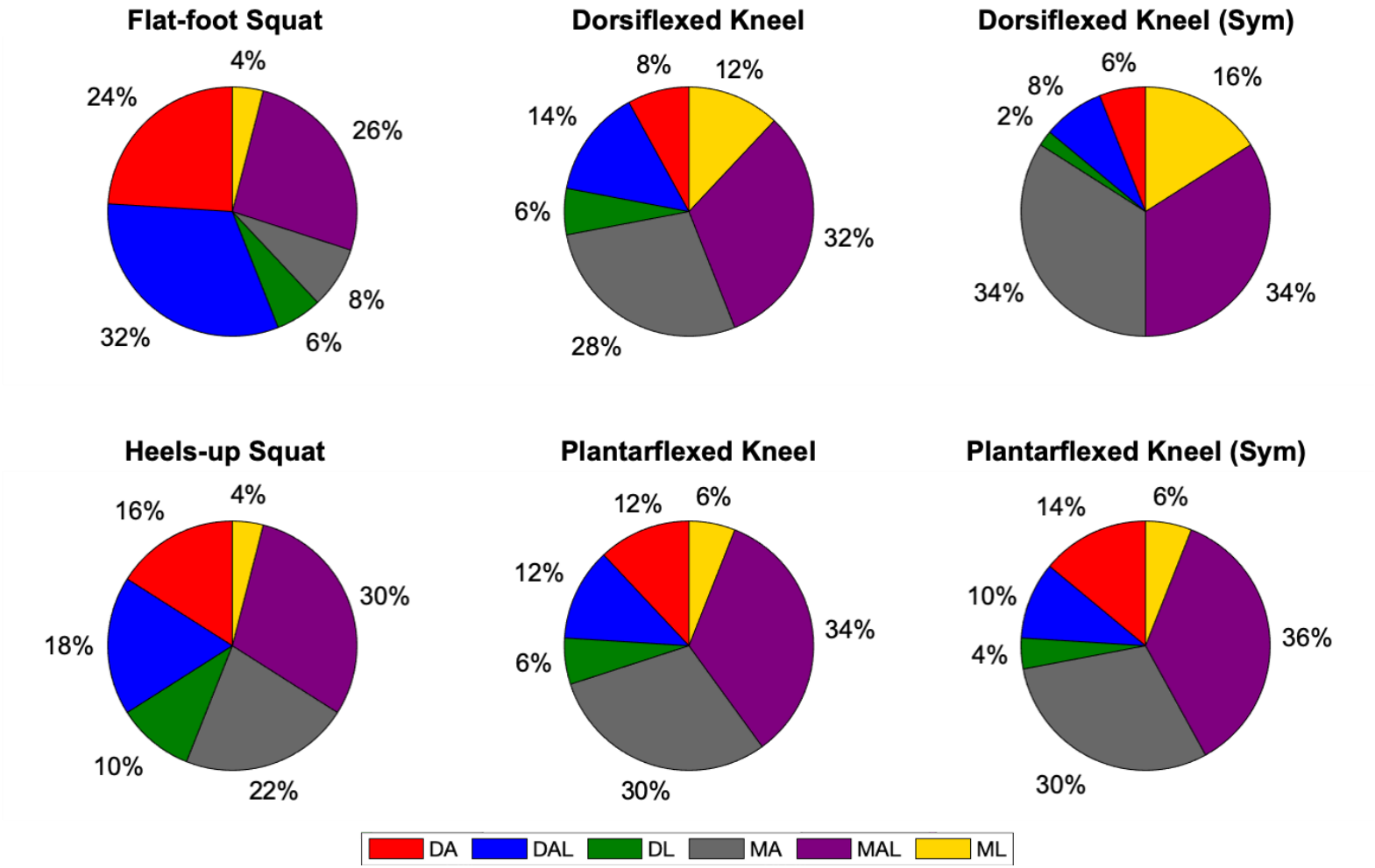

Figure 3-6: Distribution of sample in which specific marker placement demonstrated the smallest mean difference in the 3D position of the hip joint center and femoral head center for each task. The mean difference from both the lead and trail leg was utilized for the asymmetrical dorsiflexed and plantarflexed kneel.

Across the high knee flexion tasks, the mean difference tended to increase with knee flexion angle where soft tissue artifact peaked at the end of the descent phase and beginning of ascent phase, during moderate to high knee flexion (Figure 3-7 to 3-9). Although the pattern of soft tissue artifact was not identical between marker clusters throughout a movement, similar trends were found. For the squats, soft tissue artifact plateaued or decreased at approximately 100° and 120° for FS and HS, respectively (Figure 3-7). Similarly, in PK-S, soft tissue artifact plateaued at approximately 140° knee flexion; however, in DK-S, soft tissue artifact linearly increased with knee flexion (Figure 3-7). During the asymmetrical kneels, as the flexion angle increased beyond 120°, soft tissue artifact varied between the lead and trail legs. In the lead leg, soft tissue artifact abruptly decreased when transitioning between the lunge and kneel (Figure 3-8 and 3-9), wherein the individual must circumduct their leg and tuck it under their body. Soft tissue artifact for the lead leg then increased as the subject reached maximal flexion (Figure 3-8 and 3-9). Conversely, for the trial leg, soft tissue artifact tended to increase with knee flexion, with a small decrease occurring in some marker clusters when transitioning between the lunge and kneel (Figure 3-8 and 3-9).

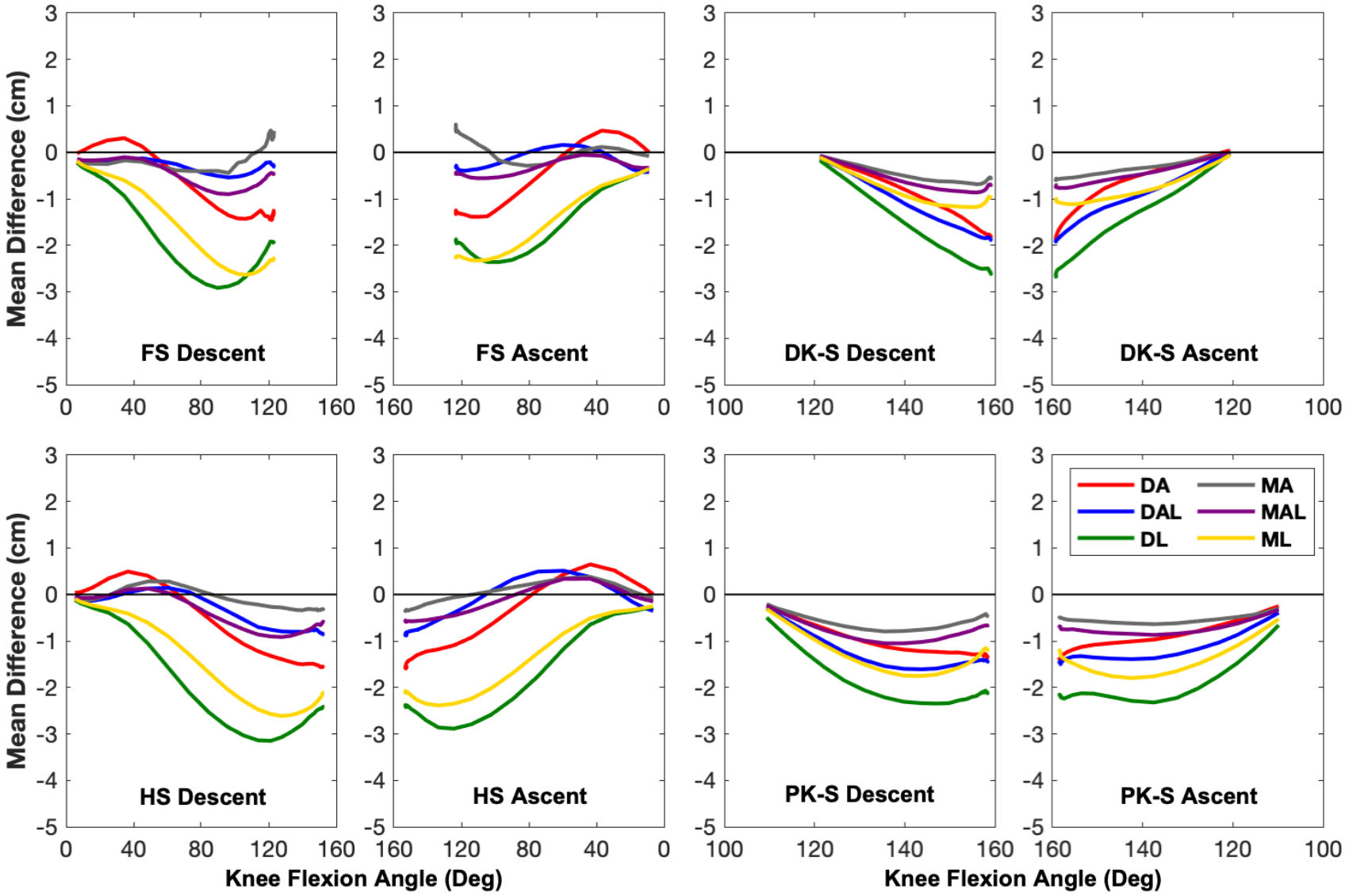

Figure 3-7: Mean difference in hip joint center and femoral head center 3D position versus mean knee flexion angle for the flat-foot (FS), heels-up squat (HS), and symmetrical dorsiflexed (DK-S) and plantarflexed kneel (PK-S) .

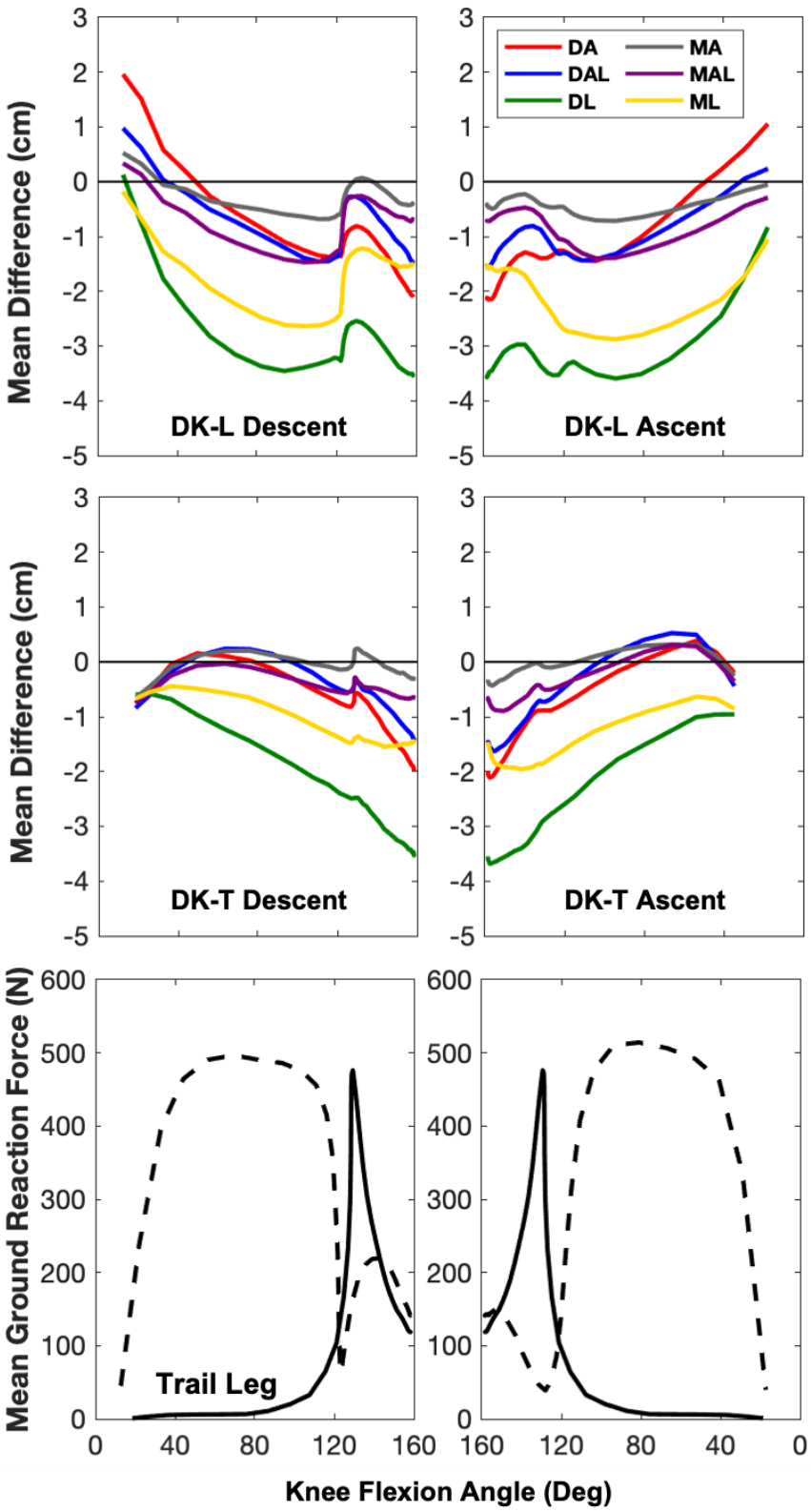

Figure 3-8: Mean difference in hip joint center and femoral head center 3D position versus mean knee flexion angle and mean vertical ground reaction force for the dorsiflexed kneel lead (DK-L) and trail (DK-T) leg.

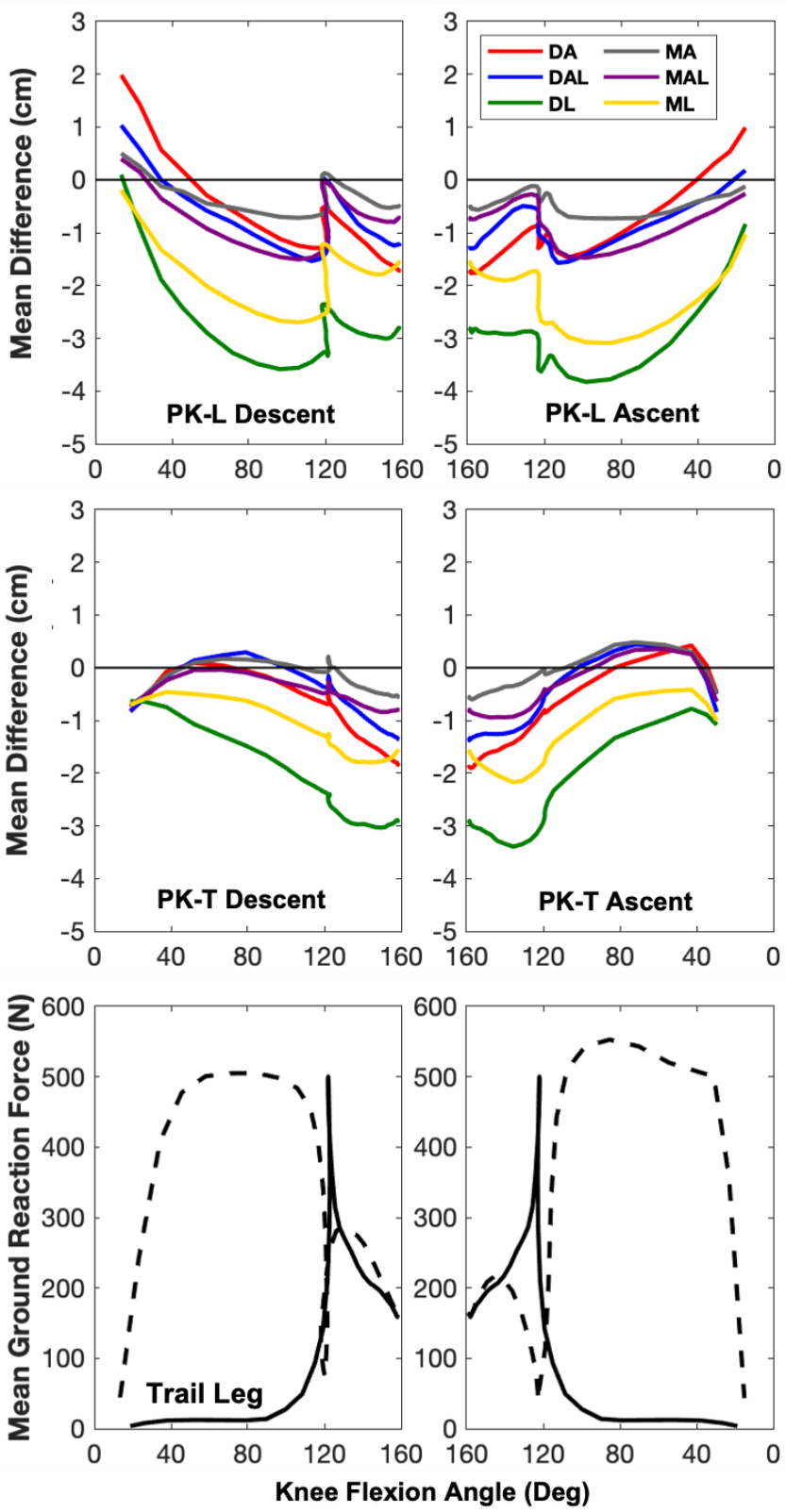

Figure 3-9: Mean difference in hip joint center and femoral head center 3D position versus mean knee flexion angle and mean vertical ground reaction force for the plantarflexed kneel lead (PK-L) and trail (PK-T) leg.

3.3.2 Soft tissue artifact subject specificity

Subject 15 was identified as an outlier and removed from analysis for the distal-anterior cluster in all movements and the mid-anterior cluster in DK. Eighteen multiple linear regression models were computed, of which ten reached statistical significance ($p < 0.05$) and did not violate the assumption of collinearity (Table 3-2). Of these ten regression models, five demonstrated a moderate fit and five demonstrated a low fit, as concluded by the R values (Table 3-2). Regression models significantly predicted soft tissue artifact for the distal-anterolateral and mid-lateral cluster in all high knee flexion tasks, the mid-anterior cluster in HS and PK, the mid-anterolateral cluster in HS only, and the distal-anterior cluster in DK only (Table 3-2, Figure 3-10 to 3-13).

For the distal-anterolateral cluster in HS and PK, distal thigh circumference explained 14% of the sample soft tissue artifact variation, while the addition of sex and thigh skinfold thickness in the DK regression model increased R_2 to 22% (Table 3-3). For the mid-lateral cluster, the models explained 16 to 26% of the sample soft tissue artifact variation, wherein only mass was included for DK and PK, while only BMI was included for HS (Table 3-3). In both HS and PK, regression models for the mid-anterior cluster explained 35 and 40% of sample variability, respectively, with the inclusion of sex, height, thigh length, and proximal and middle thigh circumference (Table 3-3). For the mid-anterolateral cluster in HS, which included mass and waist circumference, the model explained 25% of the sample variability (Table 3-3). For the distal-anterior cluster in DK, mass, height, and thigh distal circumference were included in the regression model accounting for 25% of sample variability (Table 3-3).

Unstandardized beta coefficients and partial correlations for the retained independent variables in each regression model which significantly predicted soft tissue artifact are presented in Table 3-4. For the partial correlations, 3 were classified as weak, 17 were classified as low, and 2 were classified as moderate (Table 3-4).

Table 3-2: Correlation coefficient (*R*) and coefficient of determination (R^2) for each linear regression across the six thigh marker clusters for the heels-up squat (HS) and dorsiflexed kneel (DK). Values that are bolded reached statistical significance ($p < 0.05$) and did not violate the assumption of collinearity.

Task	Distal-Anterior		Distal-Anterolateral		Distal-Lateral		Mid-Anterior		Mid-Anterolateral		Mid-Lateral	
	R	***R²***	***R***	***R²***	***R***	***R²***	***R***	***R²***	***R***	***R²***	***R***	***R²***
Heels-up Squat	0.31	0.09	**0.37**	**0.14**	0.34	0.12	**0.63**	**0.40**	**0.50**	**0.25**	**0.51**	**0.26**
Dorsiflexed Kneel	**0.50**	**0.25**	**0.47**	**0.22**	0.49	0.24	0.49	0.24	-	-	**0.41**	**0.16**
Plantarflexed Kneel	0.35	0.13	**0.38**	**0.14**	0.38	0.14	**0.59**	**0.35**	0.29	0.08	**0.46**	**0.22**

Table 3-3: Summary of regression models which reached statistical significance ($p < 0.05$) including *R*, R^2, intercept and unstandardized beta coefficients.

Independent Variables	Heels-up Squat				Dorsiflexed Kneel			Plantarflexed Kneel		
	DAL	MA	MAL	ML	DA	DAL	ML	DAL	MA	ML
R	0.37	0.63	0.50	0.51	0.50	0.47	0.41	0.38	0.59	0.46
R2	0.14	0.40	0.25	0.26	0.25	0.22	0.16	0.14	0.35	0.22
Intercept	-1.67	-4.87	-4.37	-2.33	-12.55	-0.76	-0.50	-1.16	-8.01	-0.54
Sex	-	-1.39	-	-	-	-0.89	-	-	-1.14	-
Height	-	8.58	-	-	6.55	-	-	-	11.30	-
Mass	-	-	-0.08	-	-0.07	-	0.05	-	-	0.05
BMI	-	-	-	0.23	-	-	-	-	-	-
Waist Circ	-	-	15.23	-	-	-	-	-	-	-
Thigh Length	-	-19.47	-	-	-	-	-	-	-0.23	-
Thigh Prx Circ	-	-12.18	-	-	-	-	-	-	-0.12	-
Thigh Mid Circ	-	16.67	-	-	-	-	-	-	0.16	-
Thigh Dst Circ	9.08	-	-	-	0.23	11.33	-	0.09	-	-
Thigh Skinfold	-	-	-	-	-	-0.05	-		-	-

Table 3-4: Standardized beta coefficients and partial correlations (italicized in brackets) for independent variables retained in each of the regression models that reached statistical significance ($p < 0.05$).

Independent Variables	Heels-up Squat				Dorsiflexed Kneel			Plantarflexed Kneel		
	DAL	MA	MAL	ML	DA	DAL	ML	DAL	MA	ML
Sex	-	-0.60 *(-0.46)*	-	-	-	-0.34 *(-0.27)*	-	-	-0.42 *(-0.32)*	-
Height	-	0.77 *(0.40)*	-	-	0.46 *(0.29)*	-	-	-	0.84 *(0.42)*	-
Mass	-	-	-0.86 *(-0.41)*	-	-0.64 *(-0.33)*	-	0.41 *(0.41)*	-	-	0.46 *(0.46)*
BMI	-	-	-	0.51 *(0.51)*	-	-	-	-	-	-
Waist Circ	-	-	1.07 *(0.49)*	-	-	-	-	-	-	-
Thigh Length	-	-0.48 *(-0.33)*	-	-	-	-	-	-	-0.48 *(-0.32)*	-
Thigh Prx Circ	-	0.65 *(-0.54)*	-	-	-	-	-	-	-0.55 *(-0.45)*	-
Thigh Mid Circ	-	0.60 *(0.42)*	-	-	-	-	-	-	0.52 *(0.42)*	-
Thigh Dst Circ	0.37 *(0.37)*	-	-	-	0.68 *(0.49)*	0.49 *(0.46)*	-	0.38 *(0.38)*	-	-
Thigh Skinfold	-	-	-	-	-	-0.36 *(-0.29)*	-	-	-	-

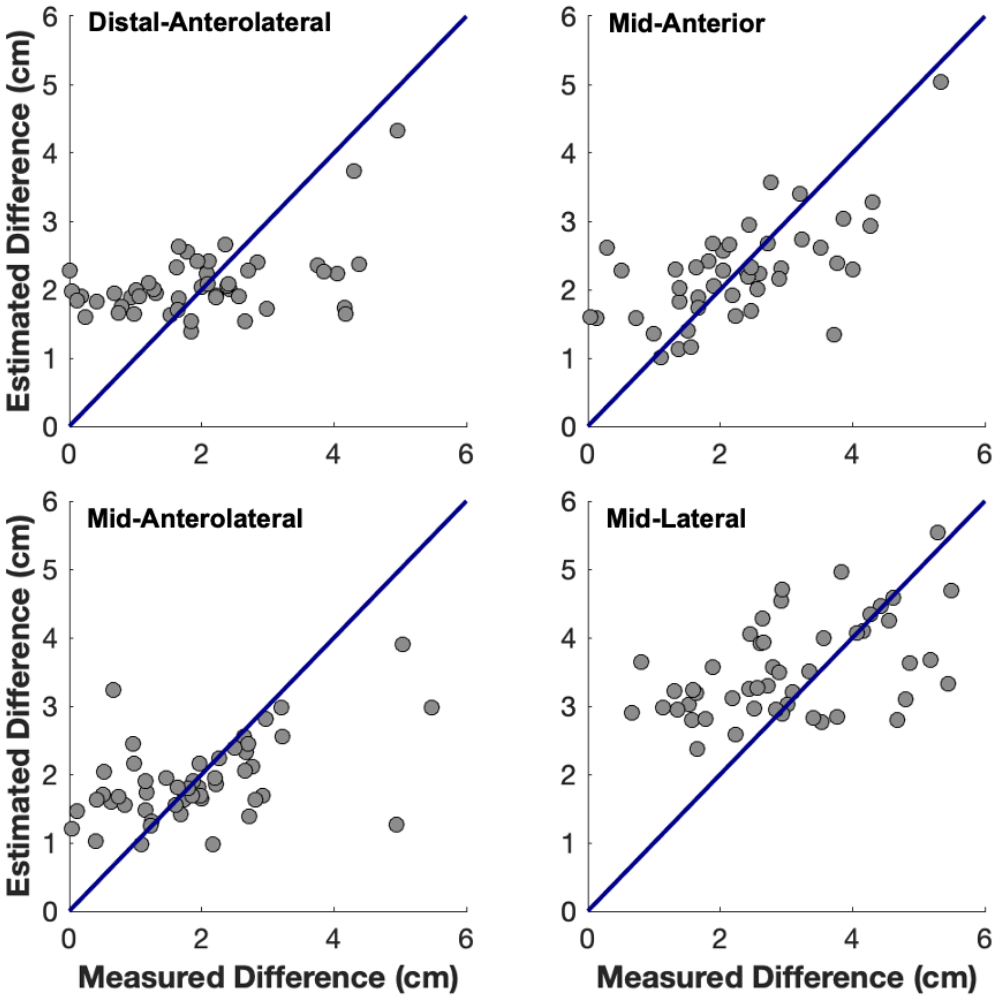

Figure 3-10: Comparison of measured and estimated difference in 3D position (cm) of hip joint center and femoral head center for heels-up squat (HS) regression models which reached statistical significance. Dark blue line indicates perfect agreement.

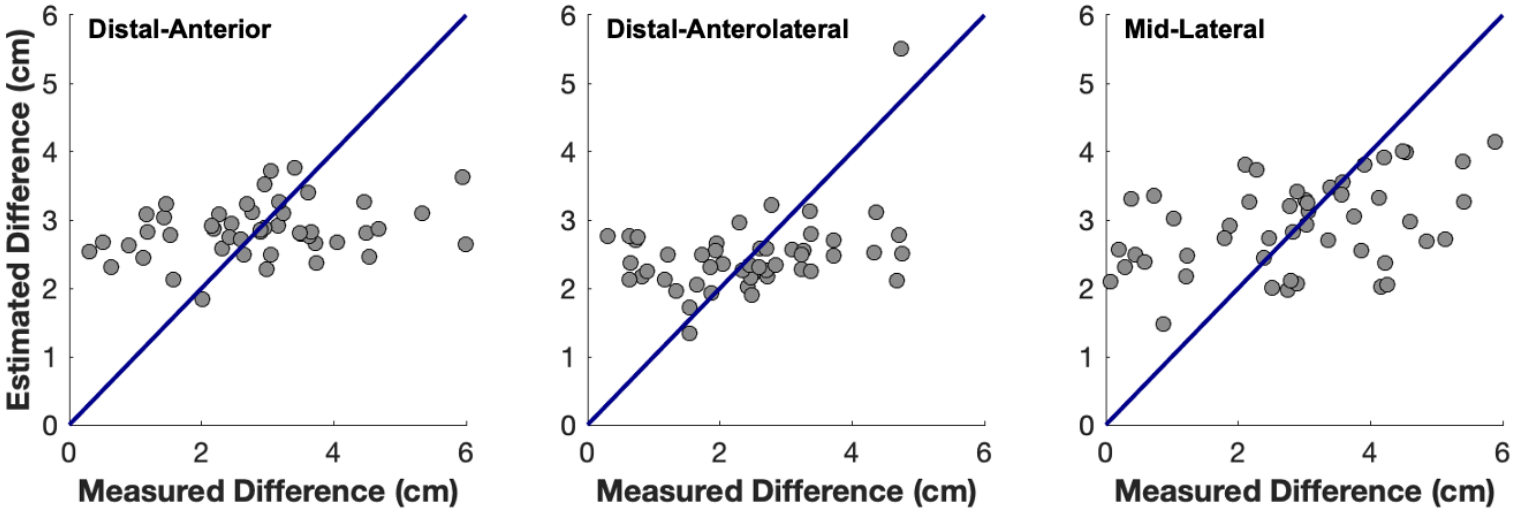

Figure 3-11: Comparison of measured and estimated difference in 3D position (cm) of hip joint center and femoral head center for the dorsiflexed kneel (DK) regression models which reached statistical significance. The dark blue line indicates perfect agreement.

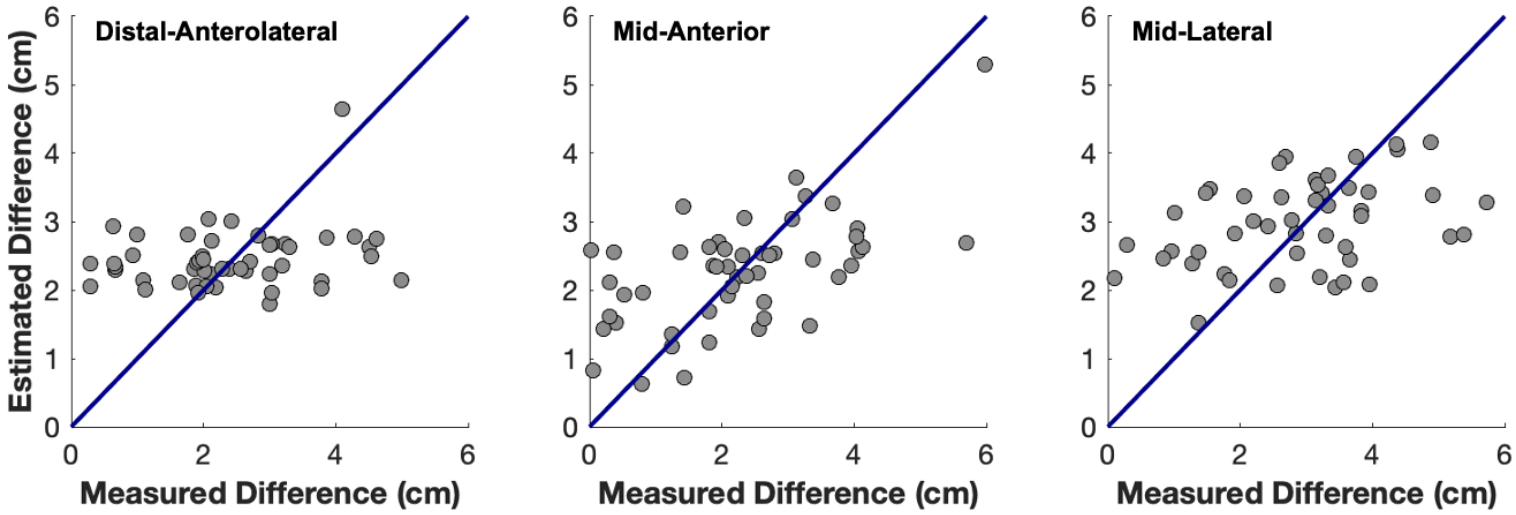

Figure 3-12: Comparison of measured and estimated difference in 3D position (cm) of hip joint center and femoral head center for the plantarflexed kneel (PK) regression models which reached statistical significance. The dark blue line indicates perfect agreement.

3.4 Discussion

3.4.1 Agreement between hip joint center and femoral head center

The agreement in the position of the hip joint center, tracked with the pelvis cluster, and the femoral head center, tracked with each of the six thigh clusters, was utilized to non-invasively describe soft tissue artifact on the thigh in high knee flexion. The mean difference, or bias, and limits of agreement demonstrated that some of the locations investigated were more optimal than others for placing marker clusters on the thigh when examining high knee flexion.

Few studies have investigated soft tissue artifact during high knee flexion activities, however deformation of the thigh during tasks which require up to approximately 100º knee flexion and during seated activities, where deformation occurs due to force application on the posterior aspect of the thigh, have been investigated. In a step-up and sit-to-stand task, peak thigh marker displacement has been recorded as high as 4.65 cm (Akbarshahi et al., 2010; Stagni et al., 2005; Tsai et al., 2011) and 7.22 cm (Kuo et al., 2011; Stagni et al., 2005), respectively. One study which measured the displacement of a marker on the lateral femoral epicondyle and found that at 120° of active knee flexion, the marker displaced posteriorly up to 4.00 cm and proximally up to 1.50 cm (Cappozzo et al., 1996). The magnitude of soft tissue artifact observed in the previous investigations is comparable to the results of the current study, particularly the mean difference, suggesting that the non-invasive method proposed is reliable. That being said, the real value of this method was its ability to make comparisons between locations on the thigh, ultimately facilitating the evaluation of different marker clusters.

Although previous studies have found that soft tissue artifact tends to be larger for the proximal thigh (Barré et al., 2013; Stagni et al., 2005), the results of the current study suggest that the clusters on the middle thigh were less vulnerable to soft tissue artifact than those on the distal thigh. This trend occurred for all movements and clusters except for the anterolateral clusters in FS, wherein the distal-anterolateral cluster had a 0.36 cm smaller mean difference than the mid-anterolateral cluster. This trend persisted when examining the limits of agreement, with the exception of the anterior clusters in HS, where the magnitude of the 95% limit was 0.05 cm greater for the distal-anterior cluster, however this is equal to sensitivity of the motion capture system. Clusters localized to the distal thigh may be more susceptible to soft tissue artifact as they are closer to the knee joint and thus may experience greater skin sliding (Sati et al., 1996) or due to muscular contractions of vastus lateralis and medialis (Cereatti et al., 2017). Additionally, the current study used rigid marker clusters attached to the segment with straps, while previous studies typically investigated individual markers adhered to segment with tape (Akbarshahi et al., 2010; Barré et al., 2013; Stagni et al., 2005). The heavier rigid marker cluster attached to the segment with straps may have attenuated soft tissue artifact resulting from oscillation of markers and/or segments (Angeloni et al., 1992; Manal et al., 2000), which presumably would have been larger on the proximal thigh as there is greater volume of soft tissue (Table 3-1).

Since the high knee flexion movements investigated did not require rapid changes in acceleration or large impacts, it is likely that the estimated soft tissue artifact was due to changes in thigh segment orientation and range of motion of adjacent joints (Bonci et al., 2014). In the symmetrical squats and kneels, soft tissue artifact tended to increase to a peak

as subjects reached maximal flexion (Figure 3-7). For the asymmetrical kneels, soft tissue artifact abruptly decreased for most marker clusters, particularly in the lead leg, as the subject transitioned from the lunge to the kneel, then tended to increase as greater knee flexion was obtained (Figure 3-8 and 3-9). Interestingly, transitioning from the lunge to the kneel requires circumduction of the lead leg, similar to the functional hip joint center trial, which may have resulted in the observed decrease in soft tissue artifact as this artifact would be included in the initial estimation of the functional hip joint center. In squatting and kneeling, onset of thigh-calf contact occurs at approximately 120 to 125°, then contact area progressively increases with knee flexion, proximally along the thigh (Kingston & Acker, 2018); thereby resulting in significant topographic deformation of the posterior and medial and lateral thigh. Although the onset of thigh-calf contact was not quantified in the present study, the results of the mean difference versus knee flexion angle suggest that some change in soft tissue artifact occurs at the approximate knee flexion angle that thigh-calf contact would occur (Figure 3-7 to 3-9). Of the marker clusters tested, thigh-calf contact would likely have the largest effect on the lateral clusters; and therefore, could partially explain the larger mean difference observed for more laterally placed clusters. For clusters on the mid-thigh, the mid-lateral cluster had the largest mean difference, followed by the mid-anterolateral, then mid-anterior, across all movements. Alternatively, for the distal-thigh clusters, the mean difference was always largest for the distal-lateral cluster while the distal-anterior and distal-anterolateral cluster performed similarly. These results are similar to previous studies which utilized a marker array to quantify soft tissue artifact of the thigh and found that soft tissue artifact was generally lowest on the anterior thigh during knee flexion-extension, and step-up and sit-to-stand tasks (Stagni et al., 2005).

The Bland-Altman analysis was initially designed to evaluate the agreement between two methods (Bland & Altman, 1986); however, the current study proposes performing multiple Bland-Altman analyses simultaneously, and subsequently comparing the results. The bias provides information on the systematic difference between the position of hip joint center and femoral head center; thereby providing insight into the accuracy of the marker cluster across the sample. The limits of agreement, which are calculated using the standard deviation of the differences and define the upper and lower limits in which 95% of the differences are expected to fall (Bland & Altman, 1986), afford conclusions on the consistency of the marker cluster across the sample. With this method, it is important to reflect on both the bias and limits of agreement when evaluating the accuracy and reliability of each of the marker clusters. For example, the relative order of the bias and limits of agreement for the marker clusters, particularly for those on the middle thigh, were not the same. The mid-lateral cluster demonstrated the highest agreement, followed by the mid-anterolateral, then mid-anterior cluster, opposite to the order of the mean differences. However, for the mid-lateral cluster, the line of equality (i.e. difference of 0 indicating perfect agreement) fell outside the limits for FS, HS, and DK-T, indicating that in high knee flexion there would be zero soft tissue artifact (i.e. no difference in the hip joint center and femoral head center) in only 5% of cases. Therefore, in attempting to narrow down what marker clusters might be best for high flexion by comparing results of the Bland-Altman analysis, it is believed that both the mean difference and limits of agreement should be considered sequentially.

One must also consider results of the Bland-Altman analysis within the context of a clinically meaningful value. In this case, at what distance would the difference between the

hip joint center and femoral head center be considered unacceptable? Studies which simulate error in anatomical landmarks during calibration then calculate subsequent kinematic and kinetic outcomes are useful for determining this threshold. One study which simulated mislocation of the hip joint center along X, Y, or Z found that 3.00 cm significantly affected angles and moments for the hip, and marginally affected angles and moments for the knee (Stagni et al., 2000). Using 3.00 cm as a threshold for the mean difference, reveals that the anterior and anterolateral marker clusters would be appropriate for all high flexion movements studied, the mid-lateral cluster would be appropriate for investigations of kneeling but not squatting, and the distal-lateral would not be appropriate for use in high knee flexion. That being said, the aforementioned study was completed for gait which requires much smaller changes in hip and knee range of motion than the high knee flexion movements examined herein, and the study did not consider simultaneous error that could occur in other anatomical landmarks used to construct the anatomical coordinate systems (e.g. knee joint center, femoral condyles). In the current study, since rigid marker clusters were utilized, it can be assumed that error in the position of the hip joint center would also be present, in part, at other anatomical landmarks on the thigh. Although it is unlikely that the error at other anatomical landmarks would be identical to that of the hip joint center, some soft tissue artifact is likely still present. Mislocation of the femoral condyles by 1.50 cm during sit-to-stand and step-up tasks, resulted in RMS errors of 6.8°, 5.4°, and 6.0° of knee flexion-extension, abduction-adduction, and internal-external rotation (Stagni et al., 2006). Similarly, an investigation of inter-examiner calibration of anatomical landmarks revealed that mean differences of up to 1.92 cm in the calibration of the femoral condyles and the hip joint center, can lead to differences in thigh

angles of 3.0°, 2.5°, and 5.1° about Z, X, and Y, respectively (Della Croce et al., 1999). A 1.50 cm threshold for the mean difference, would leave only the mid-anterior and mid-anterolateral cluster appropriate for analyzing high knee flexion movements, as well as the distal-anterolateral cluster in squatting.

Unfortunately, while the mean differences may yield the mid-anterior and mid-anterolateral cluster appropriate for both kneeling and squatting tasks, the magnitude of the limits of agreement exceeded the proposed thresholds. However, it is important to note that current study performed a 'worst case' Bland-Altman analysis by utilizing the mean of the peak difference in the hip joint center and femoral head center across the trials, and by simultaneously evaluating the total error in X, Y, and Z. When acknowledging only the mean difference, the mid-anterior and mid-anterolateral thigh were the most appropriate locations to evaluate kinematics in high knee flexion. Between these two marker clusters, the mid-anterolateral cluster tended to have narrower limits of agreement (Figure 5-1 to 5-8) and a smaller mean of peak difference for the majority of subjects across the tasks (Figure 5-9). Additionally, the mid-anterior cluster was more vulnerable to marker obstruction by the trunk and/or upper limbs as indicated by the smaller sample size in FS and HS. Thus, an anterolateral cluster placement, at the mid-thigh level if sufficiently visible, would be optimal for investigations which evaluate high knee flexion.

3.4.2 Soft tissue artifact subject specificity

The current study assessed the accuracy in which local and global subject anthropometry could predict soft tissue artifact using multiple linear regression. It was hypothesized that there would be a moderate fit between predicted soft tissue artifact and subject anthropometrics. This was partially supported as, of the eighteen (six per activity)

regression models performed, five demonstrated a moderate fit and five demonstrated a low fit. These results not only support previous findings that soft tissue artifact is subject specific, but also suggest that there is some interaction between subject, location, and task specificity.

Of the ten significant regression models, global and local (i.e. thigh) measures of anthropometry were included in regression models with the same frequency; where mass and distal thigh circumference were most commonly retained. Additionally, four of the regression models only retained measures of global anthropometry, two models only retained measures of local anthropometry, and four models retained measures of both global and local anthropometry. For models which included both global and local measures of anthropometry, standardized beta coefficients and partial correlation coefficients, which provide insight into the strength of the effect that an independent variable has on the dependent variable, were similar between anthropometric measures. Together, these results lead us to reject the hypothesis that local measures of the thigh anthropometry would have a stronger effect on soft tissue artifact than global measures of subject anthropometry. Evidently, it appears that local and global measures of anthropometry similarly influence soft tissue artifact on the thigh; however, the effect of any anthropometric measure was not particularly strong given the low fit and variance explained by the partial correlations and regression models.

Although it would seem reasonable that individuals with a greater volume of soft tissue would exhibit greater soft tissue artifact, the relationship between anthropometry and soft tissue artifact appears to be more complex. Previous studies which observed less soft tissue artifact in individuals with a larger BMI (Barré et al., 2013; Clément et al., 2018),

hypothesized that greater volume of adipose tissue may act to dampen the effect of muscular contractions, thereby reducing overall soft tissue artifact (Clément et al., 2018). Findings of the current study support the hypothesis that the composition or type of soft tissue (i.e. adipose versus muscle) modifies soft tissue artifact, particularly when examining the unstandardized beta coefficients and partial correlations for the measures of thigh skinfold thickness, thigh circumference, and sex. For thigh skinfold thickness, the negative coefficients indicate that greater subcutaneous adiposity was associated with decreased soft tissue artifact. Negative coefficients were also observed for the proximal thigh circumference, which typically holds greater adipose tissue, while positive coefficients were observed for both the middle and distal thigh circumference. Furthermore, negative coefficients were observed for sex, which indicated that being female was associated with a decrease in soft tissue artifact. Of note, females had greater proximal thigh circumferences and thigh skinfold thickness (i.e. greater adipose tissue), but smaller middle and distal thigh circumferences than males (Table 3-1). These results indicate that adipose tissue, which oscillates or wobbles during motion, may contribute less to total soft tissue artifact, and in some cases reduce artifact, while movement of soft tissue from muscular contractions may increase soft tissue artifact. This is similar to the results of Bonci et al. (2014) who found soft tissue oscillation of the thigh contributed less than approximately 11% to total soft tissue artifact, while 89% of soft tissue movement was explained by changes in the position of the hip and knee, when attempting to model artifact of a running task.

Alternatively, positive unstandardized beta coefficients and partial correlations, were observed for global measures of soft tissue, including height, BMI, waist

circumference, and mass for the mid-lateral cluster in DK and PK. As well, the negative coefficient for sex also supports these findings, wherein females tended to have smaller values for height, mass, BMI, and waist circumference (Table 3-1). While global measures of anthropometry may provide insight into total soft tissue volume, thereby indicating that an increase in total soft tissue volume may increase soft tissue artifact, these values poorly summarize soft tissue composition and distribution. Providing support to the complexity of global measures in describing local soft tissue artifact, mass was positively associated with soft tissue artifact for the mid-lateral cluster in DK and PK, but negatively associated with soft tissue artifact for the distal-anterior cluster in DK and the mid-anterolateral cluster in HS. Although the standardized beta coefficients and partial correlations indicate that local and global measures of anthropometry may be similarly correlated with soft tissue artifact, local measures likely provide greater insight into the relationship between soft tissue composition and distribution and soft tissue artifact and should therefore be preferentially considered when evaluating soft tissue artifact subject specificity.

Although there were similarities in the anthropometric variables that were retained for the same marker cluster between different high knee flexion movements (e.g. same five independent variables were retained for the mid-anterior cluster in HS and PK), inclusion varied considerably between the different marker clusters. These findings suggest that some marker clusters may be more vulnerable to the volume, composition, and/or distribution of soft tissue present. For example, soft tissue artifact for the distal-anterolateral cluster was significantly correlated with distal thigh circumference in all tasks, suggesting that soft tissue volume and/or composition modifies soft tissue artifact of the distal-anterolateral thigh. Additionally, soft tissue artifact for the mid-anterior cluster

was significantly correlated with sex which may suggest that soft tissue artifact of the mid-anterior thigh is influenced by factors beyond anthropometric variability. However, given the low to moderate fit (R = 0.37 to 0.63) and percentage of variation explained (14 to 40%) by any given regression model, it is likely that other factors such as movement patterns during task completion, muscle recruitment patterns, and joint range of motion also play a role in the magnitude and pattern of soft tissue artifact.

When first performing these regression models, it seemed reasonable that the results could not only provide insight into why soft tissue artifact varied between individuals but could also inform marker cluster placement. For example, anthropometric measures taken at the start of a data collection could be input into the regression models to predict optimal marker cluster placement (i.e. the marker clusters which predicted the smallest differences the position of hip joint center and femoral head center should be implemented in the subsequent collection). However, the results of the current study, specifically the lack of significant regression models for all clusters and poor model fit for models that did reach statistical significance, call into question adjusting marker placement on a subject-by-subject basis, when only anthropometry is considered. Furthermore, these results suggest that soft tissue artifact is not only extremely subject specific, but this subject specificity extends beyond simply anthropometric variability and interacts with marker location and the task examined.

Despite substantial variability in the regression models, for studies which investigate a specific population (e.g. overweight or obese) it may be possible that the results regression models can be used to inform optimal cluster placement. For example, selection of the distal-anterior cluster in HS, and the mid-anterolateral cluster in DK and

PK may be optimal as the regression results for these marker clusters indicated that they were least affected by subject anthropometry (i.e. lowest *R* regardless of significance in Table 3-2). However, predictive ability of the regression models on a new data set and investigation into different sample populations is warranted prior to implementing these population-specific marker configurations, as only young and healthy university aged subjects were evaluated herein. Additionally, the use of multiple linear regression assumed that there was a linear relationship between an anthropometric variable and soft tissue artifact. While linear correlations between anthropometric measures and soft tissue artifact have been tested previously, the relationship may in fact be more complex, and thus, investigation into different relationships may improve model fit.

3.5 Limitations

A number of methodological limitations for the current study are acknowledged. First, the method of quantifying soft tissue artifact was built on the assumption that pelvis soft tissue artifact was minimal. Although it is recognized that soft tissue artifact of the pelvis and specifically of the hip joint center occurs, Fiorentino et al. (2016) found that in six tasks which required rotation of the hip about all axes of rotation, the hip joint center remained within the pelvis acetabulum during motion, with an RMS error of 2.8 ± 0.7 mm. These results imply that the hip joint center is relatively robust to soft tissue artifact. As well, this magnitude of error in hip joint center location would likely minimally affect the results of the current study, given that the magnitude of soft tissue artifact estimated in the current study is greater than 0.028 cm.

Second, the effect of marker cluster distance from the hip joint center must be acknowledged as a potential confounder in the results, where marker clusters that are in

closer proximity to the hip joint center would theoretically have the highest agreement (i.e. marker clusters on the mid-thigh exhibit a lower mean difference and narrower limits of agreement than clusters on the distal-thigh). Although this trend was apparent in the data, we do not believe the differences between the marker clusters were solely the result of distance from the hip joint center as the magnitude of the mean difference between the marker clusters was quite similar (within centimetres). Additionally, the closest cluster to the hip joint center (the mid-lateral cluster) did not demonstrate the smallest mean difference across the marker clusters. Interestingly, when thigh length was retained in the regression models, for the mid-anterior cluster in HS and PK, the unstandardized beta coefficient and partial correlation coefficient were negative. This would indicate that for the mid-anterior cluster, marker clusters which would be further away from the hip joint center with a longer thigh, demonstrated less soft tissue artifact. Although this in no way eliminates questions of distance from the hip joint center on the method proposed, it does provide support that the results of the current study were not simply due to distance.

Additionally, although the Bland-Altman plots were completed for each direction, it is important to note that these were within the global (laboratory) coordinate system not the thigh local coordinate system. Therefore, conclusions cannot be made regarding how the directional change in the hip joint center position may affect thigh and knee angles. Future studies should consider how error in anatomical landmarks may propagate to error in meaningful kinematic and kinetic outcomes. Despite an abundance of research seeking to quantify and compensate for soft tissue artifact, few studies have defined thresholds for error in marker position that would be ‘accurate enough.’

Lastly, the relatively low anthropometric variability present in the sample population may have contributed to the low percentage of variation explained by the regression models. This limitation is further supported as subject 15, who was taller (1.84 cm) and had much lower thigh adiposity (skinfold thickness = 6.9 mm) than the sample population, was identified as an outlier and removed from the four regression models. Future work should consider increasing the anthropometric variability, both in terms of local and global measures, to increase the predictive ability of the regression models.

3.6 Conclusions

The overarching evidence that soft tissue artifact varies due to marker cluster location on the thigh, subject anthropometry, and high knee flexion tasks begs the question of: how should future data collections be conducted in attempt to reduce the complex effects of soft tissue artifact? Three evidence-based recommendations have emerged from the study findings. First, it is recommended that marker clusters be placed on the anterolateral aspect of the thigh when investigating high knee flexion. Additionally, the cluster should be placed towards the middle of the thigh, given that marker visibility is not disrupted. In cases where an anterolateral cluster placement is not feasible, a lateral placement should not be used. Second, the low to moderate model fit and percentage of variation explained from the regression models suggests that subject anthropometry alone cannot inform marker placement. Additionally, due to the consistent bias across the different marker clusters and high knee flexion tasks but a relatively wide limits of agreement, the lack of sufficient regression models for all marker clusters in multiple tasks, and inconsistency in retained anthropometric variables in the regression models, it is not recommended that thigh marker placement be adjusted on a subject-by-subject basis.

Lastly, it is recommended that researchers report marker cluster placement in published work to facilitate stronger comparisons between investigations. Although it is unlikely that motion capture data will enable quantification of intricate changes in joint position and orientation that can be observed with bone fixation or imaging techniques, standardization of data collections will enable more reliable and reproducible data to be obtained.

Chapter 4 - Sensitivity of Knee Joint Angles and Moments to Thigh Marker Cluster Location and Global Optimization

4.1 Introduction

Accurate and reliable kinematic and kinetic data is necessary for drawing biomechanical conclusions on task demands, understanding mechanisms of tissue damage and degeneration, and facilitating guidelines for injury and disease diagnosis, treatment, and rehabilitation. Unfortunately, multiple sources of error may impede the ability to obtain accurate data; where in optical motion capture collections, soft tissue artifact is often cited as one of the largest sources of error (Andriacchi & Alexander, 2000; Cappozzo, 1991). Soft tissue artifact refers to movement of muscle, adipose tissue, and skin relative to bone, thereby leading to inaccuracies in the position of skin markers (Leardini et al., 2005). When examining the lower limb, the thigh typically exhibits the largest error. Error in estimated knee joint angles has been recorded as high as 8.4° in gait (Reinschmidt, van den Bogert, Lundberg, et al., 1997), 15.8° in running (Li et al., 2012), and 7.3° in stair climbing (Li et al., 2012). Although error in kinetic outcomes have received less attention, knee joint moments, particularly flexion-extension moments, have been found to be underestimated during gait and stair climbing as a result of soft tissue artifact (Kuo et al., 2011; Tsai et al., 2011). Evidently, methods for attenuating soft tissue artifact are essential for improving kinematic and kinetic accuracy, as well as standardizing data collections and processing methods.

One method that has been proposed to reduce soft tissue artifact is adjusting the placement of marker clusters on a segment. Multiple studies have compared knee joint angles estimated from marker clusters formed from different individual markers adhered to the thigh (i.e. non-rigid marker clusters) and a constant shank cluster (Akbarshahi et al.,

2010; Barré et al., 2015; Cappozzo et al., 1996; Stagni et al., 2005). It was found that while some marker clusters perform more optimally than others, this largely depended on the task and axis of rotation analyzed (Akbarshahi et al., 2010; Barré et al., 2015; Cappozzo et al., 1996; Stagni et al., 2005). To date, no study has investigated how placement of rigid marker clusters – marker clusters formed from individual markers on a rigid object that is then adhered to the segment – affects estimated knee joint angles and moments, despite that rigid marker clusters are more commonly recommended in data collections (Angeloni et al., 1992; Cappozzo et al., 1995; Manal et al., 2000).

In addition to adjusting marker placement during data collections, data processing methods have been proposed which may contribute to attenuation of soft tissue artifact. One example is global optimization, in which constraints are applied on the degrees-of-freedom of adjacent segments to minimize the potential for unrealistic joint motion or dislocation (Lu & O'Connor, 1999). Global optimization has been investigated in the context of walking (Lu & O'Connor, 1999; Reinbolt et al., 2005), running (Bonnet et al., 2017; Gasparutto et al., 2015; Richard et al., 2017), hopping and cutting (Potvin et al., 2017; Richard et al., 2017), sit-to-stand and step-up (Richard et al., 2017; Stagni et al., 2009), squatting (Clément et al., 2015), and quasi-static knee flexion to 110° (Charbonnier et al., 2017). While global optimization has been successful in partially compensating for soft tissue artifact, the results are quite variable and, in some cases, the magnitude of error in position relative to the known position of bone is still quite large (Andersen et al., 2010; Charbonnier et al., 2017; Clément et al., 2015; Richard et al., 2017). However, global optimization can be advantageous because does not require additional steps during data collection and can be easily implemented in biomechanics software that has this capability.

Thus, global optimization presents a promising avenue for attenuating soft tissue artifact in a variety of tasks. Specifically, tasks which require large changes in joint range of motion require further investigations, as soft tissue artifact is known to increase with joint angle, thereby increasing the likelihood of unphysiological joint motion (Cappozzo et al., 1996; Fuller et al., 1997; Kuo et al., 2011; Tsai et al., 2011).

Although it is known that soft tissue artifact may be attenuated by data collection and processing techniques, studies typically evaluate these two pathways in isolation (i.e. the effectiveness of global optimization is presented for one marker cluster set). Since no marker set or compensation techniques has been effective in completely eliminating soft tissue artifact, and there are often varying results on their effectiveness in the literature, it seems reasonable that a combination of collection and processing techniques should be simultaneously evaluated.

The objective of the current study was to compare knee joint angles and moments in high knee flexion between thigh marker clusters localized to six different areas of the thighs with and without global optimization. Rigid marker clusters were placed on the middle and distal third of the thighs, and on the anterior, lateral, and anterolateral aspect of the thigh while subjects completed squatting and kneeling. Maximum and minimum knee joint angles and moments about each axis of rotation were assessed with and without global optimization which was implemented in Visual3D, using the inverse kinematics (IK) constraints model function to constrain motion of the ankle, knee, and hip (Lu & O'Connor, 1999). Three-way repeated measures ANOVAs were also performed to evaluate the effect of marker cluster location, global optimization condition, and high knee flexion task on peak knee joint angles and moments. Following the ANOVAs, effect sizes,

defined by the partial eta squared definition (η_p^2), were calculated for each global optimization condition and task to determine if global optimization decreased the effect of marker cluster location. Reliability between marker cluster estimated angles and moments was also assessed with intraclass correlation coefficients (ICCs). It was hypothesized that there would be a two-way interaction between marker cluster location and global optimization condition in which global optimization would attenuate differences between marker clusters, and thus there would be less differences between marker clusters when IK constraints were applied. Additionally, it was hypothesized that global optimization would result in a decrease in effect sizes and an increase in ICCs. If this occurred, this could be interpreted as global optimization partially compensating for soft tissue artifact on the thigh in high knee flexion, since it would indicate that global optimization reduced the effects of local soft tissue deformation between marker cluster locations.

4.2 Methods

4.2.1 Data collection

The data for this study was obtained from the experiment described in the previous chapter. Accordingly, specific details of the data collection can be found in section 3.2. For the present study, only the symmetrical high knee flexion movements were analyzed including HS, DK-S, and PK-S to facilitate stronger comparisons between marker clusters localized to opposite legs.

4.2.2 Data processing

Knee joint angles about all axes of rotation for each of the six thigh clusters were calculated using a Z-X-Y Cardan sequence (flexion(+)-extension, abduction(+)-adduction, external(+)-internal rotation) in Visual3D (C-Motion, Version 2.05, Germantown, MD,

USA) using the thigh anatomical coordinate system for each of the individual thigh clusters and the shank anatomical coordinate system from the single shank cluster. Anatomical coordinate systems definitions are detailed in Table 5-1 and 5-2.

External knee joint moments in all three planes of motion for each of the six thigh clusters were calculated using a bottom-up rigid link model from the measured ground reaction force. Knee joint moments were normalized to percent body weight multiplied by height (%BW*H) and expressed in the tibial coordinate system (Mündermann et al., 2004). Data were then truncated based on the pelvis marker vertical position decreasing 1 cm below mean height at the start and end of the trial, and visually examined to ensure consistent truncation.

A second set of knee joint angles and moments were calculated with the use of global optimization to restrict lower limb joint translation. This was accomplished by implementing the Visual3D IK constraints model function, whereby knee and hip translation were constrained. Restriction of ankle translation and rotation about X (inversion-eversion) and Y (internal-external rotation) were recommended following consultation with the software manufacturer to ensure physiological lower limb motion. This step was only necessary when utilizing the IK constrained model because the foot marker clusters were nearly collinear, to ensure visibility during PK. For the IK model, all segments were equally weighted at 1.00 to ensure consistent accuracy with the motion capture data. Additionally, the Levenberg-Marquardt optimization approach was selected for computational efficiency.

Flexion, abduction and external rotation were defined as positive, while extension, adduction, and internal rotation were defined as negative for both knee joint angles and

moments. The mean of maximal flexion, maximal and minimal abduction-adduction, and maximal and minimal external-internal rotation were calculated for each subject across the trials for a given tasks and input into the following statistical analyses.

4.2.3 Statistical analysis

All statistical procedures were completed in SPSS (IBM Corp., Version 26.0, Armonk, NY). Listwise elimination of missing data was used, in which subjects with an incomplete data set were excluded.

Three-way repeated measures ANOVAs were performed to evaluate the effect of marker cluster (six levels), global optimization condition (two levels), and task (three levels) on the mean of the peak knee joint angle and moment (ten dependent variables). Mauchly's test was used to evaluate sphericity, and when violated, a Greenhouse-Geisser corrected *p*-value was used to evaluate significance. Significance was determining using an alpha level of 0.05, and when the results of an ANOVA indicated significance, *post hoc* pairwise comparisons were evaluated with a Bonferroni correction.

The effect of marker cluster location for each task and global optimization condition was evaluated using η_p^2. This measure of effect size was interpreted using the following criteria: 0 to 0.05 is a small effect, 0.06 to 0.13 is a medium effect, and ≥ 0.14 is a large effect (Cohen, 2013) and compared within tasks between global optimization conditions.

ICC(2,1) were calculated using a two-way mixed effects model for absolute agreement. The single measure ICC was reported as only one marker cluster is used for measuring kinematics in actual application (Koo & Li, 2016). ICC reliability strength were defined with the following criteria: 0 to 0.5 is poor reliability, 0.5 and 0.75 is moderate

reliability, 0.75 to 0.9 is good reliability, and 0.9 to 1.0 is excellent reliability (Koo & Li, 2016).

4.3 Results

Knee joint angle and moment revealed similar time histories between marker clusters throughout completion of the high knee flexion tasks (Figure 5-9 to 5-14). The timing of the peaks were consistent between marker clusters with the exception of the abduction-adduction moment where some clusters measured an abduction moment while others simultaneously measured an adduction moment (Figure 5-13).

Three-Way ANOVAs

Due to listwise elimination of missing data, thirty-nine subjects were included in the knee joint angle analysis, and thirty-seven subjects were included in the knee joint moment analysis, described below. Subjects were excluded as a result of missing all trials due to marker cluster obstruction, instrumental error, poor placement of feet and/or knees on force plates, or difficulty implementing global optimization. The results of the three-way ANOVAs revealed significant three-way interactions (marker cluster × global optimization condition × task) for each peak angle and moment (Table 4-1).

Table 4-1: Three-way interaction *F* statistic, *p* value, and effect size for each three-way ANOVA.

Dependent Variable	*F* Statistic	*P* Value	Effect Size
Peak Angle			
Flexion	32.14	< 0.001	0.46
Abduction	15.45	< 0.001	0.29
Adduction	28.94	< 0.001	0.43
External Rotation	5.56	< 0.001	0.13
Internal Rotation	45.15	< 0.001	0.54
Peak Moment			
Flexion	8.36	< 0.001	0.19
Abduction	13.44	< 0.001	0.27
Adduction	9.09	< 0.001	0.42
External Rotation	6.75	< 0.001	0.16
Internal Rotation	5.70	< 0.001	0.14

Attenuation of differences between marker clusters with the use of global optimization depended on the outcome measure examined, with *post hoc* pairwise differences between marker clusters, global optimization condition, and task presented in Table 5-7 to 5-16. The maximum mean differences between marker clusters in estimating the peak flexion angle and moment were reduced from an average 8.9 to 6.2° and 0.7 to 0.3 %BW*H with global optimization (Figure 4-1 and 4-2).

For the peak abduction angle, global optimization increased the maximum mean difference from an average 5.2 to 10.4° (Figure 4-3). Global optimization attenuated the maximum mean difference for the peak abduction moment in HS (1.2 to 0.7 %BW*H) but increased it in DK-S (0.7 to 1.3 %BW*H) and PK-S (1.2 to 1.4 %BW*H) (Figure 4-4).

For the peak adduction angle, global optimization did not attenuate differences between marker clusters as the maximum mean difference increased from an average 4.9 to 7.0° (Figure 4-5). When examining the peak adduction moment, global optimization did

not affect the maximum mean difference in HS (0.5 %BW*H), but the difference increased from 1.0 to 1.3 %BW*H in DK-S and 0.6 to 1.1 %BW*H in PK-S (Figure 4-6).

While global optimization marginally attenuated differences between marker clusters for the peak external rotation angle in HS (6.3 to 5.7°), the maximum mean difference increased in DK-S (8.6 to 14.8°) and PK-S (7.7 to 13.5°) (Figure 4-7). There were no differences in the peak external rotation moment without global optimization, however some differences emerged when global optimization was applied (Figure 4-8; Table 5-14).

For the peak internal rotation angle, global optimization attenuated differences in HS (8.0 to 4.5°) and DK-S (9.8 to 8.2°), while PK-S marginally increased (10.7 to 11.4°) (Figure 4-9). For the peak internal rotation moment, there were no significant differences between marker clusters without global optimization; however, significant differences were observed between marker clusters when global optimization was applied (Figure 4-10; Table 5-16).

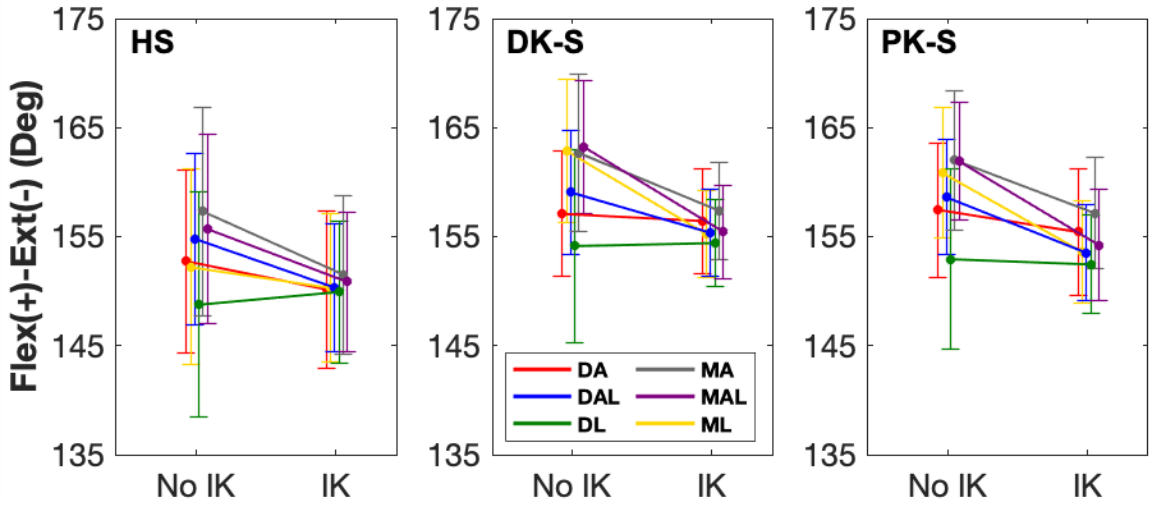

Figure 4-1: Interaction plots for peak knee flexion angle (marker cluster × IK) in each task. Significant differences between marker clusters, global optimization condition, and tasks are detailed in Table 5-7.

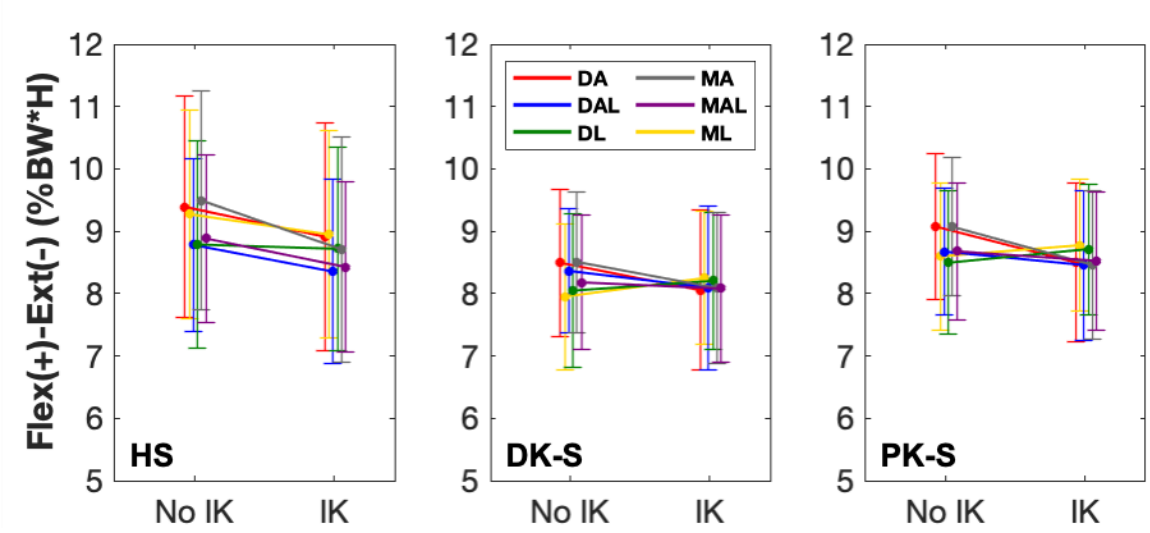

Figure 4-2: Interaction plots for peak knee flexion moment (marker cluster × IK) in each task. Significant differences between marker clusters, global optimization condition, and tasks are detailed in Table 5-8.

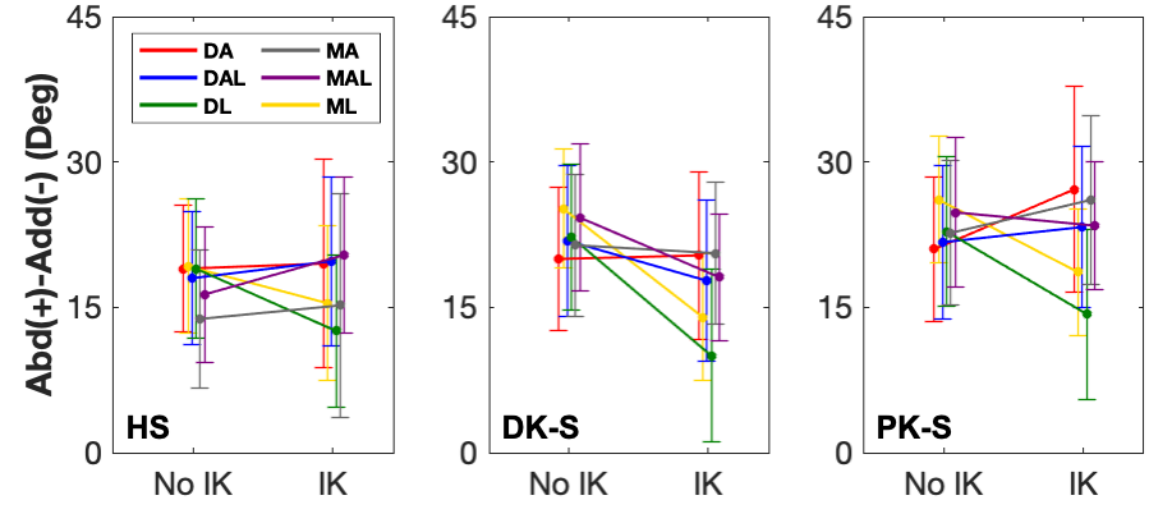

Figure 4-3: Interaction plots for peak knee abduction angle (marker cluster × IK) in each task. Significant differences between marker clusters, global optimization condition, and tasks are detailed in Table 5-9.

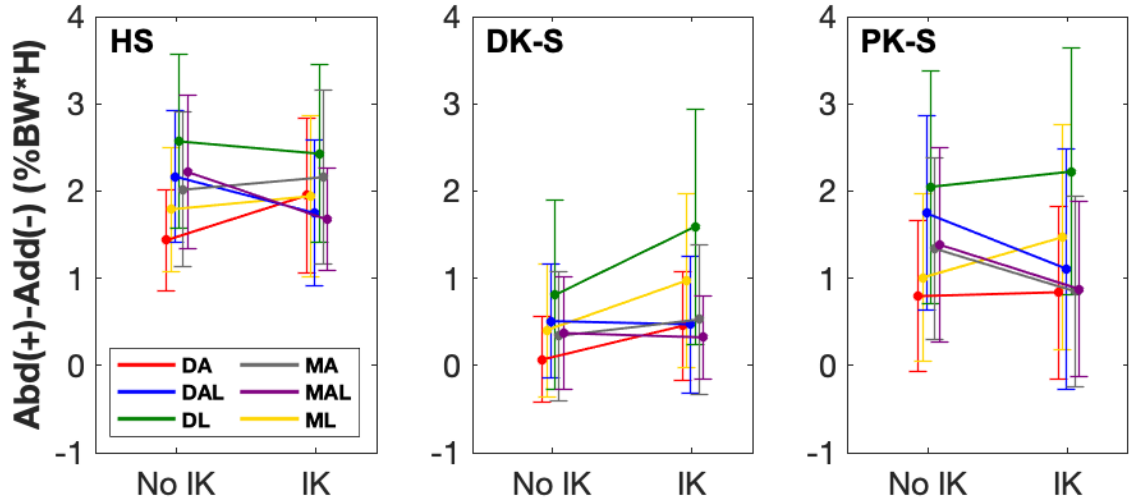

Figure 4-4: Interaction plots for peak knee abduction moment (marker cluster × IK) in each task. Significant differences between marker clusters, global optimization condition, and tasks are detailed in Table 5-10.

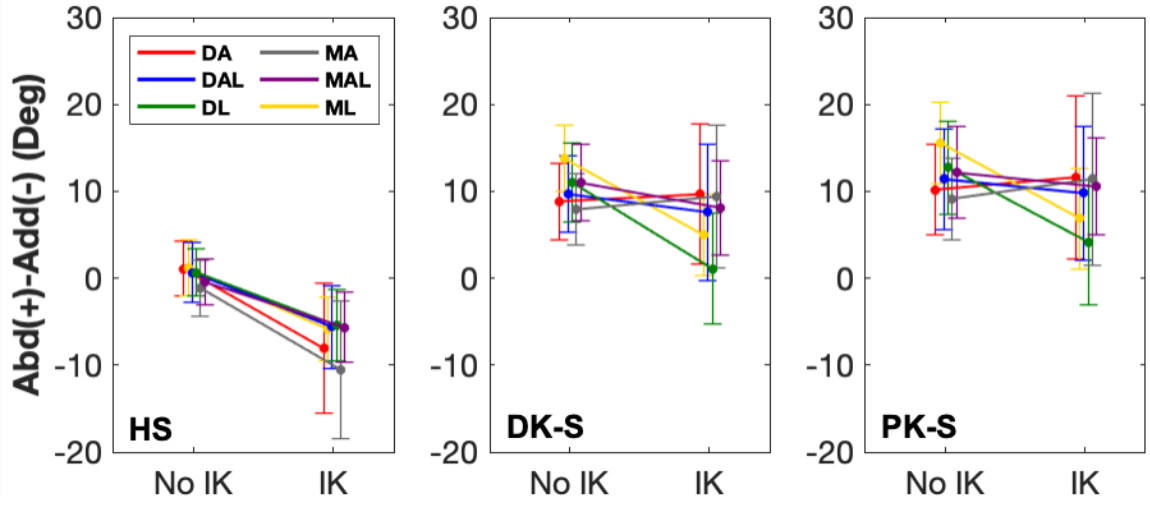

Figure 4-5: Interaction plots for peak knee adduction angle (marker cluster × IK) in each task. Significant differences between marker clusters, global optimization condition, and tasks are detailed in Table 5-11.

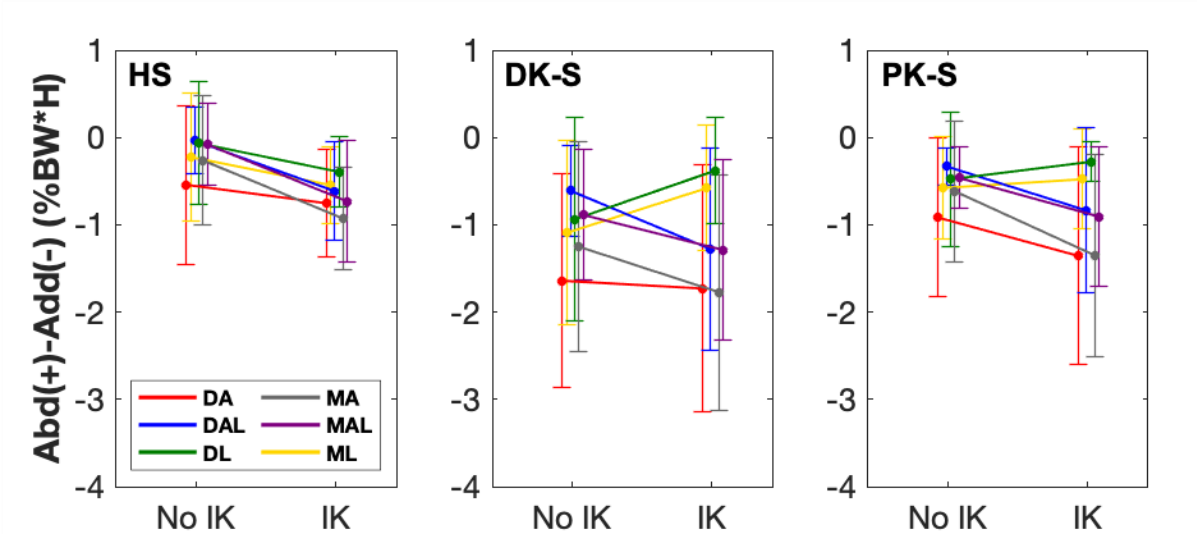

Figure 4-6: Interaction plots for peak knee adduction moment (marker cluster × IK) in each task. Significant differences between marker clusters, global optimization condition, and tasks are detailed in Table 5-12.

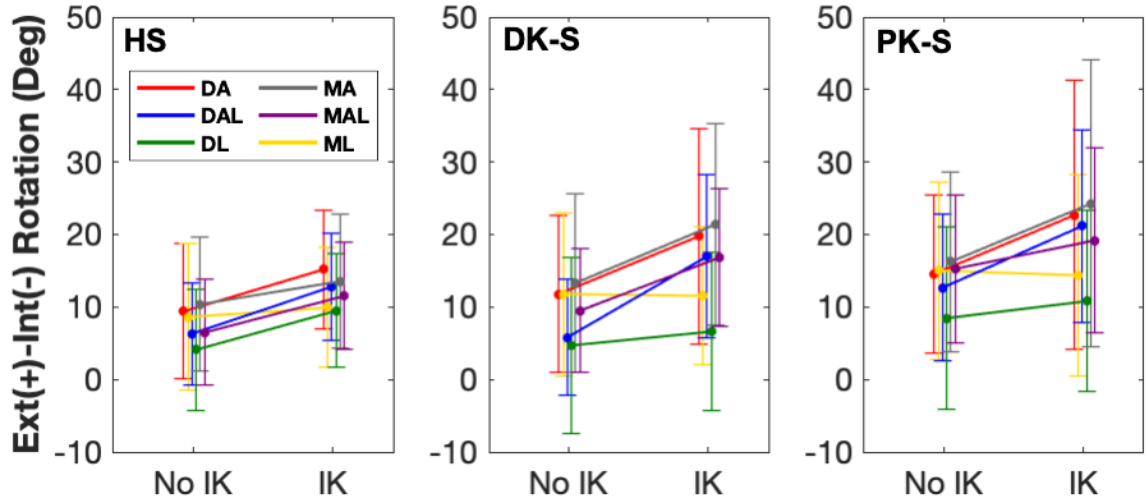

Figure 4-7: Interaction plots for peak knee external rotation angle (marker cluster × IK) in each task. Significant differences between marker clusters, global optimization condition, and tasks are detailed in Table 5-13.

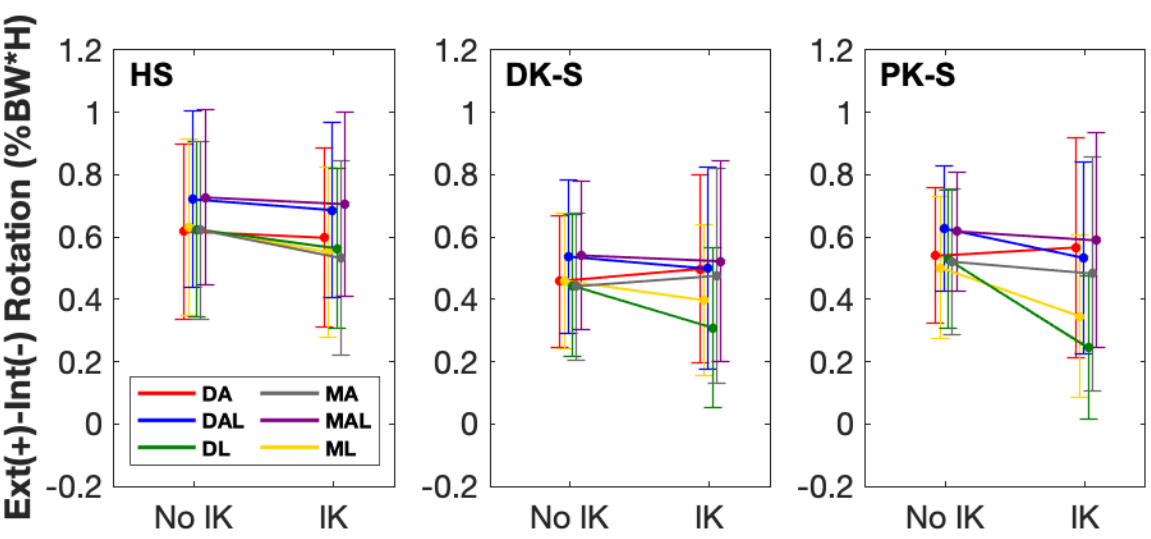

Figure 4-8: Interaction plots for peak knee external rotation moment (marker cluster × IK) in each task. Significant differences between marker clusters, global optimization condition, and tasks are detailed in Table 5-14.

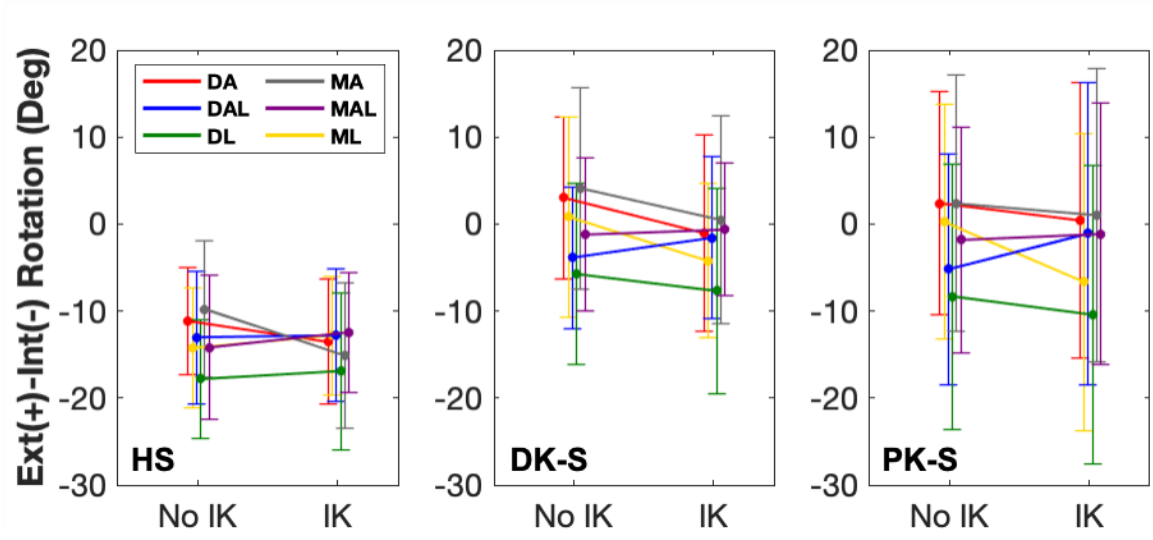

Figure 4-9: Interaction plots for peak knee internal rotation angle (marker cluster × IK) in each task. Significant differences between marker clusters, global optimization condition, and tasks are detailed in Table 5-15.

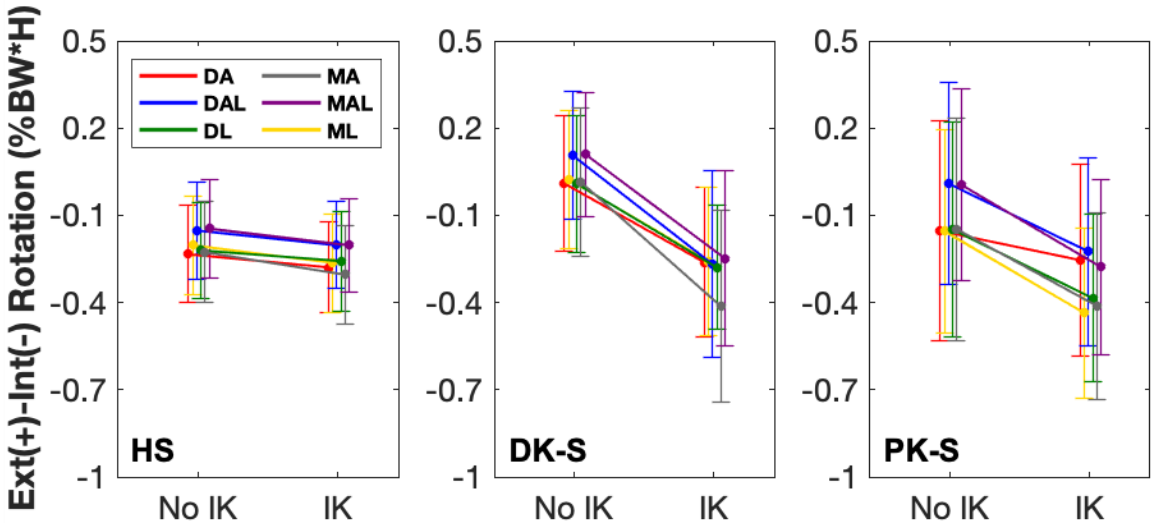

Figure 4-10: Interaction plots for peak knee internal rotation moment (marker cluster × IK) in each task. Significant differences between marker clusters, global optimization condition, and tasks are detailed in Table 5-16.

Effect Sizes

Due to listwise elimination of data, for both the effect size and ICC calculations, 45 subjects were included in the knee joint angle analysis, and 45, 44, and 43 were included in the knee joint moment analysis for HS, DK-S, and PK-S, respectively. Sixty effect size calculations were performed, of which 8 were classified as small, 15 were classified as medium, and 37 were classified as large (Table 4-2). Effect sizes tended to be larger for knee joint angles than moments (Table 4-2).

Global optimization had varying effects on η_p^2, depending on the movement and outcome measure (Table 4-2). For peak angles in HS, η_p^2 decreased for all variables, resulting in a decrease in classification from large to medium for all measures except the peak external rotation angle which remained classified as large (Table 4-2). With global optimization, η_p^2 for the peak flexion moment decreased from medium to small, and η_p^2 for the peak abduction moment decreased from large to medium (Table 4-2). The η_p^2 for the

peak adduction and external and internal rotation moment was classified as large and small, respectively, with and without global optimization (Table 4-2).

In DK-S, η_p^2 for all peak angles was classified as large without global optimization (Table 4-2). Although global optimization decreased η_p^2 for all axes of rotation except the peak abduction angle, only the effect for peak internal rotation angle was reduced from large to medium (Table 4-2). For the peak flexion moment, global optimization reduced η_p^2 from medium to small. The η_p^2 for peak internal rotation moment was classified as medium with and without global optimization (Table 4-2). With global optimization, the η_p^2 for the peak abduction and adduction moment increased, thereby remaining classified as large, and the peak external rotation moment increased from small to medium (Table 4-2).

With and without global optimization, the η_p^2 for all peak angles in PK-S were classified as large. Furthermore, applying global optimization increased η_p^2 for all angles except the peak flexion and internal rotation angle, which remained classified as large (Table 4-2). Global optimization decreased η_p^2 from medium to small for the peak flexion moment, and from large to medium for the peak adduction moment (Table 4-2). Alternatively, η_p^2 for the peak abduction and internal rotation moment remained classified as large and medium, respectively. The η_p^2 for peak external rotation moment increased from medium to large (Table 4-2).

Table 4-2: Effect sizes (η_p^2) for peak knee joint angles and moments in each task with (IK) and without (no IK) global optimization. Small effect sizes (< 0.06) are italicized. Effect size comparisons (with and without global optimization) which resulted in a decrease in classification are bolded.

Task	Flexion		Abduction		Adduction		External Rot		Internal Rot	
	No IK	IK	No IK	IK	No IK	IK	No IK	IK	No IK	IK
Peak Angle										
HS	**0.39**	**0.13**	**0.25**	**0.12**	**0.20**	**0.12**	0.24	0.18	**0.38**	**0.12**
DK-S	0.50	0.22	0.19	0.34	0.39	0.27	0.32	0.27	**0.32**	**0.09**
PK-S	0.43	0.31	0.20	0.39	0.39	0.18	0.20	0.23	0.23	0.23
Peak Moment										
HS	**0.07**	***0.02***	*0.31*	*0.11*	0.25	0.24	***0.01***	***0.01***	***0.01***	***0.02***
DK-S	**0.09**	***0.03***	0.16	0.28	0.32	0.36	*0.05*	0.11	0.06	0.06
PK-S	**0.08**	***0.02***	0.29	0.30	0.18	0.06	0.08	0.23	0.10	0.11

Intraclass Correlation Coefficients

A total of sixty ICCs (10 dependent variables × 3 tasks × 2 IK conditions) were performed to quantify the reliability between marker clusters in estimating peak knee joint angles and moments with and without global optimization for each task. Coefficients were classified as: 31 poor, 27 moderate, 1 good, and 1 excellent (Table 4-3). Knee joint moments tended to have higher reliability coefficients than knee joint angles (Table 4-3). Global optimization increased reliability coefficients to a new classification for 2 variables, the peak flexion angle in HS increased from good to excellent and the peak flexion angle in PK increased from poor to moderate reliability (Table 4-3). Alternatively, global optimization did not change reliability classification for 12 variables and decreased reliability classification for 16 variables (Table 4-3).

Table 4-3: Intraclass correlation coefficients (ICC) for peak knee joint angles and moments in each task with (IK) and without (no IK) global optimization. ICC classified as moderate to excellent (> 0.50) are italicized. ICC comparisons (with and without global optimization) which resulted in an increase in classification are bolded.

Task	Flexion		Abduction		Adduction		External Rot		Internal Rot	
	No IK	IK	No IK	IK	No IK	IK	No IK	IK	No IK	IK
Peak Angle										
HS	***0.75***	***0.92***	*0.60*	0.38	*0.57*	0.20	*0.68*	*0.57*	*0.53*	0.49
DK-S	*0.52*	*0.67*	*0.72*	0.42	*0.52*	0.33	*0.65*	0.43	*0.59*	0.30
PK-S	**0.45**	***0.66***	*0.70*	0.37	*0.59*	0.34	*0.67*	*0.55*	*0.69*	*0.72*
Peak Moment										
HS	*0.63*	*0.60*	0.38	0.45	*0.64*	0.49	*0.55*	0.48	0.34	0.36
DK-S	0.40	0.38	0.46	0.32	*0.61*	0.33	*0.55*	0.36	*0.61*	0.41
PK-S	0.45	0.42	0.43	0.48	0.46	0.06	*0.65*	0.32	*0.73*	0.45

4.4 Discussion

The current study compared knee joint angles and moments estimated from marker clusters localized to six different areas of the thighs with and without global optimization to determine the effectiveness of changing marker placement and/or utilizing global optimization in attenuating soft tissue artifact. The hypothesis that there would be two-way interactions between marker cluster location and global optimization condition, as well as decreased effect sizes and increased ICC with global optimization was partially supported. Global optimization was partially effective at attenuating differences in angles and moments between marker clusters in the sagittal plane, however in the frontal and transverse plane, angles and moments estimated from the different marker clusters were typically more variable when global optimization was applied. The differences in peak knee joint angles and moments between the marker cluster without global optimization will be discussed prior to assessing the effects of global optimization.

4.4.1 Angles and moments between marker clusters

Across the different tasks, there were significant differences between marker clusters (without global optimization) in estimating the peak knee joint angles for all axes of rotation, with a mean difference of an average 8.9° flexion, 5.2° abduction, 4.9° adduction, 7.5° external rotation, and 9.5° internal rotation. When estimating peak knee joint moments there were significant differences between marker clusters for peak flexion, abduction, and adduction, with a maximum mean difference between marker clusters of 0.6, 1.0, and 0.7 %BW*H on average, respectively. The peak external and internal rotation moments had an average mean difference of only 0.1 %BW*H. Additionally, across the axes of rotation, the angle and moment waveforms between marker clusters were temporally and spatially similar; however, in some cases, specifically for abduction and adduction moments, the variability between marker clusters was quite high. Collectively, these results demonstrate that marker cluster placement on the thigh can alter knee joint kinematics and kinetics; thus, not only is it important to be consistent with marker placement, but a given marker placement may be more representative of underlying bone motion.

Although there are multiple sources of error that may result in differences between marker clusters (i.e. calibration errors or optical distortion), it can be assumed that the dissimilarities are in part due to variability in local soft tissue artifact experienced by each of the clusters. Soft tissue artifact results from multiple sources including skin sliding, muscle and adipose deformation and oscillation, muscular contractions, and gravity; however, since definitive bone motion was not quantified in the current study, the results do not afford conclusions on the magnitude and direction of soft tissue artifact experienced

by the different marker clusters. Instead, the results demonstrate the sensitivity of kinematic and kinetic outcomes to marker placement, thereby demonstrating that adjustment of marker placement in high knee flexion is a feasible option for more accurately measuring bone motion.

The difference between the marker clusters should be interpreted within the context of the knee joint's physiological motion about a specific axis of rotation. For example, previous soft tissue artifact studies have presented error due to soft tissue artifact as a percent of joint range of motion, in which the percent error typically ranged from approximately 7-15% flexion-extension, 70-80% abduction-adduction, and 23-43% external-internal rotation angle in a step-up task and sit-to-stand (Akbarshahi et al., 2010; Stagni et al., 2005). Presenting the current data in a similar manner (maximum mean difference between marker clusters as a percent of the sample mean peak angle for each task) yields differences of approximately 6% of the mean of the peak flexion angle, up to 20-28% for abduction, 61-183% for adduction, 45-69% for external rotation, and 50-350% for internal rotation. While the aforementioned studies (Akbarshahi et al., 2010; Stagni et al., 2005) compared marker clusters and bone kinematics, one study which compared the precision of marker clusters in determining knee abduction-adduction found the mean difference in peak adduction angle between marker clusters was 4.7° (9.0 to 13.7°) in lateral cutting and 13.9° (1.9 to 15.8°) in a vertical drop jump (Mok et al., 2015). Although the latter study utilized non-rigid marker clusters and investigated tasks which likely elicit greater soft tissue oscillation than those of the current study, the magnitude of difference between marker clusters relative to the peak angles were similar.

In addition to differences in kinematic outcomes, the moments between marker clusters differed by up to 5-7% of the mean of the peak flexion moment, up to 52-100% for abduction, 71-100% for adduction, 12-16% for external rotation, and 33-100% for internal rotation. Previous studies which investigated the percent error of knee joint moment during stair ascent and sit-to-stand relative to peak the moment measured with fluoroscopy, ranged from 0.4-12.8% for peak flexion-extension moment, 0.1-16.2% for peak the abduction-adduction moment, and 0.5-13.5% for the peak external-internal rotation moment (Kuo et al., 2011; Tsai et al., 2011). While magnitudes of under 10% for the flexion angle and moment are unlikely to be detrimental to data obtained, the difference for the other axes of rotation calls into question the precision of the data and highlights the need for consistency in marker placement. For example, for protocols that require subjects to complete multiple laboratory sessions or compare data to the contralateral limb, small variations in marker placement on the thigh, may have significant effects on estimated kinematics and kinetics; thereby casting doubt on the effect of a given intervention or the demands of a given task. Additionally, although systematic differences between marker clusters were not consistent across all subjects, as soft tissue artifact is highly subject specific (Barré et al., 2013; Clément et al., 2018; Garling et al., 2007; Stagni et al., 2005), researchers should take care in ensuring that marker placement is similar between subjects completing the same laboratory protocol and when combining data from multiple data sets.

Kinematic and kinetic outcomes in activities of daily living which require low to moderate knee flexion range of motion are often utilized to explore injury and disease etiology (Bouchouras et al., 2015; Donohue et al., 2015; Graci et al., 2012; Yamazaki et al., 2010; Zeller et al., 2003) and assess the effectiveness of a given treatment (Acker et al.,

2011; Myles et al., 2002; Sumner et al., 2019; Verdini et al., 2017). Therefore, it is extremely important that variation in kinematics and kinetics are reflective of changes in the independent variable (i.e. population or intervention). The differences between marker clusters observed in the current study exceeded those previously reported between populations or when evaluating the effectiveness of an intervention. For example, when comparing high knee flexion kinematics between male Muslims with a total knee replacement and healthy controls, the mean difference for kneeling and squatting, respectively, was 1.4 and 8.0° flexion, 7.4 and 7.2° abduction, 2.4 and 0.5° adduction, 4.9 and 7.0° external rotation, and 7.8 and 6.2° internal rotation (Acker et al., 2011). The small differences between the populations highlights the importance of consistent marker placement, as a small change in marker placement could result in changes larger than the change that could be attributed to the intervention.

Comparisons for kinetic outcomes in activities of daily living which require low to moderate knee flexion have also been performed. For example, differences in knee joint moments between those with anterior cruciate ligament injuries and healthy controls are often investigated as there is an association between anterior cruciate ligament injuries and knee osteoarthritis (Andriacchi & Mündermann, 2006; Chaudhari et al., 2008; Kessler et al., 2008). Zabala et al. (2013) found significant differences between knee flexion-extension and adduction moments during stair ascent and descent between anterior cruciate ligament reconstructed, the contralateral limb, and healthy controls; however, differences were within 1.5 and 0.6 %BW*H, respectively. Like the kinematic outcomes, these differences are close to or within the differences between marker clusters presented herein.

While the ANOVAs highlighted differences between the marker clusters, the ICCs provide some indication of reliability between the marker clusters. The results of the ICCs were somewhat concerning as reliability was most frequently classified as moderate for angles and poor for moments. Low coefficients were likely observed because the ICCs were calculated for absolute agreement and single measure, which will result in smaller values than when consistency and/or average measures are used (Koo & Li, 2016). Absolute agreement was chosen as this definition considers the extent to which one marker cluster equals another as opposed to the consistency definition which considers systematic differences between marker clusters, which were likely to vary considerably across subjects (Akbarshahi et al., 2010; Cappozzo et al., 1996; Stagni et al., 2005). As well, the single measure definition was reported as only one marker cluster is typically used on a segment during data collection. It is possible however that taking the average of multiple marker clusters would not only enhance reliability, but also accuracy in measuring bone motion. Like the results of the ANOVAs, the ICCs call into question the reliability of marker clusters localized to different areas of the thigh in estimating peak knee joint angles and moments in high knee flexion.

In summary, these findings reveal that marker cluster placement significantly affects estimates for peak knee joint angles and moment in high knee flexion tasks. In some cases, particularly for those in the frontal and transverse plane, the differences between marker clusters were similar to the angle and/or moment experienced by the knee joint in high knee flexion movements. Additionally, the differences in angles and moments between marker clusters may exceed values previously found between population groups or as a result of a given intervention. It is recommended that researchers take extreme care

in selecting marker placement when evaluating high knee flexion or similar tasks and ensure consistent placement between subjects, bilaterally on a single subject's extremities, and when multiple laboratory sessions are required.

4.4.2 Global optimization

Global optimization was partially effective in attenuating differences in angles and moments between marker clusters, however this was highly axis and task dependent. Global optimization, significant differences were observed between marker clusters for all outcome measures except for the peak knee flexion moment in DK-S. Differences between marker clusters were most effectively attenuated for the peak flexion angle and moment, wherein the maximum mean difference between marker clusters decreased 2.7° and 0.4 %BW*H. Global optimization also attenuated the maximum mean difference for the peak abduction moment (0.5 %BW*H), external rotation angle (0.6°), and internal rotation angle (3.5°) in HS. The maximum mean difference in peak internal rotation angle also decreased in DK-S (1.6°) with global optimization. However, while there were no differences in the peak external or internal rotation moment between marker clusters without global optimization, applying global optimization resulted in significant differences between some marker clusters. Additionally, of the thirty effect size comparisons (with and without global optimization), global optimization only effectively decreased the effect size classification for 12 variables (included in this is 2 effect sizes which remained classified as small). Similarly, for the ICCs, global optimization increased reliability classification for 2 variables. Collectively, these results demonstrate that global optimization partially attenuated differences between in kinematic and kinetic outcome between marker clusters, most frequently for outcomes in the sagittal plane and for HS.

While the results of three-way ANOVAs exemplify absolute differences between marker clusters, these results were best summarized by examining the change in effect sizes. Based on the assumption that if there was no soft tissue artifact, all marker clusters would estimate the same peak angles and moments, a decrease in the effect size with global optimization suggests that global optimization may be effective in partially compensating for soft tissue artifact. For the peak knee joint angles, all effect sizes were initially classified as large without global optimization. With global optimization most effect sizes decreased, however the decrease was only large enough to warrant a change in effect size for angles in HS (with the exception of the external rotation angle) and the internal rotation angle in DK. Additionally, for peak knee joint moments the effect size classification decreased or did not change from a small effect for the peak flexion moment in all tasks, the peak abduction moments in HS, and the peak adduction moment in PK. Despite a change in effect size classification for only 12 variables, some of the changes in effect size were quite striking. For example, although an effect remained classified as large, the decrease was larger than the difference between a small and large effect (i.e. 0.13). Moreover, since the effect size was determined using η_p^2, this value indicates the percentage of variation in the peak angle or moment accounted for by the different marker clusters (Cohen, 2013; Lakens, 2013). For instance, η_p^2 decreased from 0.50 to 0.22 for the flexion angle in DK-S; thus, there was 28% decrease in the percentage of variation associated with marker cluster location with global optimization. It is also worth noting that smaller effect sizes were observed for moments compared to angles, thus suggesting that kinematic outcomes may be more susceptible to soft tissue artifact than kinetic outcomes. This is reasonable as differences in knee joint moments between the thigh

marker clusters would only result if there was a change in the position of the knee joint center (Kuo et al., 2011; Tsai et al., 2011).

If global optimization was compensating for soft tissue artifact, one would expect an increase in precision and reliability between marker clusters, and thus an increase in ICCs. However, ICCs, which already tended to demonstrate poor to moderate reliability, more frequently decreased with global optimization, suggesting an increase in within-subject variability. More specifically, ICC reliability classification increased for 2 variables (the flexion angle in HS and PK), did not change for 12 variables, and decreased for 16 variables. Conversely, the results of the ANOVAs and the effect size calculations indicate a decrease in the differences in the sample means for the marker clusters. Taken together, these findings suggest that while global optimization may decrease differences across the sample, within-subject variability (which is likely more indicative of individual soft tissue artifact) may not be effectively compensated for, particularly when evaluating angles and moments in the frontal and transverse plane. Utilizing different IK chain possibilities (i.e. different degrees-of-freedom constraints or segment weighting factors), different methods to solve the optimization solution (i.e. Visual3D also offers quasi-Newton and simulated annealing methods), and potentially the production of models which include subject specific constraints (e.g. joint range of motion or anthropometry) may improve the compensation ability of global optimization model. Additionally, the differences in the ability of the global optimization model for the different tasks, particularly that the models performed better in HS compared to DK-S and PK-S, suggests that changes to the model may be required to improve its applicability in more complex tasks as the global optimization method was initially designed for use in walking (Lu & O'Connor, 1999).

Although the results of the current study alone do not afford conclusions on accuracy of marker placement, when coupled with the Bland-Altman results in Chapter 3, the marker cluster which may be most likely to represent bone motion was the mid-anterolateral cluster. Peak angles and moments estimated by the mid-anterolateral cluster tended to fall between other marker clusters; however, this trend was variable with the task and global optimization condition. However, these results suggest that the mid-anterolateral cluster may be closest to the mean kinematic and kinetic measurements, which could be considered the best representation of bone motion (Bland & Altman, 1986). Additionally, if global optimization was effectively compensating for soft tissue artifact, one would expect marker clusters which were most susceptible to soft tissue artifact, to undergo the largest changes when IK constraints were applied. Based on the results from Chapter 3, we would expect the distal-lateral and mid-lateral cluster to require the largest compensation. Interestingly, the lateral clusters not only tended to display similar trends (i.e. both increased, decreased, or did not change) when global optimization was implemented but they also tended to undergo larger changes in angles or moments in the frontal and transverse plane compared to the other marker clusters (Figure 4-3 to 4-10).

In conclusion, global optimization represents a feasible option for attenuating differences between marker clusters; however, improvements must be made to the tool to improve subject specificity. While there was a decrease in the sample mean differences between the clusters with global optimization, as indicated by changes in the frequency and magnitude of the significant difference in the ANOVAs and decreases in effect sizes, within-subject variability tended to increase, as indicated by increases in ICCs. Global optimization more effectively attenuated differences between marker clusters when

estimating the peak flexion angle and moment, while differences between angles and moments in the frontal and transverse plane were only reduced for some marker clusters. These findings cast doubt on the ability to reliably estimate knee joint abduction-adduction and external-internal rotation in high knee flexion. The current research demonstrates that while global optimization, implemented in Visual3D using IK constraints, can attenuate some differences in angles and moments between marker clusters, global optimization alone cannot eliminate all variability between marker clusters, and thus is likely only moderately effective in compensating for soft tissue artifact.

4.5 Limitations

Although soft tissue artifact is considered one of the largest sources of error in measuring kinematics from motion capture data, it is recognized that other sources of error are present, and thus may have affected the results of the current study. Three methodological limitations are acknowledged. First, some of the differences between the marker clusters may have resulted in part because marker clusters were localized to opposite legs (i.e. the distal-anterior, distal-anterolateral, mid-anterior, and mid-anterolateral cluster on one leg while the distal-anterolateral and mid-anterolateral cluster were on the other leg). Thus, differences between anterior/lateral and anterolateral clusters would likely be due to both differences in soft tissue artifact and differences in movement strategy between the legs. However, since the tasks investigated were symmetrical and the marker clusters were compared within a trial, it is unlikely that differences between marker clusters on opposite legs were solely the result of different movement strategies between the legs.

An additional methodological limitation to the current study is that the use of the current gold standard for defining the thigh coordinate system – the functional knee joint center and functional axis on the distal end of the segment – may result in slightly different coordinate system definitions between the clusters as these landmarks were estimated for each thigh marker cluster independently from the functional knee joint trial. Although the differences in thigh coordinate system definition may have amplified or attenuated differences between the thigh marker clusters, we believe it would not have been justified to utilize the same joint center and axis definitions between the marker clusters as this would not be implemented in a typical motion capture data collection. Moreover, it is likely that differences between marker clusters were attenuated by this coordinate system definition as soft tissue artifact experienced by the different marker clusters during the functional knee trial would be included in the estimation of the position of the knee joint center and functional axis. Thus, soft tissue artifact between marker clusters may in fact be compensated for by utilizing the functional knee joint center and axis for coordinate system definition.

While global optimization was effective in reducing variability in the sagittal plane kinematics, the difficulties faced when attempting to implement IK constraints in Visual3D should be acknowledged. Although constructing an IK model was a straight-forward process, utilizing the IK optimization algorithm to calculate kinematics and kinetics was quite challenging. To obtain the postures, the model often underwent unphysiological motion of the lower limbs, such as 360° of axial rotation of the shank or feet or gimbal lock occurring in the knee joint. This instability in the model unfortunately led to exclusion of trials and in some cases, subjects. Recommendations by the software provider to restrict

foot rotation relative to the shank decreased the frequency of unphysiological motion but did not prevent it entirely. Future improvements to the model should address this instability and make recommendations for additional processing steps which can be taken to improve the predictive ability of the model.

Lastly, despite that the current sample size (n of 50 with 28 females and 22 males), was sufficient for statistical testing with sex as an additional independent variable, sex was not included in in the current ANOVAs. Instead, sex was considered in the regression equations found in Chapter 3. This was decided *a priori* as it was hypothesized that much of the variability in marker cluster location between the sexes would likely have resulted from anthropometric variability. Thus, we felt investigating anthropometry as continuous rather than discrete variables would provide greater insight into their effects on soft tissue artifact. Additionally, it is important to note that inclusion of sex as an additional independent variable would not have distinguished between optimal marker placement for males and females, but rather demonstrated possible differences in marker cluster reliability, global optimization conditions, and/or tasks between the sexes.

4.6 Conclusions

While the results of the current study cannot speak to accuracy of marker clusters in tracking bone motion, they provide evidence on the precision between marker clusters, thereby tapping into necessary standardization procedures when utilizing optical motion capture. Peak knee joint angles and moments were different between the thigh marker clusters; however, the differences observed were inconsistent across high knee flexion tasks and axes of rotation. These findings suggest that specific marker clusters may be more representative of bone motion depending on the task demands and the axis of rotation

of interest. Additionally, these results highlight the importance of consistency in marker placement between and within subjects to enhance scientific reproducibility.

Global optimization represents a feasible method to reduce differences between marker clusters when estimating flexion angles and moments in high knee flexion, but improvements to the optimization procedures are warranted to increase its applicability for other planes of motion and more complex tasks. Additionally, given that global optimization differentially affected the thigh marker clusters across the sample, future investigations into attenuating soft tissue artifact should consider changes in kinematic and kinetic outcomes with marker placement and compensation methodologies, simultaneously.

The results of the current study indicate that estimated angles and moments varied considerably with marker cluster location, global optimization condition, and the different high knee flexion tasks. These findings emphasize the need for researchers to report all data processing steps in published work. Researchers must be transparent and specific when describing methodological procedures to ultimately facilitate comparability and reproducibility in the field.

Chapter 5 - Novel Contributions and Future Directions

The two studies presented in the current thesis probed the location, subject, and task specificity of soft tissue artifact in high knee flexion through data collection and processing methods, to ultimately make recommendations for attenuating soft tissue artifact.

The first study developed a non-invasive method, making use of the difference in the position of the functional hip joint center tracked by the pelvis cluster and different thigh clusters, to compare thigh marker cluster susceptibility to soft tissue artifact. This method could be applied to other tasks or segments to evaluate marker placements which may be least vulnerable to soft tissue artifact. The results indicated that a mid-anterolateral cluster is likely most accurate in high flexion as it was least vulnerable to thigh-calf contact while maintaining marker visibility. As well, soft tissue artifact was shown to increase with knee flexion, which aligns with results from previous studies (Cappozzo et al., 1996; Kuo et al., 2011; Tsai et al., 2011).

The association between local and global measures of subject anthropometry and soft tissue artifact was then explored using backward stepwise regressions. It was found that while soft tissue artifact was extremely subject specific, subject anthropometry could be utilized to moderately predict soft tissue artifact for specific marker clusters in squatting and kneeling. Additionally, the results demonstrated that measures which differentiate between segment adipose and muscle tissue may more effectively explain the relationship between anthropometry and soft tissue artifact.

While the first study used changes in the position of the functional hip joint center to estimate soft tissue artifact, the second study explored the sensitivity of knee joint angles and moments to marker placement, thereby demonstrating the extent to which soft tissue

artifact may affect clinically meaningful outcomes. The results indicated that marker placement can significantly affect peak knee joint angles and moments, particularly in the frontal and transverse plane. These findings were similar to previous studies, which found that appropriate marker placement can improve the accuracy of determining bone motion in tasks which require low to moderate knee flexion (Akbarshahi et al., 2010; Barré et al., 2013; Cappozzo et al., 1996; Stagni et al., 2005). These results extend beyond studies which examine high knee flexion tasks; researchers must ensure consistent marker placement within and between subjects.

Additionally, the second study investigated if global optimization could partially compensate for differences between marker clusters in estimating peak knee joint angles and moments. By applying IK constraints in Visual3D to limit the degrees-of-freedom of the joints of the lower limb, the results demonstrated that while global optimization may attenuate some differences between marker clusters, largely in the sagittal plane and for squatting, global optimization was less effective on a subject-by-subject basis.

This thesis investigated the precision and reliability of different marker clusters in high knee flexion, a task that has previously been large unexplored. The results suggest that marker placement can significantly alter kinematic and kinetic outcomes which ultimately compromises the ability to compare results between studies and make conclusions on mechanisms for injury and disease. While there is a need to address the accuracy of the marker placements and global optimization procedures tested in the current thesis, the results exemplify the need for standardization in data collection and processing procedures. Researchers must be consistent in marker placement within and between subjects during data collection and report all methodological steps in published work. The

importance of standardization must not be overlooked as it facilitates the ability to repeat, compare, and reproduce scientific investigations – the foundation of inductive reasoning and scientific advancement.

References

Acker, S. M., Cockburn, R. A., Krevolin, J., Li, R. M., Tarabichi, S., & Wyss, U. P. (2011). Knee Kinematics of High-Flexion Activities of Daily Living Performed by Male Muslims in the Middle East. *The Journal of Arthroplasty*, *26*(2), 319–327. https://doi.org/10.1016/J.ARTH.2010.08.003

Acker, S. M., Kutzner, I., Bergmann, G., Deluzio, K. J., & Wyss, U. P. (2018). In Vivo Tibiofemoral Joint Contact Forces During High Flexion Activities. *Orthopaedic Proceedings, Vol. 94-B, No. SUPP_XXV*.

Akbarshahi, M., Schache, A. G., Fernandez, J. W., Baker, R., Banks, S. A., & Pandy, M. G. (2010). Non-invasive assessment of soft-tissue artifact and its effect on knee joint kinematics during functional activity. *Journal of Biomechanics*, *43*(7), 1292–1301. https://doi.org/10.1016/J.JBIOMECH.2010.01.002

Alexander, E. J., & Andriacchi, T. P. (2001). Correcting for deformation in skin-based marker systems. *Journal of Biomechanics*, *34*(3), 355–361. https://doi.org/10.1016/S0021-9290(00)00192-5

Altman, D. G., & Bland, J. M. (1983). Measurement in Medicine: The Analysis of Method Comparison Studies. *The Statistician*, *32*(3), 307–317. https://doi.org/10.2307/2987937

Andersen, M. S., Benoit, D. L., Damsgaard, M., Ramsey, D. K., & Rasmussen, J. (2010). Do kinematic models reduce the effects of soft tissue artefacts in skin marker-based motion analysis? An in vivo study of knee kinematics. *Journal of Biomechanics*, *43*(2), 268–273. https://doi.org/10.1016/J.JBIOMECH.2009.08.034

Andersen, M. S., Damsgaard, M., Rasmussen, J., Ramsey, D. K., & Benoit, D. L. (2012). A linear soft tissue artefact model for human movement analysis: Proof of concept using in vivo data. *Gait & Posture*, *35*(4), 606–611. https://doi.org/10.1016/J.GAITPOST.2011.11.032

Andriacchi, T. P., & Alexander, E. J. (2000). Studies of human locomotion: past, present and future. *Journal of Biomechanics*, *33*(10), 1217–1224. https://doi.org/10.1016/S0021-9290(00)00061-0

Andriacchi, T. P., Alexander, E. J., Toney, M. K., Dyrby, C., & Sum, J. (1998). A Point Cluster Method for In Vivo Motion Analysis: Applied to a Study of Knee Kinematics. In *Journal of Biomechanical Engineering* (Vol. 120, Issue 6). American Society of Mechanical Engineers. https://doi.org/10.1115/1.2834888

Andriacchi, T. P., & Mündermann, A. (2006). The role of ambulatory mechanics in the initiation and progression of knee osteoarthritis. *Current Opinion in Rheumatology*, *18*(5), 514–518. https://doi.org/10.1097/01.bor.0000240365.16842.4e

Andriacchi, T. P., Mündermann, A., Smith, R. L., Alexander, E. J., Dyrby, C. O., & Koo, S. (2004). A Framework for the in Vivo Pathomechanics of Osteoarthritis at the Knee. *Annals of Biomedical Engineering*, *32*(3), 447–457. https://doi.org/10.1023/B:ABME.0000017541.82498.37

Angeloni, C., Cappozzo, A., Catani, F., & Leardini, A. (1992). Quantification of relative displacement between bones and skin- and plate-mounted markers. *In Proceedings of the VlIIth Meeting of European Society of Biomechanics*, 279.

Babyak, M. (2004). What You See May Not Be What You Get: A Brief, Nontechnical Introduction to Overfitting in Regression-Type Models. *Psychosomatic Medicine*,

66(3), 441–421. https://doi.org/10.1300/j120v12n27_14
Baker, P., Reading, I., Cooper, C., & Coggon, D. (2003). Knee disorders in the general population and their relation to occupation. *Occupational and Environmental Medicine*, *60*(10), 794–797. https://doi.org/10.1016/j.echo.2013.12.006
Barré, A., Aissaoui, R., & Aminian, K. (2017). Assessment of the lower limb soft tissue artefact at marker-cluster level with a high-density marker set during walking. *Journal of Biomechanics*, *62*, 21–26. https://doi.org/10.1016/J.JBIOMECH.2017.04.036
Barré, A., Jolles, B. M., Theumann, N., & Aminian, K. (2015). Soft tissue artifact distribution on lower limbs during treadmill gait: Influence of skin markers' location on cluster design. *Journal of Biomechanics*, *48*(10), 1965–1971. https://doi.org/10.1016/J.JBIOMECH.2015.04.007
Barré, A., Thiran, J.-P. P., Jolles, B. M., Theumann, N., & Aminian, K. (2013). Soft tissue artifact assessment during treadmill walking in subjects with total knee arthroplasty. *IEEE Transactions on Biomedical Engineering*, *60*(11), 3131–3140. https://doi.org/10.1109/TBME.2013.2268938
Bell, A. L., Pedersen, D. R., & Brand, R. A. (1990). A comparison of the accuracy of several hip center location prediction methods. *Journal of Biomechanics*, *23*(6), 617–621. http://www.ncbi.nlm.nih.gov/pubmed/2341423
Benedetti, M. G., Catani, F., Leardini, A., Pignotti, E., & Giannini, S. (1998). Data management in gait analysis for clinical applications. *Clinical Biomechanics*, *13*(3), 204–215. https://doi.org/10.1016/S0268-0033(97)00041-7
Benoit, D. L., Damsgaard, M., & Andersen, M. S. (2015). Surface marker cluster translation, rotation, scaling and deformation: Their contribution to soft tissue artefact and impact on knee joint kinematics. *Journal of Biomechanics*, *48*(10), 2124–2129. https://doi.org/10.1016/J.JBIOMECH.2015.02.050
Benoit, D. L., Ramsey, D. K., Lamontagne, M., Xu, L., Wretenberg, P., & Renström, P. (2006). Effect of skin movement artifact on knee kinematics during gait and cutting motions measured in vivo. *Gait & Posture*, *24*(2), 152–164. https://doi.org/10.1016/J.GAITPOST.2005.04.012
Bland, J. M., & Altman, D. G. (1986). Statistical methods for assessing agreement between two methods of clinical measurement. *Lancet (London, England)*, *1*(8476), 307–310. http://www.ncbi.nlm.nih.gov/pubmed/2868172
Bonci, T., Camomilla, V., Dumas, R., Chèze, L., & Cappozzo, A. (2014). A soft tissue artefact model driven by proximal and distal joint kinematics. *Journal of Biomechanics*, *47*(10), 2354–2361. https://doi.org/10.1016/J.JBIOMECH.2014.04.029
Bonnet, V., Richard, V., & Venture, G. (2017). Joint kinematics estimation using a multi-body kinematics optimisation and an extended Kalman filter, and embedding a soft tissue artefact model. *Journal of Biomechanics*, *62*, 148–155. https://doi.org/10.1016/J.JBIOMECH.2017.04.033
Bouchouras, G., Patsika, G., Hatzitaki, V., & Kellis, E. (2015). Kinematics and knee muscle activation during sit-to-stand movement in women with knee osteoarthritis. *Clinical Biomechanics*, *30*(6), 599–607. https://doi.org/10.1016/j.clinbiomech.2015.03.025
Camomilla, V., Bonci, T., & Cappozzo, A. (2017). Soft tissue displacement over pelvic anatomical landmarks during 3-D hip movements. *Journal of Biomechanics*, *62*, 14–20. https://doi.org/10.1016/J.JBIOMECH.2017.01.013

Camomilla, V., Bonci, T., Dumas, R., Chèze, L., & Cappozzo, A. (2015). A model of the soft tissue artefact rigid component. *Journal of Biomechanics*, *48*(10), 1752–1759. https://doi.org/10.1016/J.JBIOMECH.2015.05.007

Camomilla, V., Cereatti, A., Chèze, L., & Cappozzo, A. (2013). A hip joint kinematics driven model for the generation of realistic thigh soft tissue artefacts. *Journal of Biomechanics*, *46*(3), 625–630. https://doi.org/10.1016/J.JBIOMECH.2012.09.018

Camomilla, V., Cereatti, A., Vannozzi, G., & Cappozzo, A. (2006). An optimized protocol for hip joint centre determination using the functional method. *Journal of Biomechanics*, *39*(6), 1096–1106. https://doi.org/10.1016/J.JBIOMECH.2005.02.008

Camomilla, V., Donati, M., Stagni, R., & Cappozzo, A. (2009). Non-invasive assessment of superficial soft tissue local displacements during movement: A feasibility study. *Journal of Biomechanics*, *42*(7), 931–937. https://doi.org/10.1016/J.JBIOMECH.2009.01.008

Canetti, E. F. D., Schram, B., Orr, R. M., Knapik, J., & Pope, R. (2020). Risk factors for development of lower limb osteoarthritis in physically demanding occupations: A systematic review and meta-analysis. *Applied Ergonomics*, *86*, 103097. https://doi.org/10.1016/j.apergo.2020.103097

Cappello, A., Cappozzo, A., La Palombara, P. F., Lucchetti, L., & Leardini, A. (1997). Multiple anatomical landmark calibration for optimal bone pose estimation. *Human Movement Science*, *16*(2–3), 259–274. https://doi.org/10.1016/S0167-9457(96)00055-3

Cappello, A., Stagni, R., Fantozzi, S., & Leardini, A. (2005). Soft Tissue Artifact Compensation in Knee Kinematics by Double Anatomical Landmark Calibration: Performance of a Novel Method During Selected Motor Tasks. *IEEE Transactions on Biomedical Engineering*, *52*(6), 992–998. https://doi.org/10.1109/TBME.2005.846728

Cappozzo, A. (1991). Three-dimensional analysis of human walking: Experimental methods and associated artifacts. *Human Movement Science*, *10*(5), 589–602. https://doi.org/10.1016/0167-9457(91)90047-2

Cappozzo, A., Cappello, A., Croce, U. D., & Pensalfini, F. (1997). Surface-marker cluster design criteria for 3-D bone movement reconstruction. *IEEE Transactions on Biomedical Engineering*, *44*(12), 1165–1174. https://doi.org/10.1109/10.649988

Cappozzo, A., Catani, F., Della Croce, U., & Leardini, A. (1995). Position and orientation in space of bones during movement: anatomical frame definition and determination. *Clinical Biomechanics*, *10*(4), 171–178. https://doi.org/10.1016/0268-0033(95)91394-T

Cappozzo, A., Catani, F., Leardini, A., Benedetti, M. G., Della Croce, U., & Croce, U. Della. (1996). Position and orientation in space of bones during movement: experimental artefacts. *Clinical Biomechanics*, *11*(2), 90–100. https://doi.org/10.1016/0268-0033(95)00046-1

Cereatti, A., Bonci, T., Akbarshahi, M., Aminian, K., Barré, A., Begon, M., Benoit, D. L., Charbonnier, C., Dal Maso, F., Fantozzi, S., Lin, C.-C., Lu, T.-W., Pandy, M. G., Stagni, R., & van den Bogert, A. J. (2017). Standardization proposal of soft tissue artefact description for data sharing in human motion measurements. *Journal of Biomechanics*, *62*, 5–13. https://doi.org/10.1016/J.JBIOMECH.2017.02.004

Cereatti, A., Della Croce, U., & Cappozzo, A. (2006). Reconstruction of skeletal movement using skin markers: comparative assessment of bone pose estimators.

Journal of NeuroEngineering and Rehabilitation, *3*(1), 7. https://doi.org/10.1186/1743-0003-3-7

Cereatti, A., Donati, M., Camomilla, V., Margheritini, F., & Cappozzo, A. (2009). Hip joint centre location: An ex vivo study. *Journal of Biomechanics*, *42*(7), 818–823. https://doi.org/10.1016/J.JBIOMECH.2009.01.031

Charbonnier, C., Chagué, S., Kolo, F. C., Duthon, V. B., & Menetrey, J. (2017). Multi-body optimization with subject-specific knee models: performance at high knee flexion angles. *Computer Methods in Biomechanics and Biomedical Engineering*, *20*(14), 1571–1579. https://doi.org/10.1080/10255842.2017.1390568

Chaudhari, A. M. W., Briant, P. L., Bevill, S. L., Koo, S., & Andriacchi, T. P. (2008). Knee kinematics, cartilage morphology, and osteoarthritis after ACL injury. *Medicine and Science in Sports and Exercise*, *40*(2), 215–222. https://doi.org/10.1249/mss.0b013e31815cbb0e

Chehab, E. F. F., Andriacchi, T. P., & Favre, J. (2017). *Speed, age, sex, and body mass index provide a rigorous basis for comparing the kinematic and kinetic profiles of the lower extremity during walking*. *58*, 11–20. http://www.ncbi.nlm.nih.gov/pubmed/28501342

Chèze, L., Fregly, B. J., & Dimnet, J. (1995). A solidification procedure to facilitate kinematic analyses based on video system data. *Journal of Biomechanics*, *28*(7), 879–884. https://doi.org/10.1016/0021-9290(95)95278-D

Chiari, L., Croce, U. Della, Leardini, A., & Cappozzo, A. (2005). Human movement analysis using stereophotogrammetry: Part 2: Instrumental errors. *Gait & Posture*, *21*(2), 197–211. https://doi.org/10.1016/J.GAITPOST.2004.04.004

Chong, H. C., Tennant, L. M., Kingston, D. C., & Acker, S. M. (2017). Knee joint moments during high flexion movements: Timing of peak moments and the effect of safety footwear. *The Knee*, *24*(2), 271–279. https://doi.org/10.1016/J.KNEE.2016.12.006

Clément, J., de Guise, J. A., Fuentes, A., & Hagemeister, N. (2018). Comparison of soft tissue artifact and its effects on knee kinematics between non-obese and obese subjects performing a squatting activity recorded using an exoskeleton. *Gait & Posture*, *61*, 197–203. https://doi.org/10.1016/J.GAITPOST.2018.01.009

Clément, J., Dumas, R., Hagemeister, N., & de Guise, J. A. (2015). Soft tissue artifact compensation in knee kinematics by multi-body optimization: Performance of subject-specific knee joint models. *Journal of Biomechanics*, *48*(14), 3796–3802. https://doi.org/10.1016/J.JBIOMECH.2015.09.040

Coggon, D., Croft, P., Kellingray, S., Barrett, D., McLaren, M., & Cooper, C. (2000). Occupational physical activities and osteoarthritis of the knee. *Arthritis & Rheumatism*, *43*(7), 1443–1449. https://doi.org/10.1002/1529-0131(200007)43:7<1443::AID-ANR5>3.0.CO;2-1

Cohen, J. (2013). *Statistical Power Analysis for the Behavioral Sciences* (Second).

D'Lima, D. D., Patil, S., Steklov, N., Slamin, J. E., & Colwell, C. W. (2006). Tibial Forces Measured In Vivo After Total Knee Arthroplasty. *The Journal of Arthroplasty*, *21*(2), 255–262. http://www.ncbi.nlm.nih.gov/pubmed/16520216

Dal Maso, F., Raison, M., Lundberg, A., Arndt, A., & Begon, M. (2014). Coupling between 3D displacements and rotations at the glenohumeral joint during dynamic tasks in healthy participants. *Clinical Biomechanics*, *29*(9), 1048–1055.

https://doi.org/10.1016/J.CLINBIOMECH.2014.08.006
Davis, R. B., Õunpuu, S., Tyburski, D., & Gage, J. R. (1991). A gait analysis data collection and reduction technique. *Human Movement Science*, *10*(5), 575–587. https://doi.org/10.1016/0167-9457(91)90046-Z
De Rosario, H., Page, A., Besa, A., Mata, V., & Conejero, E. (2012). Kinematic description of soft tissue artifacts: quantifying rigid versus deformation components and their relation with bone motion. *Medical & Biological Engineering & Computing*, *50*(11), 1173–1181. https://doi.org/10.1007/s11517-012-0978-5
Della Croce, U., Cappozzo, A., Kerrigan, D. C., Cappozzo, I. A., Kerrigan, I. D. C., Cappozzo, A., & Kerrigan, D. C. (1999). Pelvis and lower limb anatomical landmark calibration precision and its propagation to bone geometry and joint angles. *Med. Biol. Eng. Comput*, *37*(2), 155–161. https://doi.org/10.1007/bf02513282
Della Croce, U., Leardini, A., Chiari, L., & Cappozzo, A. (2005). Human movement analysis using stereophotogrammetry: Part 4: assessment of anatomical landmark misplacement and its effects on joint kinematics. *Gait & Posture*, *21*(2), 226–237. https://doi.org/10.1016/J.GAITPOST.2004.05.003
Donohue, M. R., Ellis, S. M., Heinbaugh, E. M., Stephenson, M. L., Zhu, Q., & Dai, B. (2015). *Differences and correlations in knee and hip mechanics during single-leg landing, single-leg squat, double-leg landing, and double-leg squat tasks*. https://doi.org/10.1080/15438627.2015.1076413
Dumas, R., Camomilla, V., Bonci, T., Chèze, L., & Cappozzo, A. (2014). Generalized mathematical representation of the soft tissue artefact. *Journal of Biomechanics*, *47*(2), 476–481. https://doi.org/10.1016/J.JBIOMECH.2013.10.034
Dumas, R., & Cheze, L. (2009). Soft tissue artifact compensation by linear 3D interpolation and approximation methods. *Journal of Biomechanics*, *42*(13), 2214–2217. https://doi.org/10.1016/J.JBIOMECH.2009.06.006
Ehrig, R. M., Taylor, W. R., Duda, G. N., & Heller, M. O. (2006). A survey of formal methods for determining the centre of rotation of ball joints. *Journal of Biomechanics*, *39*(15), 2798–2809. https://doi.org/10.1016/J.JBIOMECH.2005.10.002
Faul, F., Erdfelder, E., Lang, A. G., & Buchner, A. (2007). G*Power 3: A flexible statistical power analysis program for the social, behavioral, and biomedical sciences. *Behavior Research Methods*, *39*(2), 175–191. https://doi.org/10.3758/BF03193146
Felson, D. T. (2013). Osteoarthritis as a disease of mechanics. *Osteoarthritis and Cartilage*, *21*(1), 10–15. https://doi.org/10.1016/j.joca.2012.09.012
Fiorentino, N. M., Atkins, P. R., Kutschke, M. J., Foreman, K. B., & Anderson, A. E. (2016). In-vivo quantification of dynamic hip joint center errors and soft tissue artifact. *Gait & Posture*, *50*, 246–251. https://doi.org/10.1016/J.GAITPOST.2016.09.011
Fregly, B. J., Besier, T. F., Lloyd, D. G., Delp, S. L., Banks, S. A., Pandy, M. G., & D'Lima, D. D. (2012). Grand challenge competition to predict in vivo knee loads. *Journal of Orthopaedic Research*, *30*(4), 503–513. https://doi.org/10.1002/jor.22023
Fuller, J., Liu, L.-J., Murphy, M. C., & Mann, R. W. (1997). A comparison of lower-extremity skeletal kinematics measured using skin- and pin-mounted markers. *Human Movement Science*, *16*(2–3), 219–242. https://doi.org/10.1016/S0167-9457(96)00053-X
Furnee, H. (1997). *Three-Dimensional Analysis of Human Locomotion* (P. Allard, A.

Cappozzo, A. Lumberg, & K. Vaughan (eds.); 1st ed.). Wiley.
Gamage, S. S. H. U. H. U., & Lasenby, J. (2002). New least squares solutions for estimating the average centre of rotation and the axis of rotation. *Journal of Biomechanics*, *35*(1), 87–93. https://doi.org/10.1016/S0021-9290(01)00160-9
Garling, E. H., Kaptein, B. L., Mertens, B., Barendregt, W., Veeger, H. E. J., Nelissen, R. G. H. H., & Valstar, E. R. (2007). Soft-tissue artefact assessment during step-up using fluoroscopy and skin-mounted markers. *Journal of Biomechanics*, *40*, S18–S24. https://doi.org/10.1016/J.JBIOMECH.2007.03.003
Gasparutto, X., Sancisi, N., Jacquelin, E., Parenti-Castelli, V., & Dumas, R. (2015). Validation of a multi-body optimization with knee kinematic models including ligament constraints. *Journal of Biomechanics*, *48*(6), 1141–1146. https://doi.org/10.1016/j.jbiomech.2015.01.010
Graci, V., Van Dillen, L. R., & Salsich, G. B. (2012). Gender differences in trunk, pelvis and lower limb kinematics during a single leg squat. *Gait and Posture*, *36*(3), 461–466. https://doi.org/10.1016/j.gaitpost.2012.04.006
Grimpampi, E., Camomilla, V., Cereatti, A., de Leva, P., & Cappozzo, A. (2014). Metrics for Describing Soft-Tissue Artefact and Its Effect on Pose, Size, and Shape of Marker Clusters. *IEEE Transactions on Biomedical Engineering*, *61*(2), 362–367. https://doi.org/10.1109/TBME.2013.2279636
Grood, E. S., & Suntay, W. J. (1983). A joint coordinate system for the clinical description of three-dimensional motions: application to the knee. *Journal of Biomechanical Engineering*, *105*(2), 136–144. https://doi.org/10.1115/1.3138397
Gruber, K., Ruder, H., Denoth, J., & Schneider, K. (1998). A comparative study of impact dynamics: wobbling mass model versus rigid body models. *Journal of Biomechanics*, *31*(5), 439–444. https://doi.org/10.1016/S0021-9290(98)00033-5
Hara, R., Sangeux, M., Baker, R., & McGinley, J. (2014). Quantification of pelvic soft tissue artifact in multiple static positions. *Gait & Posture*, *39*(2), 712–717. https://doi.org/10.1016/J.GAITPOST.2013.10.001
Harrington, M. E., Zavatsky, A. B., Lawson, S. E. M., Yuan, Z., & Theologis, T. N. (2007). Prediction of the hip joint centre in adults, children, and patients with cerebral palsy based on magnetic resonance imaging. *Journal of Biomechanics*, *40*(3), 595–602. https://doi.org/10.1016/J.JBIOMECH.2006.02.003
Hemmerich, A., Brown, H., Smith, S., Marthandam, S. S. K., & Wyss, U. P. (2006). Hip, knee, and ankle kinematics of high range of motion activities of daily living. *Journal of Orthopaedic Research*, *24*(4), 770–781. https://doi.org/10.1002/jor.20114
Henriksen, M., Creaby, M. W., Lund, H., Juhl, C., & Christensen, R. (2014). Is there a causal link between knee loading and knee osteoarthritis progression? A systematic review and meta-analysis of cohort studies and randomised trials. *BMJ Open*, *4*(7), e005368. https://doi.org/10.1136/bmjopen-2014-005368
Hofer, J. K., Gejo, R., McGarry, M. H., & Lee, T. Q. (2011). Effects on tibiofemoral biomechanics from kneeling. *Clinical Biomechanics*, *26*(6), 605–611. https://doi.org/10.1016/J.CLINBIOMECH.2011.01.016
Holden, J. P., Orsini, J. A., Siegel, K. L., Kepple, T. M., Gerber, L. H., & Stanhope, S. J. (1997). Surface movement errors in shank kinematics and knee kinetics during gait. *Gait & Posture*, *5*(3), 217–227. https://doi.org/10.1016/S0966-6362(96)01088-0
Howarth, S. J., & Callaghan, J. P. (2009). The rule of 1 s for padding kinematic data prior

to digital filtering: Influence of sampling and filter cutoff frequencies. *Journal of Electromyography and Kinesiology*, *19*(5), 875–881. https://doi.org/10.1016/J.JELEKIN.2008.03.010

Howarth, S. J., & Callaghan, J. P. (2010). Quantitative assessment of the accuracy for three interpolation techniques in kinematic analysis of human movement. *Computer Methods in Biomechanics and Biomedical Engineering*, *13*(6), 847–855. https://doi.org/10.1080/10255841003664701

Iwaki, H., Pinskerova, V., & Freeman, M. A. (2000). Tibiofemoral movement 1: the shapes and relative movements of the femur and tibia in the unloaded cadaver knee. *The Journal of Bone and Joint Surgery. British Volume*, *82*(8), 1189–1195. https://doi.org/10.1302/0301-620x.82b8.10717

Jensen, L. K. (2005). Knee-straining work activities, self-reported knee disorders and radiographically determined knee osteoarthritis. *Scandinavian Journal of Work, Environment & Health*, *31 Suppl 2*, 68–74. http://www.ncbi.nlm.nih.gov/pubmed/16363449

Jensen, L. K. (2008). Knee osteoarthritis: influence of work involving heavy lifting, kneeling, climbing stairs or ladders, or kneeling/squatting combined with heavy lifting. *Occupational and Environmental Medicine*, *65*(2), 72–89. https://doi.org/10.1136/oem.2007.032466

Jia, R., Monk, P., Murray, D., Noble, J. A., & Mellon, S. (2017). CAT & MAUS: A novel system for true dynamic motion measurement of underlying bony structures with compensation for soft tissue movement. *Journal of Biomechanics*, *62*, 156–164. https://doi.org/10.1016/J.JBIOMECH.2017.04.015

Johal, P., Williams, A., Wragg, P., Hunt, D., & Gedroyc, W. (2005). Tibio-femoral movement in the living knee. A study of weight bearing and non-weight bearing knee kinematics using 'interventional' MRI. *Journal of Biomechanics*, *38*(2), 269–276. https://doi.org/10.1016/J.JBIOMECH.2004.02.008

Karlsson, D., & Tranberg, R. (1999). On skin movement artefact-resonant frequencies of skin markers attached to the leg. *Human Movement Science*, *18*(5), 627–635. https://doi.org/10.1016/S0167-9457(99)00025-1

Kessler, M. A., Behrend, H., Henz, S., Stutz, G., Rukavina, A., & Kuster, M. S. (2008). Function, osteoarthritis and activity after ACL-rupture: 11 Years follow-up results of conservative versus reconstructive treatment. *Knee Surgery, Sports Traumatology, Arthroscopy*, *16*(5), 442–448. https://doi.org/10.1007/s00167-008-0498-x

Kingston, D. C., & Acker, S. M. (2018). Thigh-calf contact parameters for six high knee flexion postures: Onset, maximum angle, total force, contact area, and center of force. *Journal of Biomechanics*, *67*, 46–54. https://doi.org/10.1016/j.jbiomech.2017.11.022

Koo, T. K., & Li, M. Y. (2016). A Guideline of Selecting and Reporting Intraclass Correlation Coefficients for Reliability Research. *Journal of Chiropractic Medicine*, *15*(2), 155–163. https://doi.org/10.1016/j.jcm.2016.02.012

Kuo, M.-Y., Tsai, T.-Y., Lin, C.-C., Lu, T.-W., Hsu, H.-C., & Shen, W.-C. (2011). Influence of soft tissue artifacts on the calculated kinematics and kinetics of total knee replacements during sit-to-stand. *Gait & Posture*, *33*(3), 379–384. https://doi.org/10.1016/J.GAITPOST.2010.12.007

Kutzner, I., Heinlein, B., Graichen, F., Bender, A., Rohlmann, A., Halder, A., Beier, A., & Bergmann, G. (2010). Loading of the knee joint during activities of daily living

measured in vivo in five subjects. *Journal of Biomechanics*, *43*(11), 2164–2173. https://doi.org/10.1016/J.JBIOMECH.2010.03.046

Lakens, D. (2013). Calculating and reporting effect sizes to facilitate cumulative science: a practical primer for t-tests and ANOVAs. *Frontiers in Psychology*, *4*, 863. https://doi.org/10.3389/fpsyg.2013.00863

Leardini, A., Chiari, L., Croce, U. Della, Cappozzo, A., Chiari, A., Della Croce, U., Cappozzo, A., Chiari, L., Croce, U. Della, & Cappozzo, A. (2005). Human movement analysis using stereophotogrammetry Part 3. Soft tissue artifact assessment and compensation. *Gait and Posture*, *21*(2), 212–225. https://doi.org/10.1016/j.gaitpost.2004.05.002

Legendre, P., & Legendre, L. (2012). *Numerical Ecology* (3rd ed.). Elsevier.

Leszko, F., Hovinga, K. R., Lerner, A. L., Komistek, R. D., & Mahfouz, M. R. (2011). In Vivo Normal Knee Kinematics: Is Ethnicity or Gender an Influencing Factor? *Clinical Orthopaedics and Related Research*, *469*(1), 95–106. https://doi.org/10.1007/s11999-010-1517-z

Li, K., Zheng, L., Tashman, S., & Zhang, X. (2012). The inaccuracy of surface-measured model-derived tibiofemoral kinematics. *Journal of Biomechanics*, *45*(15), 2719–2723. https://doi.org/10.1016/J.JBIOMECH.2012.08.007

Longpré, H. S., Potvin, J. R., & Maly, M. R. (2013). Biomechanical changes at the knee after lower limb fatigue in healthy young women. *Clinical Biomechanics*, *28*(4), 441–447. https://doi.org/10.1016/J.CLINBIOMECH.2013.02.010

Lu, T.-W., & O'Connor, J. J. (1999). Bone position estimation from skin marker co-ordinates using global optimisation with joint constraints. *Journal of Biomechanics*, *32*(2), 129–134. https://doi.org/10.1016/S0021-9290(98)00158-4

Lucchetti, L., Cappozzo, A., Cappello, A., & Croce, U. Della. (1998). Skin movement artefact assessment and compensation in the estimation of knee-joint kinematics. *Journal of Biomechanics*, *31*(11), 977–984. https://doi.org/10.1016/S0021-9290(98)00083-9

Manal, K., Davis, I., Galinat, B., & Stanhope, S. (2003). The accuracy of estimating proximal tibial translation during natural cadence walking: bone vs. skin mounted targets. *Clinical Biomechanics*, *18*(2), 126–131. https://doi.org/10.1016/S0268-0033(02)00176-6

Manal, K., McClay, I., Stanhope, S., Richards, J., & Galinat, B. (2000). Comparison of surface mounted markers and attachment methods in estimating tibial rotations during walking: an in vivo study. *Gait & Posture*, *11*(1), 38–45. https://doi.org/10.1016/S0966-6362(99)00042-9

McKinnon, C. D., & Callaghan, J. P. (2019). Validation of an Ultrasound Protocol to Measure Intervertebral Axial Twist during Functional Twisting Movements in Isolated Functional Spinal Units. *Ultrasound in Medicine & Biology*, *45*(3), 642–649. https://doi.org/10.1016/J.ULTRASMEDBIO.2018.10.023

Mehta, B. V., Rajani, S., & Sinha, G. (1997). Comparison of image processing techniques (Magnetic resonance imaging, computed tomography scan and ultrasound) for 3D modeling and analysis of the human bones. *Journal of Digital Imaging*, *10*(S1), 203–206. https://doi.org/10.1007/BF03168701

Miranda, D. L., Rainbow, M. J., Crisco, J. J., & Fleming, B. C. (2013). Kinematic differences between optical motion capture and biplanar videoradiography during a

jump-cut maneuver. *Journal of Biomechanics*, *46*(3), 567–573. https://doi.org/10.1016/j.jbiomech.2012.09.023

Mok, K. M., Kristianslund, E. K., & Krosshaug, T. (2015). The effect of thigh marker placement on knee valgus angles in vertical drop jumps and sidestep cutting. *Journal of Applied Biomechanics*, *31*(4), 269–274. https://doi.org/10.1123/jab.2014-0137

Mukaka, M. M. (2012). Statistics corner: A guide to appropriate use of correlation coefficient in medical research. *Malawi Medical Journal : The Journal of Medical Association of Malawi*, *24*(3), 69–71. http://www.ncbi.nlm.nih.gov/pubmed/23638278

Mündermann, A., Dyrby, C. O., D'Lima, D. D., Colwell, C. W., & Andriacchi, T. P. (2008). In vivo knee loading characteristics during activities of daily living as measured by an instrumented total knee replacement. *Journal of Orthopaedic Research*, *26*(9), 1167–1172. https://doi.org/10.1002/jor.20655

Mündermann, A., Dyrby, C. O., Hurwitz, D. E., Sharma, L., & Andriacchi, T. P. (2004). Potential strategies to reduce medial compartment loading in patients with knee osteoarthritis of varying severity: reduced walking speed. *Arthritis and Rheumatism*, *50*(4), 1172–1178. https://doi.org/10.1002/art.20132

Myles, C. M., Rowe, P. J., Walker, C. R. C., & Nutton, R. W. (2002). Knee joint functional range of movement prior to and following total knee arthroplasty measured using flexible electrogoniometry. In *Gait and Posture* (Vol. 16). www.elsevier.com/locate/gaitpost

Nagura, T., Dyrby, C. O., Alexander, E. J., & Andriacchi, T. P. (2002). Mechanical loads at the knee joint during deep flexion. *Journal of Orthopaedic Research*, *20*(4), 881–886. https://doi.org/10.1016/S0736-0266(01)00178-4

Nagura, T., Matsumoto, H., Kiriyama, Y., Chaudhari, A., & Andriacchi, T. P. (2006). Tibiofemoral joint contact force in deep knee flexion and its consideration in knee osteoarthritis and joint replacement. *Journal of Applied Biomechanics*, *22*(4), 305–313. https://doi.org/10.1123/jab.22.4.305

Nakagawa, S., Kadoya, Y., Kobayashi, A., Yamano, Y., Todo, S., Fellow, R., Sakamoto, H., Nakagawa, S., Freeman, M. A. R., Kadoya, Y., Todo, S., Kobayashi, A., Sakamoto, H., Freeman, M. A. R., & Yamano, Y. (2000). Tibiofemoral movement 3: full flexion in the living knee studied by MRI. *Journal of Bone and Joint Surgery (Br)*, *8*, 1199–1200. https://doi.org/10.1302/0301-620X.82B8.0821199

Peters, A., Galna, B., Sangeux, M., Morris, M., & Baker, R. (2010). Quantification of soft tissue artifact in lower limb human motion analysis: A systematic review. *Gait & Posture*, *31*(1), 1–8. https://doi.org/10.1016/J.GAITPOST.2009.09.004

Pollard, J. P., Porter, W. L., & Redfern, M. S. (2011). Forces and Moments on the Knee During Kneeling and Squatting. In *Journal of Applied Biomechanics* (Vol. 27). https://journals.humankinetics.com/doi/pdf/10.1123/jab.27.3.233

Potvin, B. M., Shourijeh, M. S., Smale, K. B., & Benoit, D. L. (2017). A practical solution to reduce soft tissue artifact error at the knee using adaptive kinematic constraints. *Journal of Biomechanics*, *62*, 124–131. https://doi.org/10.1016/J.JBIOMECH.2017.02.006

Reinbolt, J. A., Schutte, J. F., Fregly, B. J., Koh, B. Il, Haftka, R. T., George, A. D., & Mitchell, K. H. (2005). Determination of patient-specific multi-joint kinematic models through two-level optimization. *Journal of Biomechanics*, *38*(3), 621–626. https://doi.org/10.1016/J.JBIOMECH.2004.03.031

Reinschmidt, C., van den Bogert, A. ., Lundberg, A., Nigg, B. M., Murphy, N., Stacoff, A., & Stano, A. (1997). Tibiofemoral and tibiocalcaneal motion during walking: external vs. skeletal markers. *Gait & Posture*, *6*(2), 98–109. https://doi.org/10.1016/S0966-6362(97)01110-7

Reinschmidt, C., van den Bogert, A. J., Nigg, B. M., Lundberg, A., & Murphy, N. (1997). Effect of skin movement on the analysis of skeletal knee joint motion during running. *Journal of Biomechanics*, *30*(7), 729–732. https://doi.org/10.1016/S0021-9290(97)00001-8

Richard, V., Cappozzo, A., & Dumas, R. (2017). Comparative assessment of knee joint models used in multi-body kinematics optimisation for soft tissue artefact compensation. *Journal of Biomechanics*, *62*, 95–101. https://doi.org/10.1016/J.JBIOMECH.2017.01.030

Rozumalski, A., Schwartz, M. H., Novacheck, T. F., Wervey, R., Swanson, A., & Dykes, D. C. (2007). Quantification of pelvis soft tissue artifact. *Gait and Clinical Movement Analysis Society*, 10–11.

Rytter, S., Egund, N., Jensen, L. K., & Bonde, J. P. (2009). Occupational kneeling and radiographic tibiofemoral and patellofemoral osteoarthritis. *Journal of Occupational Medicine and Toxicology*, *4*(1), 19. https://doi.org/10.1186/1745-6673-4-19

Ryu, T. (2012). Application of Soft Tissue Artifact Compensation Using Displacement Dependency between Anatomical Landmarks and Skin Markers. *Anatomy Research International*, *2012*, 123713. https://doi.org/10.1155/2012/123713

Ryu, T., Choi, H. S., & Chung, M. K. (2009). Soft tissue artifact compensation using displacement dependency between anatomical landmarks and skin markers - a preliminary study. *International Journal of Industrial Ergonomics*, *39*, 152–158. https://doi.org/10.1016/j.ergon.2008.05.005

Sati, M., de Guise, J. A., Larouche, S., & Drouin, G. (1996). Quantitative assessment of skin-bone movement at the knee. *The Knee*, *3*(3), 121–138. https://doi.org/10.1016/0968-0160(96)00210-4

Schielzeth, H. (2010). Simple means to improve the interpretability of regression coefficients. *Methods in Ecology and Evolution*, *1*(2), 103–113. https://doi.org/10.1111/j.2041-210x.2010.00012.x

Schwartz, M. H., & Rozumalski, A. (2005). A new method for estimating joint parameters from motion data. *Journal of Biomechanics*, *38*(1), 107–116. https://doi.org/10.1016/J.JBIOMECH.2004.03.009

Smith, S. M., Cockburn, R. A., Hemmerich, A., Li, R. M., & Wyss, U. P. (2008). Tibiofemoral joint contact forces and knee kinematics during squatting. *Gait & Posture*, *27*(3), 376–386. https://doi.org/10.1016/j.gaitpost.2007.05.004

Söderkvist, I., & Wedin, P.-Å. A. (1993). Determining the movements of the skeleton using well-configured markers. *Journal of Biomechanics*, *26*(12). https://doi.org/10.1016/0021-9290(93)90098-Y

Stagni, R., Fantozzi, S., & Cappello, A. (2006). Propagation of anatomical landmark misplacement to knee kinematics: Performance of single and double calibration. *Gait & Posture*, *24*(2), 137–141. https://doi.org/10.1016/J.GAITPOST.2006.08.001

Stagni, R., Fantozzi, S., & Cappello, A. (2009). Double calibration vs. global optimisation: Performance and effectiveness for clinical application. *Gait & Posture*, *29*(1), 119–122. https://doi.org/10.1016/J.GAITPOST.2008.07.008

Stagni, R., Fantozzi, S., Cappello, A., & Leardini, A. (2005). Quantification of soft tissue artefact in motion analysis by combining 3D fluoroscopy and stereophotogrammetry: a study on two subjects. *Clinical Biomechanics*, *20*(3), 320–329. https://doi.org/10.1016/J.CLINBIOMECH.2004.11.012

Stagni, R., Leardini, A., Cappozzo, A., Benedetti, M. G., & Cappello, A. (2000). Effects of hip joint centre mislocation on gait analysis results. *Journal of Biomechanics*, *33*, 1479–1487. https://doi.org/10.1016/s0021-9290(00)00093-2

Stewart, A., & Marfell-Jones, M. (2011). *International Standards for Anthropometric Assessment* (3rd ed.). International Society for the Advancement of Kinanthropometry.

Steyerberg, E. W., C Eijkemans, M. J., Harrell Jr, F. E., & Habbema, J. F. (2001). Prognostic Modeling with Logistic Regression Analysis: In Search of a Sensible Strategy in Small Data Sets. *Medical DecisionMaking*, *21*(1), 45–56. https://doi.org/https://doi.org/10.1177/0272989X0102100106

Südhoff, I., Van Driessche, S., Laporte, S., de Guise, J. A., & Skalli, W. (2007). Comparing three attachment systems used to determine knee kinematics during gait. *Gait & Posture*, *25*(4), 533–543. https://doi.org/10.1016/J.GAITPOST.2006.06.002

Sumner, B., McCamley, J., Jacofsky, D. J., & Jacofsky, M. C. (2019). Comparison of Knee Kinematics and Kinetics during Stair Descent in Single- and Multi-Radius Total Knee Arthroplasty. *The Journal of Knee Surgery*. https://doi.org/10.1055/s-0039-1692652

Tashman, S., & Anderst, W. (2003). In-Vivo Measurement of Dynamic Joint Motion Using High Speed Biplane Radiography and CT: Application to Canine ACL Deficiency. *Journal of Biomechanical Engineering*, *125*(2), 238. https://doi.org/10.1115/1.1559896

Tashman, S., Kolowich, P., Collon, D., Anderson, K., & Anderst, W. (2007). Dynamic function of the ACL-reconstructed knee during running. *Clinical Orthopaedics and Related Research*, *454*, 66–73. https://doi.org/10.1097/BLO.0b013e31802bab3e

Thambyah, A., Goh, J. C. H., & De, S. Das. (2005). Contact stresses in the knee joint in deep flexion. *Medical Engineering & Physics*, *27*(4), 329–335. https://doi.org/10.1016/J.MEDENGPHY.2004.09.002

Thun, M., Tanaka, S., Smith, A. B., Halperin, W. E., Lee, S. T., Luggen, M. E., & Hess, E. V. (1987). Morbidity from repetitive knee trauma in carpet and floor layers. *British Journal of Industrial Medicine*, *44*(9), 611–620. https://doi.org/10.1136/oem.44.9.611

Tsai, T.-Y., Lu, T.-W., Kuo, M.-Y., & Hsu, H.-C. (2009). Quantification of three-dimensional movement of skin markers relative to the underlying bones during functional activities. *Biomedical Engineering: Applications, Basis and Communications*, *21*(03), 223–232. https://doi.org/10.4015/S1016237209001283

Tsai, T.-Y., Lu, T.-W., Kuo, M.-Y., & Lin, C.-C. (2011). Effects of soft tissue artifacts on the calculated kinematics and kinetics of the knee during stair-ascent. *Journal of Biomechanics*, *44*(6), 1182–1188. https://doi.org/10.1016/J.JBIOMECH.2011.01.009

Veldpaus, F. E., Woltring, H. J., & Dortmans, L. J. M. G. (1988). A least-squares algorithm for the equiform transformation from spatial marker co-ordinates. *Journal of Biomechanics*, *21*(1), 45–54. https://doi.org/10.1016/0021-9290(88)90190-X

Verdini, F., Zara, C., Leo, T., Mengarelli, A., Cardarelli, S., & Innocenti, B. (2017). Assessment of patient functional performance in different knee arthroplasty designs during unconstrained squat. *Muscles, Ligaments and Tendons Journal*, *7*(3), 514.

https://doi.org/10.11138/MLTJ/2017.7.3.514
Winter, D. A. (2009). *Biomechanics and motor control of human movement* (4th ed.). Wiley.
Wu, G., & Cavanagh, P. R. (1995). ISB recommendations for standardization in the reporting of kinematic data. *Journal of Biomechanics*, *28*(10), 1257–1261. https://doi.org/10.1016/0021-9290(95)00017-C
Wu, G., Siegler, S., Allard, P., Kirtley, C., Leardini, A., Rosenbaum, D., Whittle, M., D'Lima, D. D., Cristofolini, L., Witte, H., Schmid, O., Stokes, I., & Standardization and Terminology Committee of the International Society of Biomechanics. (2002). ISB recommendation on definitions of joint coordinate system of various joints for the reporting of human joint motion--part I: ankle, hip, and spine. International Society of Biomechanics. *Journal of Biomechanics*, *35*(4), 543–548. https://doi.org/10.1016/s0021-9290(01)00222-6
Yamazaki, J., Muneta, T., Ju, Y. J., & Sekiya, I. (2010). Differences in kinematics of single leg squatting between anterior cruciate ligament-injured patients and healthy controls. *Knee Surgery, Sports Traumatology, Arthroscopy*, *18*(1), 56–63. https://doi.org/10.1007/s00167-009-0892-z
Yao, J., Lancianese, S. L., Hovinga, K. R., Lee, J., & Lerner, A. L. (2008). Magnetic resonance image analysis of meniscal translation and tibio-menisco-femoral contact in deep knee flexion. *Journal of Orthopaedic Research*, *26*(5), 673–684. https://doi.org/10.1002/jor.20553
Zabala, M. E., Favre, J., Scanlan, S. F., Donahue, J., & Andriacchi, T. P. (2013). Three-dimensional knee moments of ACL reconstructed and control subjects during gait, stair ascent, and stair descent. *Journal of Biomechanics*, *46*(3), 515–520. https://doi.org/10.1016/j.jbiomech.2012.10.010
Zelle, J., Barink, M., De Waal Malefijt, M., & Verdonschot, N. (2009). Thigh–calf contact: Does it affect the loading of the knee in the high-flexion range? *Journal of Biomechanics*, *42*(5), 587–593. https://doi.org/10.1016/J.JBIOMECH.2008.12.015
Zelle, J., Barink, M., Loeffen, R., De Waal Malefijt, M., & Verdonschot, N. (2007). Thigh–calf contact force measurements in deep knee flexion. *Clinical Biomechanics*, *22*(7), 821–826. https://doi.org/10.1016/J.CLINBIOMECH.2007.03.009
Zeller, B. L., McCrory, J. L., Kibler, W. Ben, Uhl, T. L., Ben Kibler, W., & Uhl, T. L. (2003). Differences in Kinematics and Electromyographic Activity Between Men and Women during the Singel-Legged Squat. *American Journal of Sports Medicine*, *31*(3), 449–456. https://doi.org/10.1177/03635465030310032101
Zhao, D., Banks, S. A., D'Lima, D. D., Colwell, C. W., & Fregly, B. J. (2007). In vivo medial and lateral tibial loads during dynamic and high flexion activities. *Journal of Orthopaedic Research*, *25*(5), 593–602. https://doi.org/10.1002/jor.20362

Appendices

Appendix A: Anatomical Coordinate System Definition

The following section outlines segment coordinate system definition, utilized for calculating knee joint angles and moments in study one, in conjunction with ISB guidelines (Wu et al., 2002; Wu & Cavanagh, 1995). The digitized greater trochanter, and lateral and medial femoral condyles were identical between the thigh clusters localized to the same leg.

Table 5-1: Thigh coordinate system

Origin	Functional hip joint center (Camomilla et al., 2006; Ehrig et al., 2006)
YZ plane	Plane defined by origin, greater trochanter, and lateral and medial border of the knee joint (points projected from the lateral and medial femoral condyles along the knee functional axis of rotation)
Y-axis	Vector from the functional knee joint center to origin
X-axis	Vector perpendicular YZ plane (anterior)
Z-axis	Perpendicular vector calculated from cross-product of X-axis and Y-axis

Table 5-2: Shank coordinate system

Origin	Functional knee joint center
YZ plane	Plane defined by lateral and medial malleoli and lateral and medial border of the knee joint (points projected from the lateral and medial femoral condyles along the knee functional axis of rotation)
Y-axis	Vector from midpoint of medial and lateral malleoli to the origin
X-axis	Vector perpendicular YZ plane (anterior)
Z-axis	Perpendicular vector calculated from cross-product of X-axis and Y-axis

Appendix B: Bland-Altman Mean Difference and Limits of Agreement Values

Table 5-3: Mean of the peak difference (bolded) and limits of agreement (italicized in brackets) for the estimated position (cm) of the hip joint center and femoral head center for each task. Sym is symmetrical, lead is lead leg, and trail is trail leg. * indiciates sample size less than 50 subjects due to marker obstruction (FS: n = 31, 48, 14, 48, 47, 48; HS: n = 48, 50, 45, 50, 49, 50).

Task	Distal-Anterior	Distal-Anterolateral	Distal-Lateral	Mid-Anterior	Mid-Anterolateral	Mid-Lateral
Flat-foot Squat*	**-1.95** *(-7.68 / 3.78)*	**-0.56** *(-4.61 / 3.49)*	**-3.39** *(-7.20 / 0.42)*	**0.03** *(-4.28 / 4.35)*	**-0.92** *(-4.81 / 2.97)*	**-3.22** *(-5.57 / -0.87)*
Heels-up Squat*	**-1.94** *(-6.86 / 2.98)*	**-1.21** *(-5.50 / 3.08)*	**-3.44** *(-9.80 / 2.91)*	**-0.35** *(-5.32 / 4.63)*	**-0.90** *(-4.98 / 3.18)*	**-3.10** *(-5.76 / -0.44)*
Dorsiflexed Kneel (Sym)	**-2.26** *(-5.03 / 0.51)*	**-2.41** *(-4.81 / -0.01)*	**-3.35** *(-7.30 / 0.60)*	**-1.00** *(-3.27 / 1.28)*	**-1.26** *(-3.29 / 0.77)*	**-1.72** *(-3.72 / 0.29)*
Plantarflexed Kneel (Sym)	**-2.04** *(-5.59 / 1.51)*	**-2.08** *(-5.48 / 1.31)*	**-3.26** *(-7.43 / 0.91)*	**-0.85** *(-4.11 / 2.41)*	**-1.17** *(-4.12 / 1.79)*	**-2.18** *(-5.05 / 0.69)*
Dorsiflexed Kneel (Lead)	**-1.92** *(-8.92 / 5.08)*	**-2.01** *(-6.68 / 2.66)*	**-4.93** *(-11.86 / 2.00)*	**-0.47** *(-5.88 / 4.95)*	**-1.50** *(-5.85 / 2.85)*	**-3.02** *(-7.25 / 1.21)*
Plantarflexed Kneel (Lead)	**-1.73** *(-8.38 / 4.92)*	**-1.60** *(-6.79 / 3.59)*	**-4.56** *(-11.51 / 2.38)*	**-0.29** *(-5.92 / 5.33)*	**-1.12** *(-5.46 / 3.22)*	**-2.98** *(-6.82 / 0.86)*
Dorsiflexed Kneel (Trail)	**-2.01** *(-7.98 / 3.97)*	**-1.81** *(-5.62 / 1.99)*	**-4.67** *(-11.61 / 2.28)*	**-0.21** *(-4.91 / 4.49)*	**-1.00** *(-4.51 / 2.51)*	**-2.80** *(-5.41 / -0.18)*
Plantarflexed Kneel (Trail)	**-1.85** *(-8.04 / 4.33)*	**-1.75** *(-5.85 / 2.35)*	**-4.30** *(-10.90 / 2.30)*	**-0.39** *(-5.49 / 4.70)*	**-1.32** *(-4.83 / 2.20)*	**-2.74** *(-6.00 / 0.51)*

Table 5-4: Mean difference (bolded) and limits of agreement (italicized in brackets) for the estimated position (cm) in X (anterior-posterior) of the hip joint center and femoral head center for each movement. Sym is symmetrical, lead is lead leg, and trail is trail leg.

Movement	Distal-Anterior	Distal-Anterolateral	Distal-Lateral	Mid-Anterior	Mid-Anterolateral	Mid-Lateral
Flat-foot Squat	**-1.92** *(-6.22 / 2.38)*	**-3.14** *(-8.11 / 1.83)*	**-2.53** *(-8.06 / 2.99)*	**-0.22** *(-5.31 / 4.86)*	**-2.11** *(-7.04 / 2.82)*	**-2.00** *(-7.16 / 3.16)*
Heels-up Squat	**-1.23** *(-6.32 / 3.86)*	**-2.55** *(-7.52 / 2.41)*	**-1.91** *(-7.77 / 3.96)*	**-0.87** *(-6.04 / 4.29)*	**-1.53** *(-6.37 / 3.32)*	**-1.21** *(-6.45 / 4.03)*
Dorsiflexed Kneel (Sym)	**-1.86** *(-4.98 / 1.26)*	**-1.85** *(-4.58 / 0.88)*	**-2.32** *(-5.65 / 1.00)*	**-0.45** *(-3.54 / 2.64)*	**-0.85** *(-3.68 / 1.97)*	**-1.18** *(-3.86 / 1.50)*
Plantarflexed Kneel (Sym)	**-1.12** *(-5.85 / 3.62)*	**-1.57** *(-6.02 / 2.87)*	**-1.90** *(-7.16 / 3.36)*	**-0.17** *(-4.78 / 4.44)*	**-0.66** *(-4.85 / 3.53)*	**-1.13** *(-5.81 / 3.54)*
Dorsiflexed Kneel (Lead)	**-1.91** *(-7.78 / 3.95)*	**-2.55** *(-7.57 / 2.48)*	**-4.46** *(-10.81 / 1.89)*	**-0.52** *(-5.57 / 4.52)*	**-1.63** *(-6.52 / 3.25)*	**-2.41** *(-6.34 / 1.52)*
Plantarflexed Kneel (Lead)	**-1.72** *(-7.79 / 4.36)*	**-2.38** *(-7.60 / 2.84)*	**-4.38** *(-10.29 / 1.54)*	**-0.61** *(-5.94 / 4.73)*	**-1.58** *(-6.26 / 3.11)*	**-2.30** *(-7.32 / 2.73)*
Dorsiflexed Kneel (Trail)	**-2.51** *(-7.25 / 2.23)*	**-2.97** *(-6.60 / 0.65)*	**-4.96** *(-11.08 / 1.15)*	**-0.59** *(-4.91 / 3.72)*	**-2.02** *(-5.30 / 1.25)*	**-3.08** *(-6.01 / -0.15)*
Plantarflexed Kneel (Trail)	**-2.12** *(-7.35 / 3.11)*	**-2.75** *(-7.25 / 1.76)*	**-4.82** *(-10.71 / 1.07)*	**-0.83** *(-5.81 / 4.14)*	**-2.04** *(-6.26 / 2.18)*	**-2.64** *(-7.27 / 1.99)*

Table 5-5: Mean difference (bolded) and limits of agreement (italicized in brackets) for the estimated position (cm) in Y (vertical) of the hip joint center and femoral head center for each movement. Sym is symmetrical, lead is lead leg, and trail is trail leg.

Movement	Distal-Anterior	Distal-Anterolateral	Distal-Lateral	Mid-Anterior	Mid-Anterolateral	Mid-Lateral
Flat-foot Squat	**-2.01** *(-6.81 / 2.78)*	**-0.59** *(-5.43 / 4.24)*	**-4.33** *(-9.29 / 0.63)*	**-0.23** *(-3.98 / 3.51)*	**-1.28** *(-5.70 / 3.14)*	**-4.55** *(-7.68 / -1.41)*
Heels-up Squat	**-2.39** *(-7.97 / 3.19)*	**-0.79** *(-6.13 / 4.55)*	**-5.01** *(-11.84 / 1.83)*	**-0.03** *(-4.30 / 4.24)*	**-0.99** *(-5.54 / 3.57)*	**-4.25** *(-7.52 / -0.98)*
Dorsiflexed Kneel (Sym)	**-2.82** *(-5.55 / -0.09)*	**-2.77** *(-5.52 / -0.01)*	**-4.65** *(-8.71 / -0.58)*	**-1.53** *(-3.86 / 0.80)*	**-1.41** *(-3.73 / 0.92)*	**-2.16** *(-4.32 / 0.01)*
Plantarflexed Kneel (Sym)	**-2.99** *(-5.87 / -0.11)*	**-3.25** *(-6.37 / -0.13)*	**-5.41** *(-10.10 / -0.71)*	**-1.91** *(-4.56 / 0.75)*	**-1.97** *(-4.70 / 0.75)*	**-3.50** *(-5.95 / -1.05)*
Dorsiflexed Kneel (Lead)	**-2.67** *(-8.11 / 2.77)*	**-0.63** *(-6.02 / 4.75)*	**-5.76** *(-11.52 / -0.01)*	**-0.92** *(-5.33 / 3.50)*	**-0.85** *(-5.61 / 3.90)*	**-3.93** *(-7.30 / -0.55)*
Plantarflexed Kneel (Lead)	**-2.36** *(-7.87 / 3.14)*	**-0.65** *(-6.03 / 4.72)*	**-5.65** *(-12.32 / 1.01)*	**-0.70** *(-5.12 / 3.72)*	**-0.53** *(-5.23 / 4.16)*	**-3.85** *(-7.34 / -0.35)*
Dorsiflexed Kneel (Trail)	**-1.23** *(-7.04 / 4.57)*	**-0.22** *(-4.98 / 4.54)*	**-4.23** *(-9.90 / 1.45)*	**0.75** *(-2.76 / 4.27)*	**0.74** *(-2.80 / 4.28)*	**-1.64** *(-5.30 / 2.02)*
Plantarflexed Kneel (Trail)	**-1.60** *(-7.36 / 4.16)*	**-0.54** *(-5.68 / 4.60)*	**-5.07** *(-11.70 / 1.56)*	**0.19** *(-3.40 / 3.79)*	**0.05** *(-4.20 / 4.29)*	**-2.79** *(-6.12 / 0.54)*

Table 5-6: Mean difference (bolded) and limits of agreement (italicized in brackets) for the estimated position (cm) in Z (medial-lateral) of the hip joint center and femoral head center for each movement. Sym is symmetrical, lead is lead leg, and trail is trail leg.

Movement	Distal-Anterior	Distal-Anterolateral	Distal-Lateral	Mid-Anterior	Mid-Anterolateral	Mid-Lateral
Flat-foot Squat	**-0.31** *(-7.12 / 6.50)*	**0.01** *(-3.80 / 3.83)*	**0.23** *(-4.48 / 4.94)*	**0.16** *(-4.05 / 4.36)*	**0.23** *(-2.75 / 3.21)*	**0.01** *(-2.90 / 2.93)*
Heels-up Squat	**-0.09** *(-5.37 / 5.19)*	**-0.04** *(-4.18 / 4.11)*	**0.03** *(-4.96 / 5.02)*	**0.06** *(-4.95 / 5.08)*	**0.12** *(-2.99 / 3.22)*	**-0.11** *(-3.01 / 2.80)*
Dorsiflexed Kneel (Sym)	**0.04** *(-2.78 / 2.86)*	**-0.24** *(-2.90 / 2.41)*	**-0.03** *(-4.15 / 4.09)*	**-0.06** *(-2.04 / 1.92)*	**-0.12** *(-1.71 / 1.48)*	**-0.20** *(-2.48/ 2.07)*
Plantarflexed Kneel (Sym)	**-0.11** *(-3.53 / 3.30)*	**0.00** *(-3.38 / 3.38)*	**-0.19** *(-4.20 / 3.83)*	**-0.03** *(-2.86 / 2.80)*	**-0.03** *(-2.15 / 2.09)*	**-0.10** *(-2.48/ 2.28)*
Dorsiflexed Kneel (Lead)	**-0.11** *(-6.90 / 6.68)*	**-0.05** *(-5.16 / 5.05)*	**-0.03** *(-6.76 / 6.69)*	**0.05** *(-5.28 / 5.37)*	**0.09** *(-3.33 / 3.51)*	**-0.18** *(-4.92 / 4.56)*
Plantarflexed Kneel (Lead)	**-0.15** *(-7.01 / 6.71)*	**0.02** *(-4.68 / 4.72)*	**0.22** *(-6.35 / 6.78)*	**0.07** *(-5.47 / 5.61)*	**0.28** *(-3.14 / 3.71)*	**0.04** *(-4.38 / 4.46)*
Dorsiflexed Kneel (Trail)	**-0.13** *(-6.35 / 6.04)*	**0.01** *(-3.90 / 4.10)*	**-0.32** *(-5.88 / 5.25)*	**-0.02** *(-5.22 / 5.18)*	**0.10** *(-2.91 / 2.94)*	**-0.41** *(-4.07 / 3.29)*
Plantarflexed Kneel (Trail)	**-0.35** *(-7.01 / 6.31)*	**0.04** *(-4.11 / 4.20)*	**-0.09** *(-5.62 / 5.45)*	**0.00** *(-5.47 / 5.47)*	**0.13** *(-2.87 / 3.12)*	**-0.20** *(-3.60 / 3.19)*

Appendix C: Bland-Altman Plots for Magnitude of 3D Difference

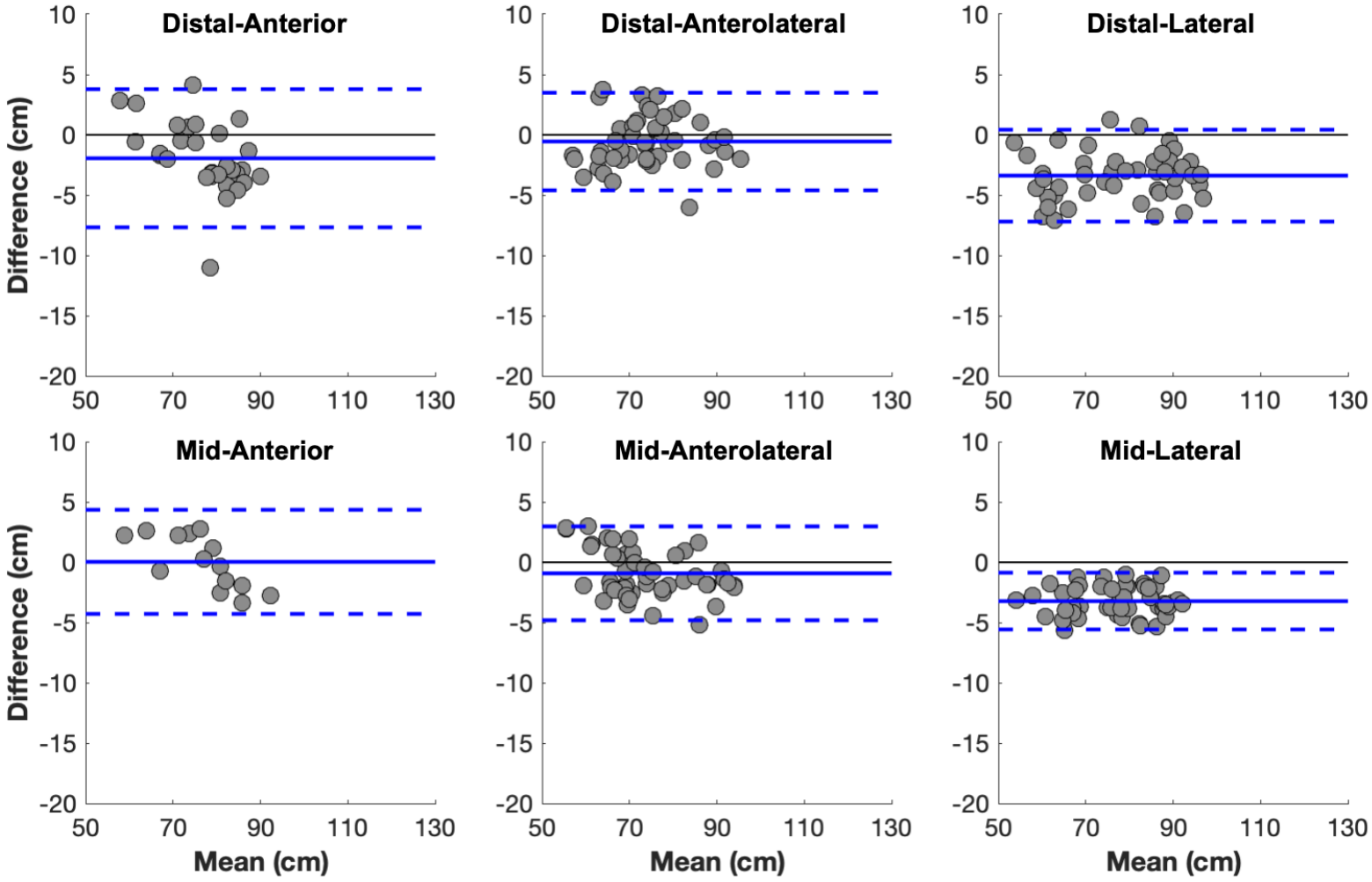

Figure 5-1: Bland-Altman plot for each marker cluster in the flat-foot squat. The solid black line indicates perfect agreement, the solid blue line is the mean difference, and the dashed line is the upper and lower limits of agreement.

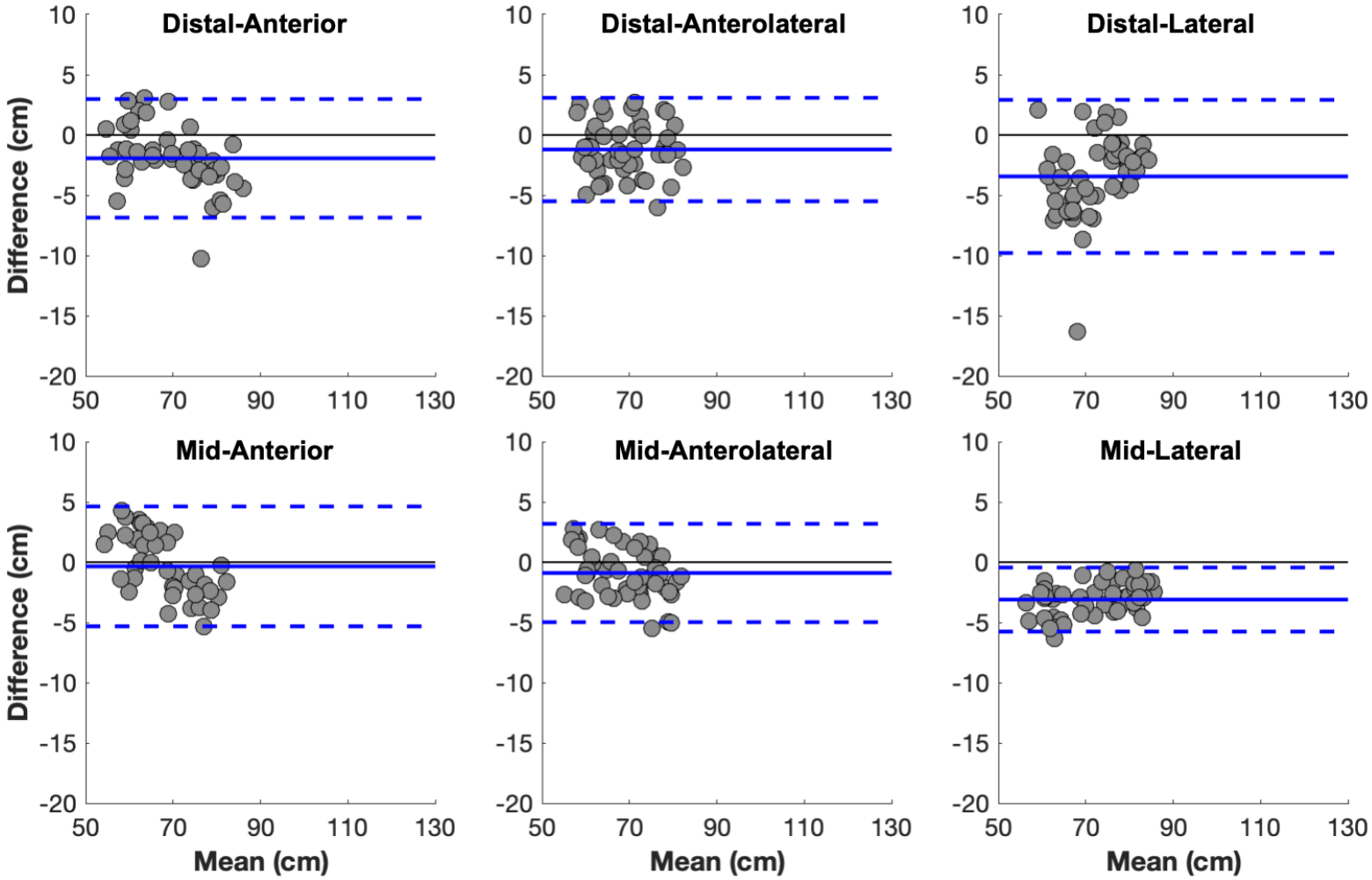

Figure 5-2: Bland-Altman plot for each marker cluster in the heels-up squat. The solid black line indicates perfect agreement, the solid blue line is the mean difference, and the dashed line is the upper and lower limits of agreement.

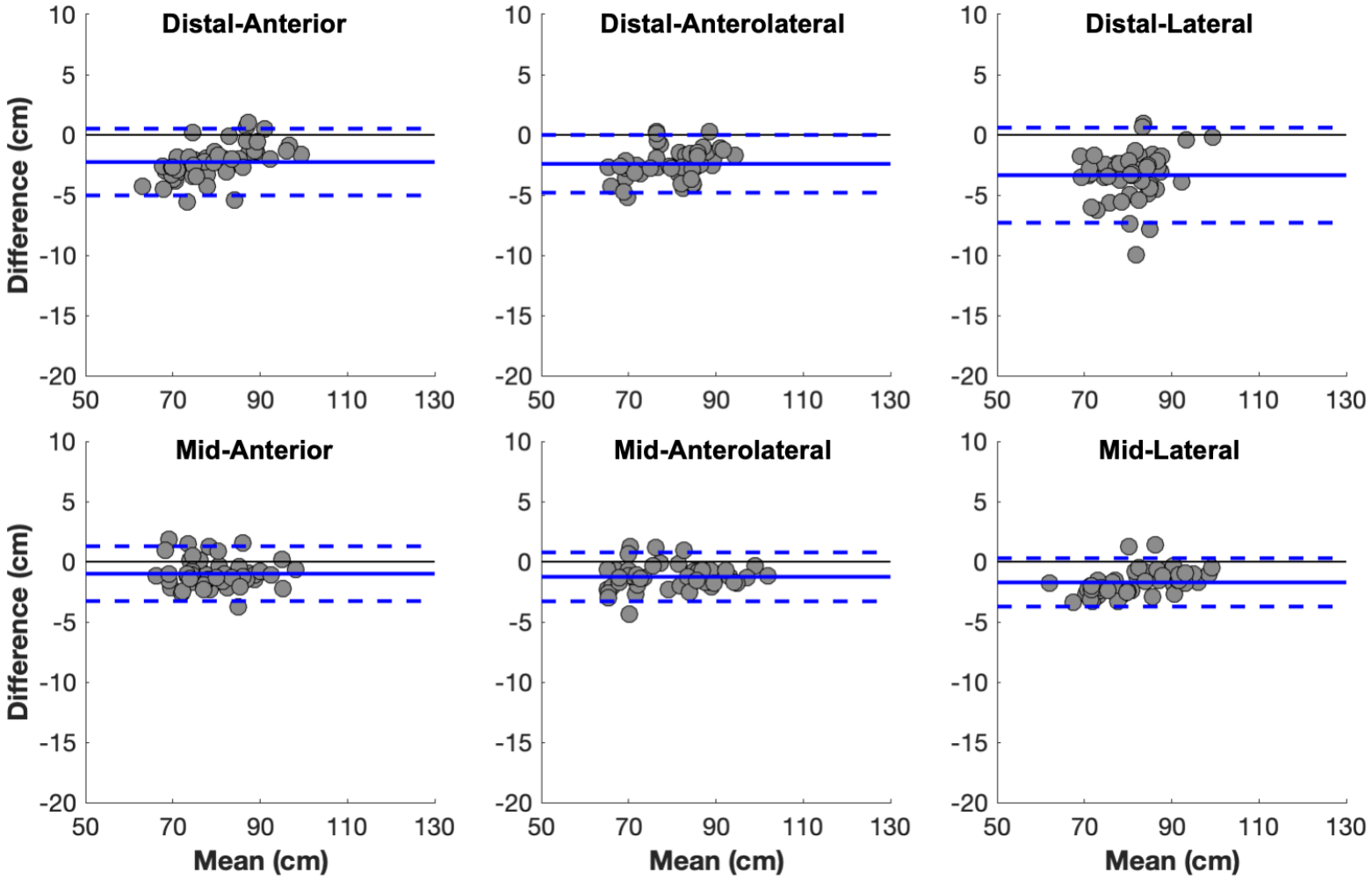

Figure 5-3: Bland-Altman plot for each marker cluster in the symmetrical dorsiflexed kneel. The solid black line indicates perfect agreement, the solid blue line is the mean difference, and the dashed line is the upper and lower limits of agreement.

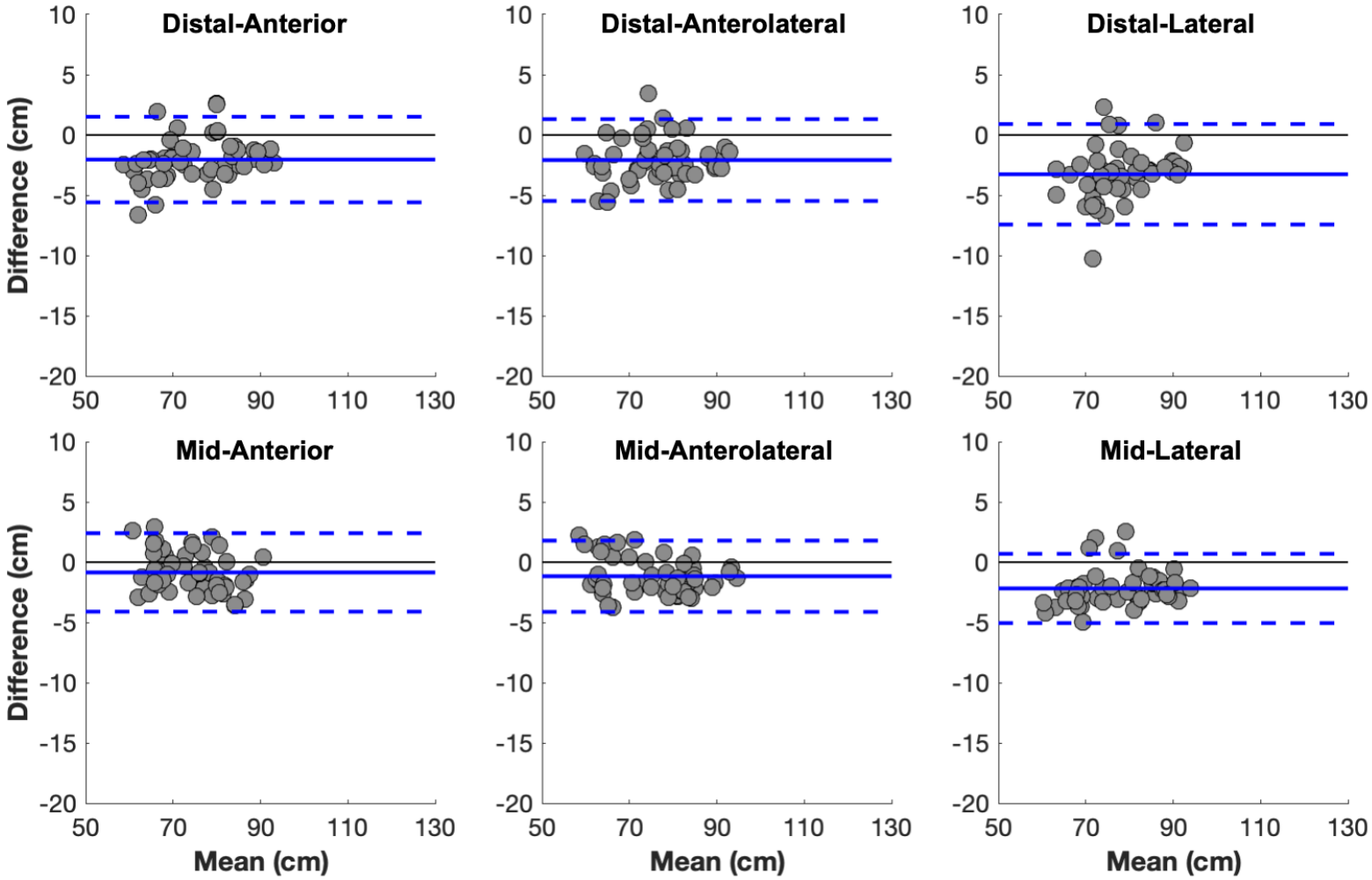

Figure 5-4: Bland-Altman plot for each marker cluster in the symmetrical plantarflexed kneel. The solid black line indicates perfect agreement, the solid blue line is the mean difference, and the dashed line is the upper and lower limits of agreement.

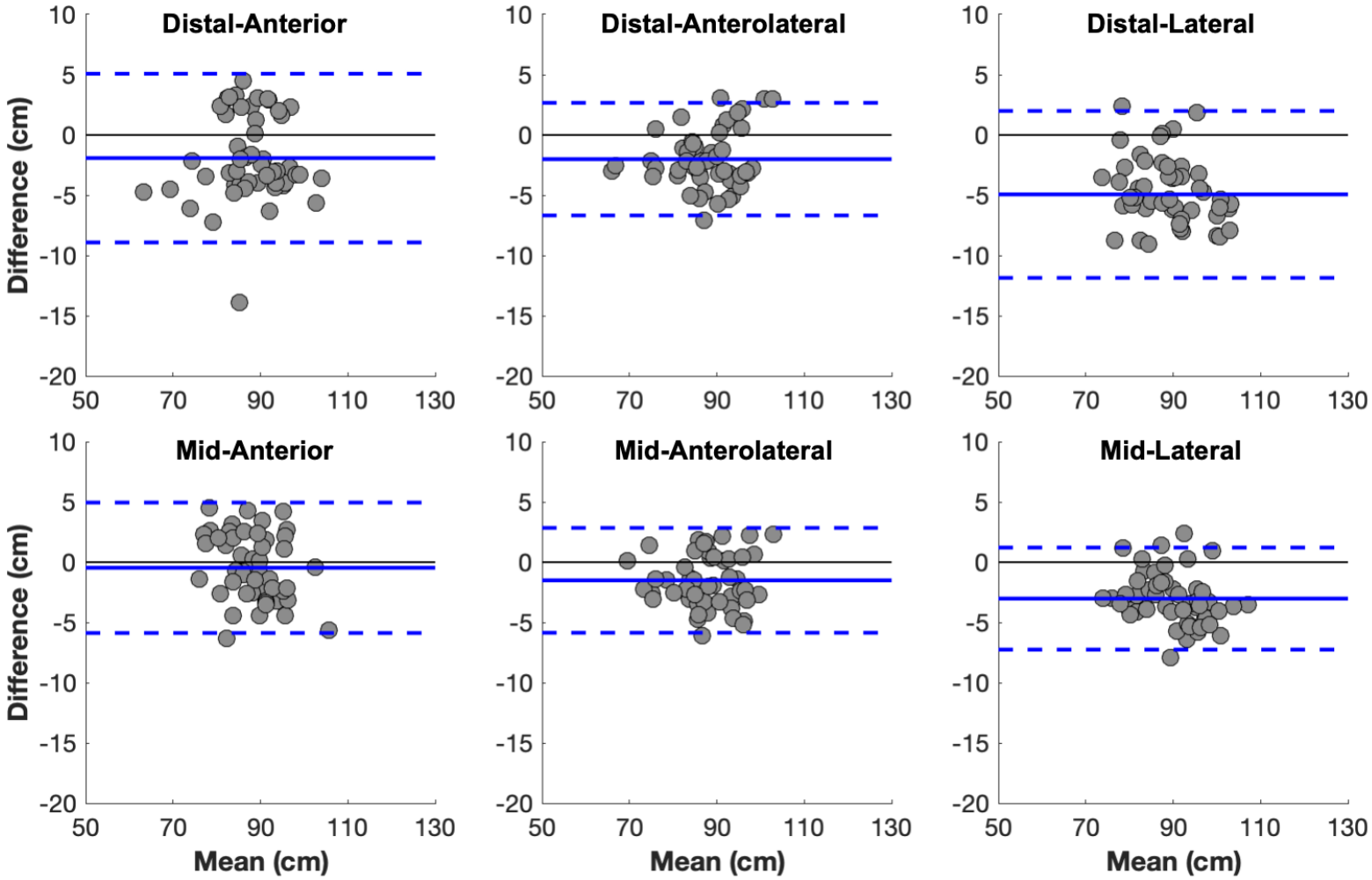

Figure 5-5: Bland-Altman plot for each marker cluster in the lead leg of the dorsiflexed kneel. The solid black line indicates perfect agreement, the solid blue line is the mean difference, and the dashed line is the upper and lower limits of agreement.

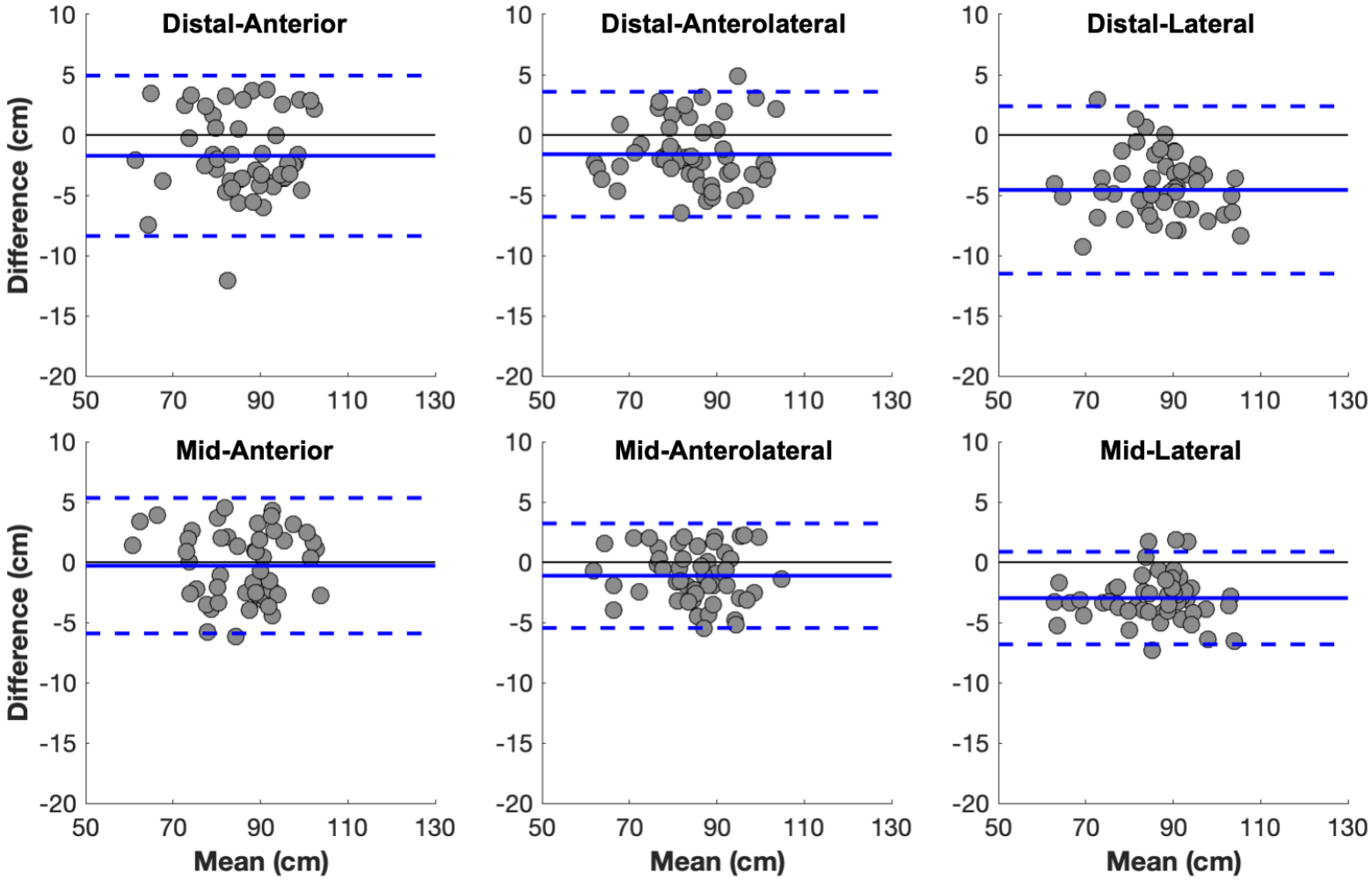

Figure 5-6: Bland-Altman plot for each marker cluster in the lead leg of the plantarflexed kneel. The solid black line indicates perfect agreement, the solid blue line is the mean difference, and the dashed line is the upper and lower limits of agreement.

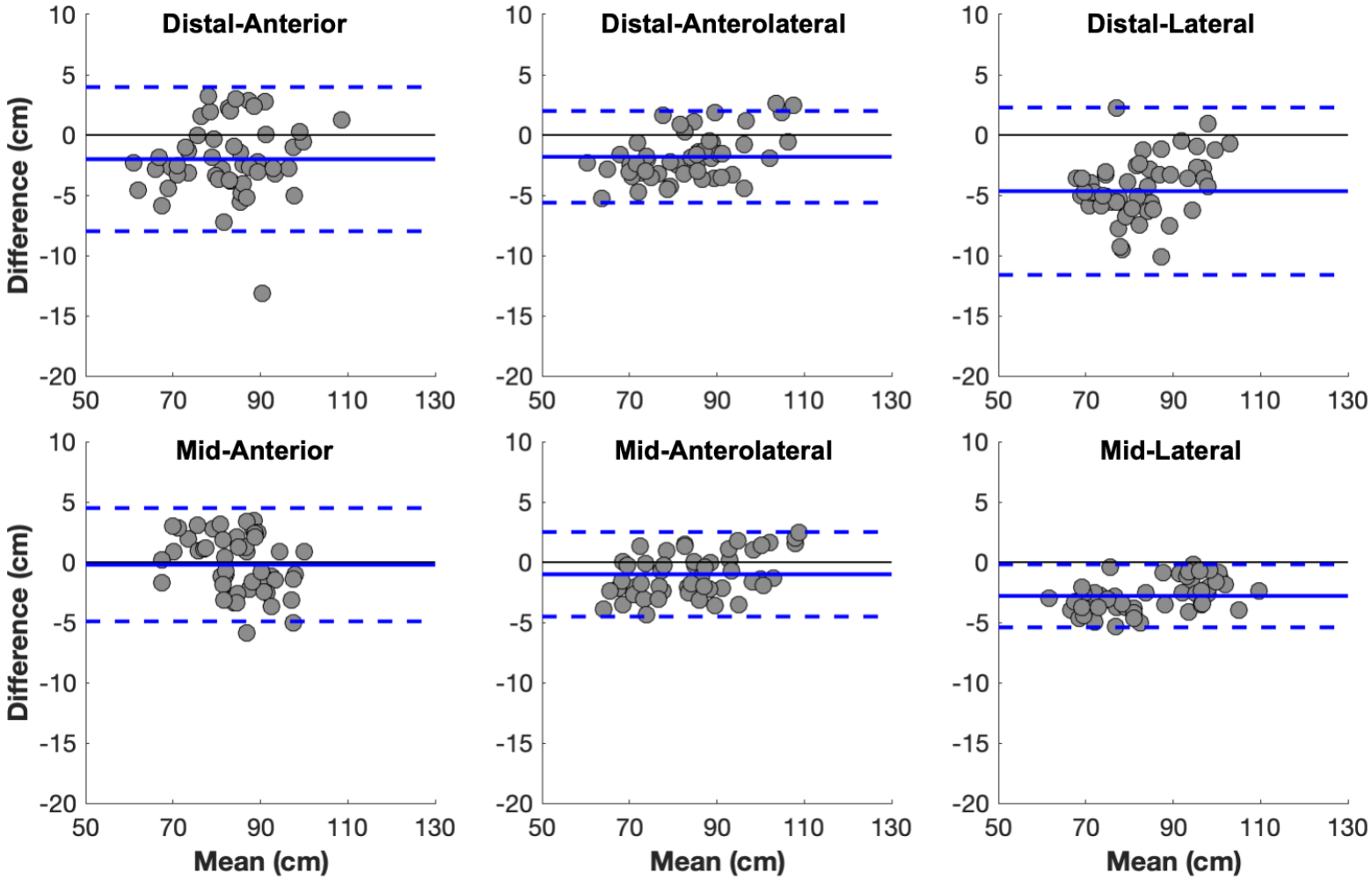

Figure 5-7: Bland-Altman plot for each marker cluster in the trail leg of the dorsiflexed kneel. The solid black line indicates perfect agreement, the solid blue line is the mean difference, and the dashed line is the upper and lower limits of agreement.

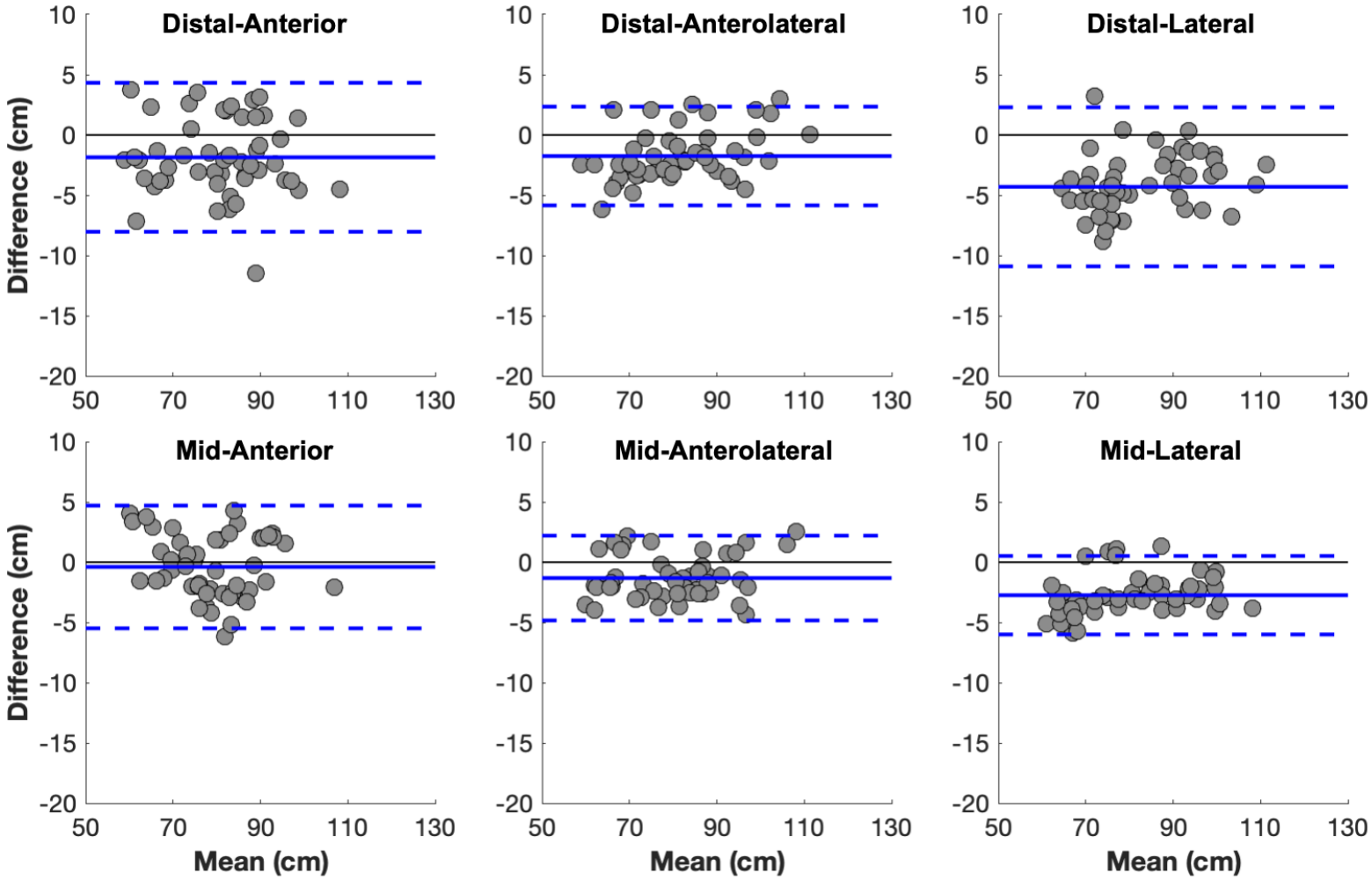

Figure 5-8: Bland-Altman plot for each marker cluster in the trail leg of the plantarflexed kneel. The solid black line indicates perfect agreement, the solid blue line is the mean difference, and the dashed line is the upper and lower limits of agreement.

Appendix D: Knee Joint Angle and Moment Time Histories

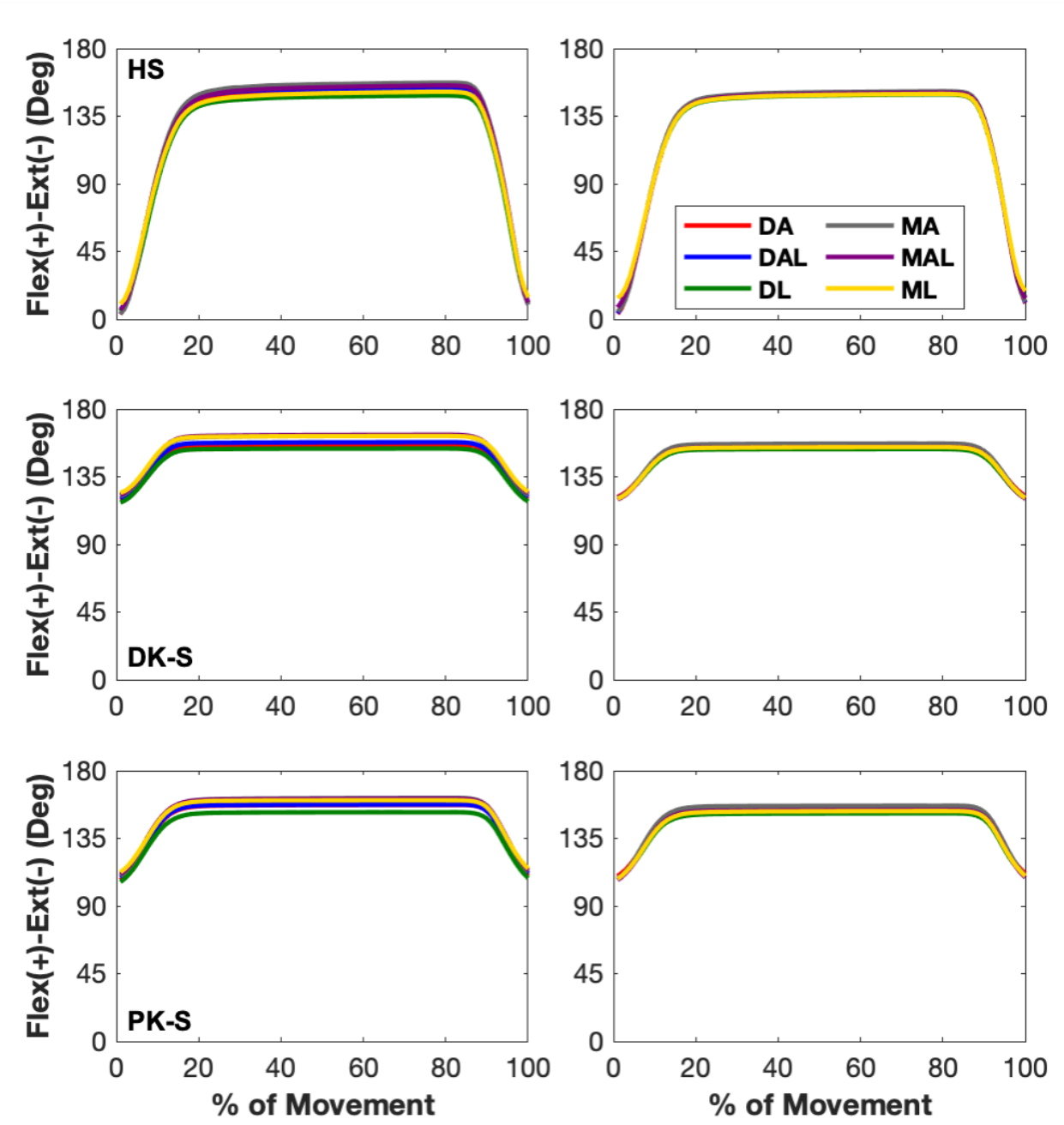

Figure 5-9: Mean knee flexion(+)-extension(-) angle for each thigh marker clusters in each task. Left column: no IK; right column: IK.

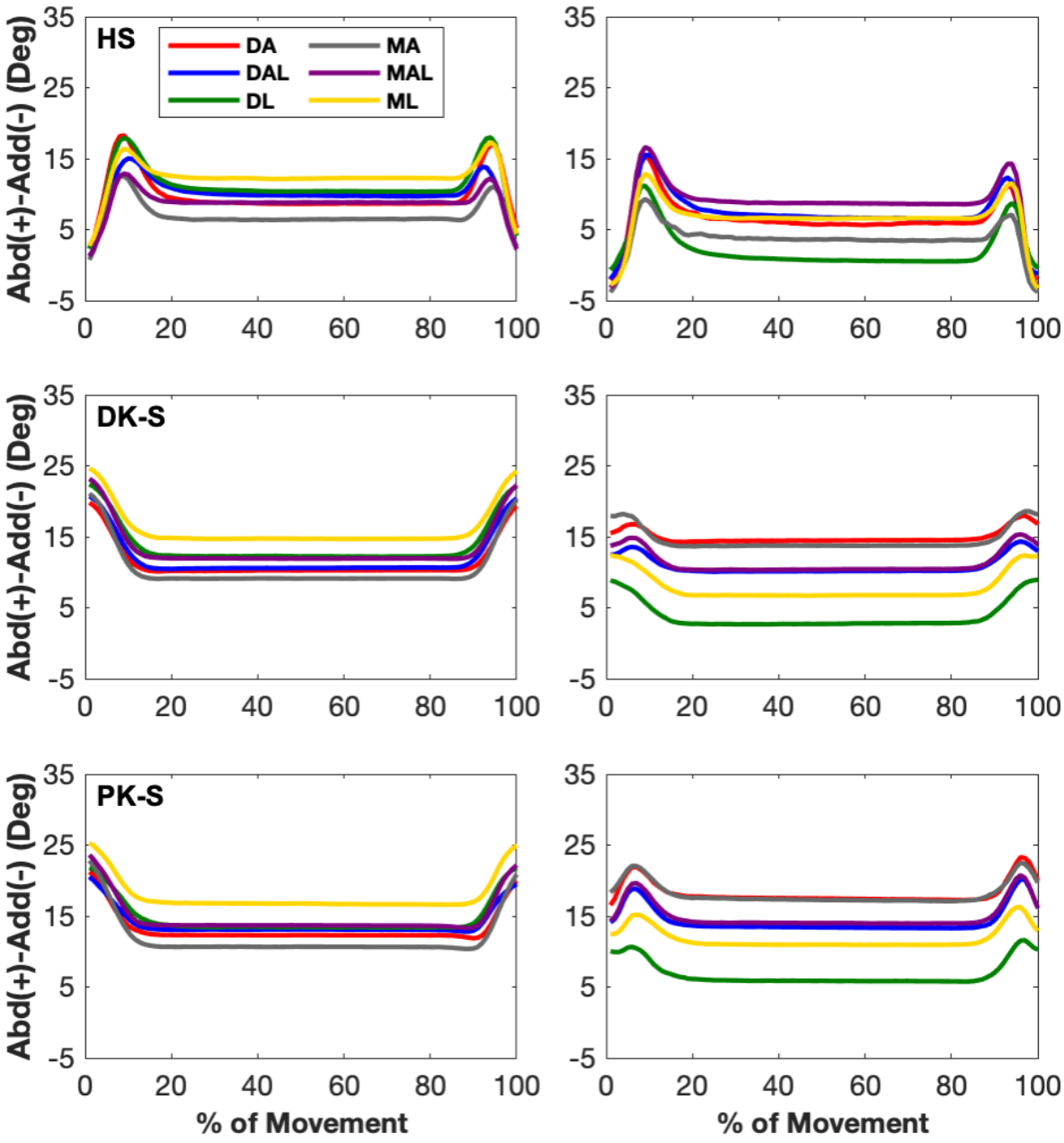

Figure 5-10: Mean knee abduction(+)-adduction(-) angle for each thigh marker clusters in each task. Left column: no IK; right column: IK.

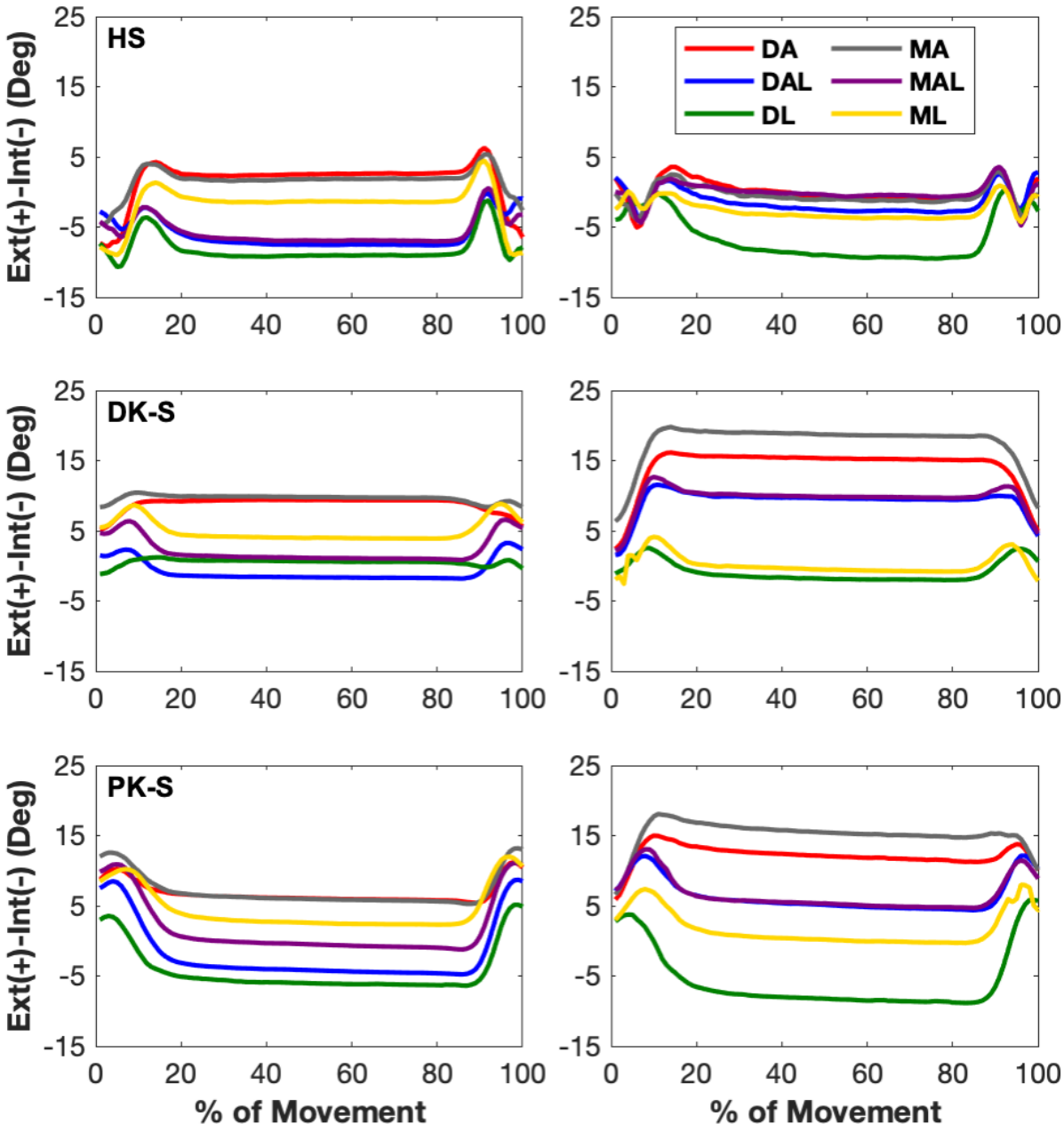

Figure 5-11: Mean knee external(+)-internal(-) rotation angle for each thigh marker clusters in each task. Left column: no IK; right column: IK.

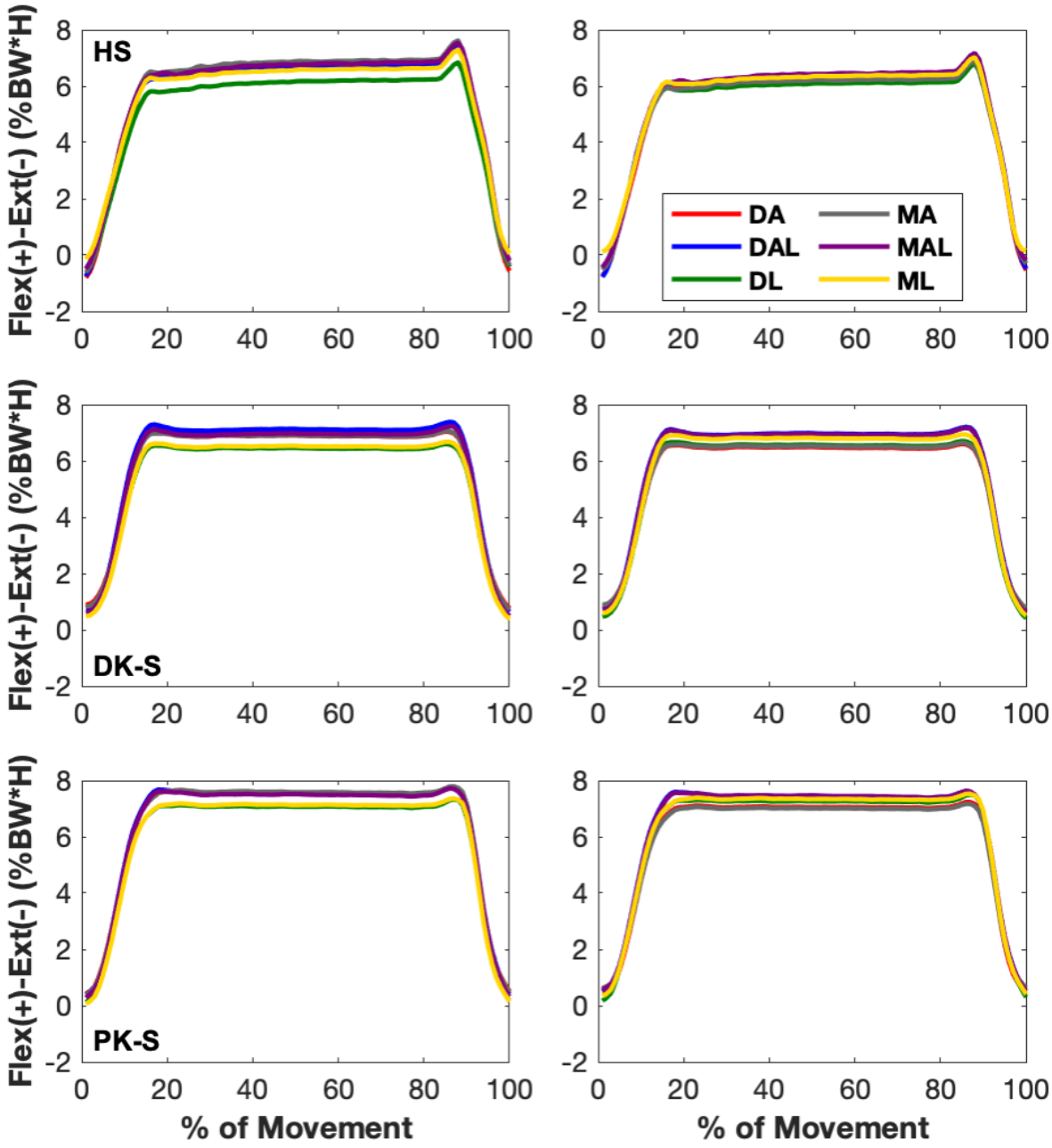

Figure 5-12: Mean knee flexion(+)-extension(-) moment for each thigh marker clusters in each task. Left column: no IK; right column: IK.

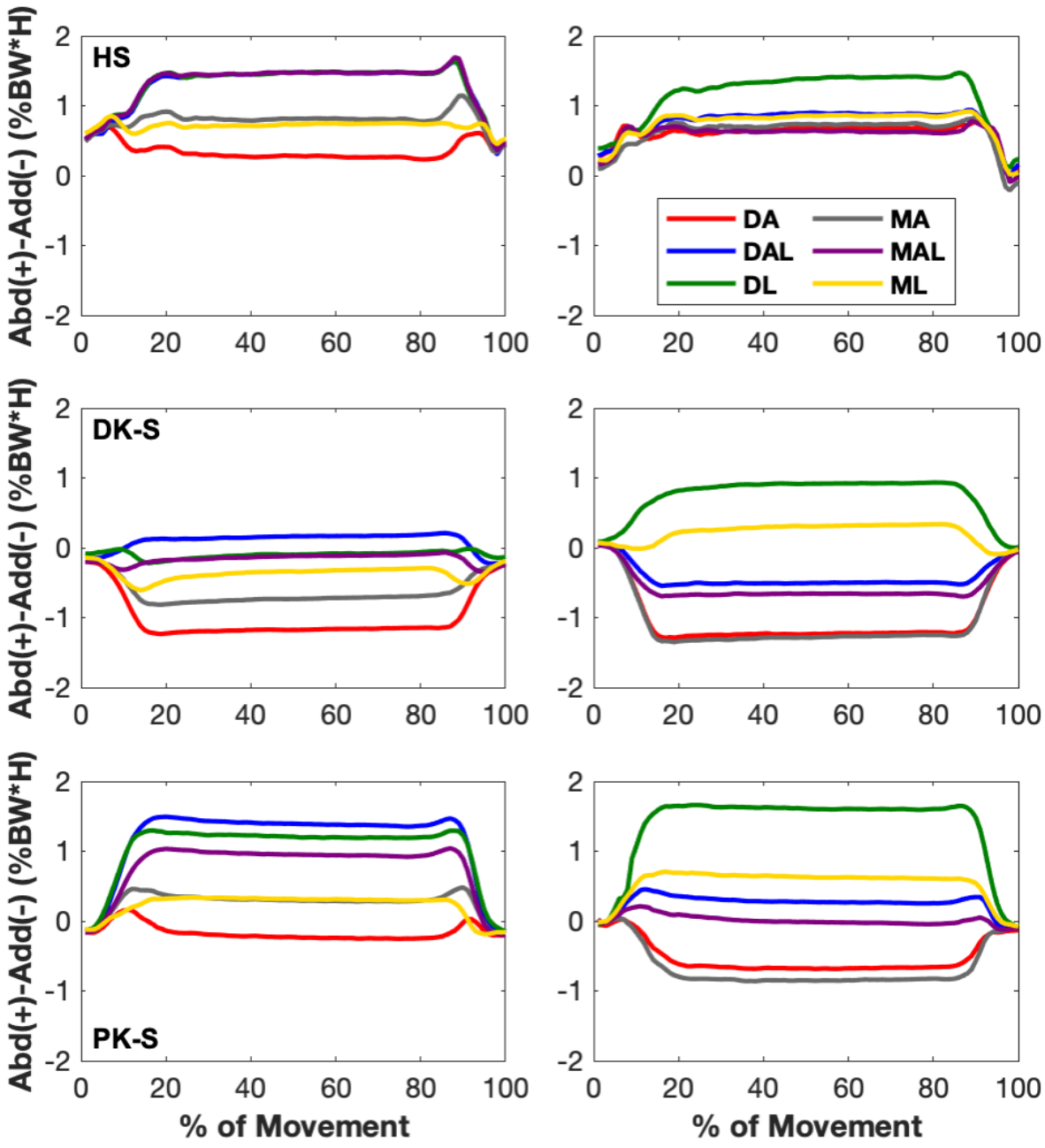

Figure 5-13: Mean knee abduction(+)-adduction(-) moment for each thigh marker clusters in each task. Left column: no IK; right column: IK.

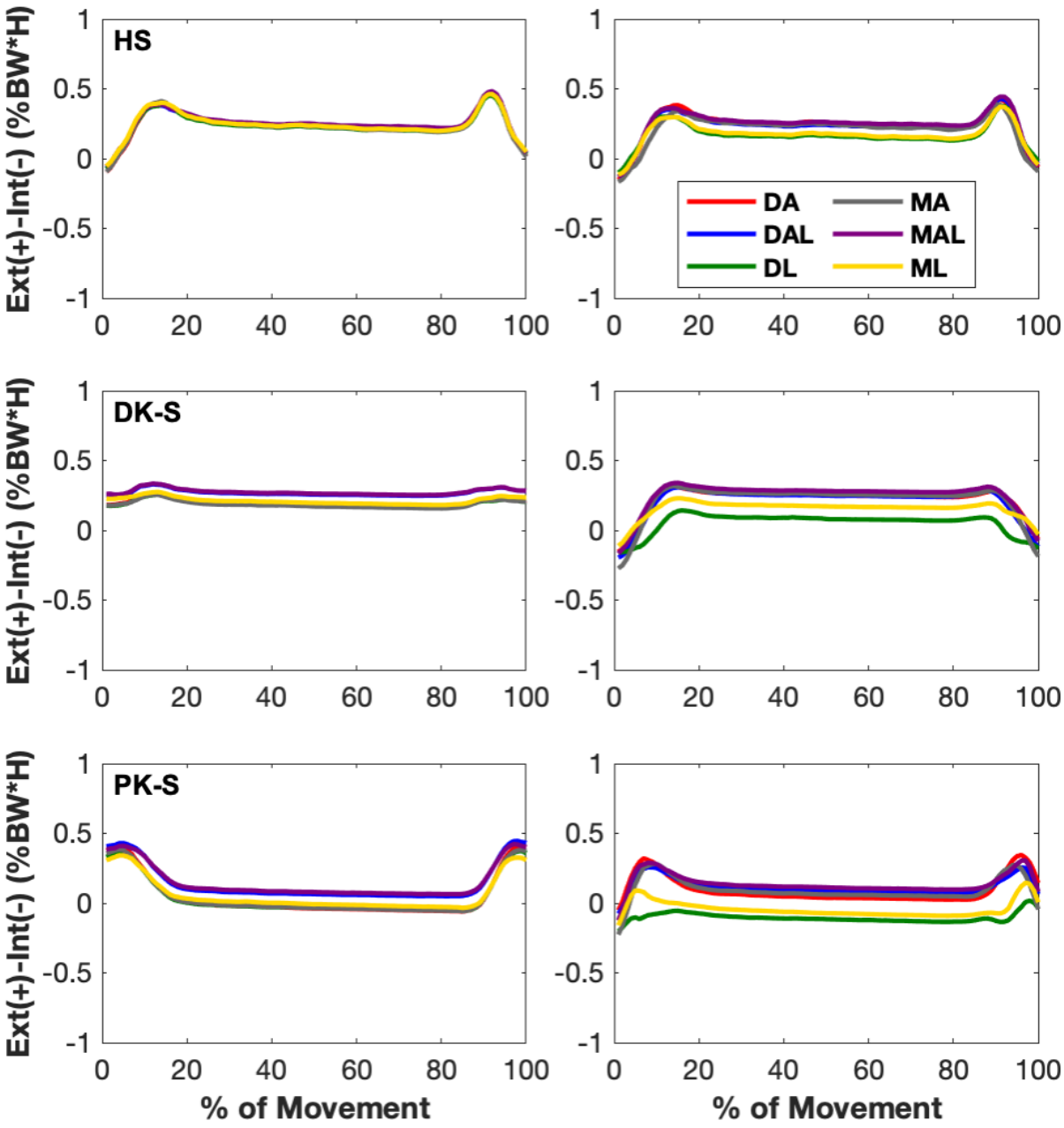

Figure 5-14: Mean knee external(+)-internal(-) rotation moment for each thigh marker clusters in each task. Left column: no IK; right column: IK.

Appendix E: Pairwise Differences in Peak Knee Joint Angles and Moments Between Marker Clusters and Tasks

The following section highlights pairwise differences between marker clusters and tasks for the two IK conditions. Each table summarizes one dependent variable (i.e. peak knee joint angle/moment).

Table 5-7: Mean and standard deviation (in brackets) peak flexion angle for each marker cluster and global optimization condition in each task. Numbers indicate significant differences between tasks, described below the table. Values with different letters across a row indicate significant differences between marker clusters.

Task	IK	DA[3]	DAL[1,4]	DL[1,2]	MA[3]	MAL[1,2]	ML[1,2]
HS	**No IK**	152.7 (8.4)$_{ab}$	154.8 (7.8)$_{a}$	148.8 (10.3)$_{c}$	157.3 (9.5)$_{d}$	155.7 (8.7)$_{d}$	152.2 (9.0)$_{b}$
	IK	150.2 (7.2)$_{a}$	150.3 (5.9)	149.9 (6.5)$_{a}$	151.5 (7.3)$_{b}$	150.8 (6.4)	150.3 (6.8)
DK-S	**No IK**	157.1 (5.8)$_{abc}$	159.1 (5.7)$_{b}$	154.1 (8.9)$_{a}$	162.7 (7.2)$_{d}$	163.3 (6.1)$_{cd}$	162.9 (6.5)$_{d}$
	IK	156.4 (4.8)$_{ab}$	155.3 (4.0)$_{bc}$	154.4 (4.0)$_{c}$	157.4 (4.5)$_{a}$	155.4 (4.3)	155.2 (4.0)$_{b}$
PK-S	**No IK**	157.5 (6.2)$_{a}$	158.6 (5.3)$_{ab}$	152.9 (8.3)$_{c}$	162.0 (6.4)$_{d}$	161.9 (5.3)$_{d}$	160.8 (6.0)$_{bd}$
	IK	155.4 (5.8)$_{a}$	153.5 (4.4)$_{a}$	152.4 (4.5)$_{b}$	157.1 (5.1)$_{c}$	154.2 (5.1)$_{a}$	153.6 (4.7)$_{a}$

1 Significant differences between all tasks without IK.

2 Significant differences between all tasks with IK.

3 Significant differences between all tasks except DK-S and PK-S in both IK conditions.

4 Significant differences between all tasks except DK-S and PK-S with IK

Global optimization significantly decreased the flexion angle for the distal-anterior, mid-anterior, and mid-anterolateral cluster in all tasks, and the distal-anterior cluster in HS and PK-S.

Table 5-8: Mean and standard deviation (in brackets) peak flexion moment for each marker cluster and global optimization condition in each task. Numbers indicate significant differences between tasks, described below the table. Values with different letters across a row indicate significant differences between marker clusters.

Task	IK	DA[2,4]	DAL[3,5]	DL[2,5]	MA[2,5]	MAL[1,5]	ML[1,5]
HS	**No IK**	9.4 (1.8)$_{ab}$	8.8 (1.4)	8.8 (1.7)$_{c}$	9.5 (1.8)$_{a}$	8.9 (1.4)	9.3 (1.7)$_{b}$
	IK	8.9 (1.8)$_{ab}$	8.4 (1.5)	8.7 (1.8)$_{ac}$	8.7 (1.8)$_{cd}$	8.4 (1.4)	8.9 (1.7)$_{bd}$
DK-S	**No IK**	8.5 (1.2)$_{ab}$	8.4 (1.0)$_{ac}$	8.0 (1.2)$_{cd}$	8.5 (1.1)$_{ab}$	8.2 (1.1)$_{bd}$	8.0 (1.2)$_{cd}$
	IK	8.1 (1.3)	8.1 (1.3)	8.2 (1.1)	8.1 (1.2)	8.1 (1.2)	8.2 (1.1)
PK-S	**No IK**	9.1 (1.2)$_{a}$	8.7 (1.0)	8.5 (1.1)$_{b}$	9.1 (1.1)$_{a}$	8.7 (1.1)	8.6 (1.1)$_{b}$
	IK	8.5 (1.3)	8.5 (1.2)	8.7 (1.0)	8.5 (1.2)$_{a}$	8.5 (1.1)	8.8 (1.1)$_{b}$

1 Significant differences between all tasks without IK.
2 Significant differences between all tasks except HS and PK-S without IK.
3 Significant differences between HS and DK-S without IK.
4 Significant difference between all tasks except HS and PK-S with IK.
5 Significant difference between DK-S and PK-S with IK.

Global optimization significantly decreased the peak knee flexion moment for the distal-anterior, distal-anterolateral, and mid-anterior cluster in all tasks, the mid-anterolateral cluster in HS and PK-S, and the mid-lateral cluster in HS but significantly increased the flexion moment for the distal-lateral and mid-lateral cluster in DK-S and PK-S.

Table 5-9: Mean and standard deviation (in brackets) peak abduction angle for each marker cluster and global optimization condition in each task. Numbers indicate significant differences between tasks, described below the table. Values with different letters across a row indicate significant differences between marker clusters.

Task	IK	DA[3]	DAL[2,4]	DL[4,5]	MA[1,2]	MAL[2,4]	ML[4,6]
HS	**No IK**	19.0 (6.5)$_{a}$	18.0 (6.8)$_{a}$	19.0 (7.2)$_{a}$	13.8 (7.1)$_{b}$	16.3 (7.0)	19.2 (6.9)$_{a}$
	IK	19.5 (10.7)$_{a}$	19.8 (8.7)$_{a}$	12.6 (7.8)$_{b}$	15.2 (11.5)$_{b}$	20.4 (8.0)$_{a}$	15.4 (8.0)$_{a}$
DK-S	**No IK**	20.0 (7.4)$_{a}$	21.9 (7.7)$_{ab}$	22.2 (7.6)$_{bc}$	21.4 (7.3)$_{bc}$	24.3 (6.5)$_{cd}$	25.2 (6.2)$_{d}$
	IK	20.4 (8.7)$_{a}$	17.7 (8.3)$_{ab}$	10.0 (8.9)$_{c}$	20.6 (7.3)$_{a}$	18.1 (7.6)$_{a}$	14.0 (6.6)$_{b}$
PK-S	**No IK**	21.0 (7.5)$_{ac}$	21.7 (7.9)$_{ab}$	22.8 (7.7)$_{bc}$	22.7 (7.7)$_{bc}$	24.8 (7.7)$_{cd}$	26.1 (6.5)$_{d}$
	IK	27.2 (10.6)$_{a}$	23.3 (8.3)$_{a}$	14.3 (8.8)$_{b}$	26.1 (8.7)$_{a}$	23.4 (6.6)$_{a}$	18.6 (6.6)$_{c}$

1 Significant differences between all tasks without IK.
2 Significant differences between all tasks with IK.
3 Significant differences between all tasks except HS and DK-S in both IK conditions.
4 Significant differences between all tasks except DK-S and PK-S without IK.
5 Significant differences between all tasks except HS and PK-S with IK.
6 Significant differences between all tasks except DK-S and PK-S with IK.

Global optimization significantly decreased the peak abduction angle for the distal-lateral and mid-lateral cluster in all tasks, and the distal-anterolateral and mid-anterolateral cluster in DK but increased the peak abduction angle for the mid-anterolateral cluster in HS.

Table 5-10: Mean and standard deviation (in brackets) peak abduction moment for each marker cluster and global optimization condition in each task. Numbers indicate significant differences between tasks, described below the table. Values with different letters across a row indicate significant differences between marker clusters.

Task	IK	DA[1,2]	DAL[1,2]	DL[1,3]	MA[1,2]	MAL[1,2]	ML[1,2]
HS	**No IK**	1.4 (0.6)$_{a}$	2.2 (0.8)$_{bc}$	2.6 (1.0)$_{b}$	2.0 (0.9)$_{cd}$	2.2 (0.9)$_{bd}$	1.8 (0.7)$_{ac}$
	IK	1.9 (0.9)$_{ab}$	1.7 (0.8)$_{ab}$	2.4 (1.0)$_{cd}$	2.2 (0.9)$_{ab}$	1.7 (0.6)$_{cd}$	1.9 (0.9)$_{ab}$
DK-S	**No IK**	0.1 (0.5)$_{a}$	0.5 (0.7)$_{bc}$	0.8 (1.1)$_{b}$	0.3 (0.7)$_{c}$	0.4 (0.7)$_{bc}$	0.4 (0.8)$_{c}$
	IK	0.5 (0.6)$_{a}$	0.5 (0.8)$_{ab}$	1.6 (1.4)$_{b}$	0.5 (0.9)$_{a}$	0.3 (0.5)$_{a}$	1.0 (1.0)$_{c}$
PK-S	**No IK**	0.8 (0.9)$_{a}$	1.7 (1.1)$_{bc}$	2.0 (1.3)$_{b}$	1.3 (1.0)$_{cd}$	1.4 (1.1)$_{d}$	1.0 (1.0)$_{acd}$
	IK	0.8 (1.0)$_{a}$	1.1 (1.4)$_{ab}$	2.2 (1.4)$_{c}$	0.8 (1.1)$_{a}$	0.9 (1.0)$_{ab}$	1.5 (1.3)$_{b}$

1 Significant differences between all tasks with no IK.
2 Significant differences between all tasks with IK.
3 Significant difference between all tasks with IK except HS and PK-S.

Global optimization significantly increased the peak abduction moment for the distal-anterior cluster in HS and DK-S and the mid-lateral cluster in PK-S but decreased the peak abduction moment for the distal-anterolateral and mid-anterolateral cluster in HS and PK-S, and the mid-anterior cluster in PK-S.

Table 5-11: Mean and standard deviation (in brackets) peak adduction angle for each marker cluster and global optimization condition in each task. Numbers indicate significant differences between tasks, described below the table. Values with different letters across a row indicate significant differences between marker clusters.

Task	IK	DA[1,2]	DAL[1,2]	DL[1,2]	MA[1,3]	MAL[1,2]	ML[1,2]
HS	**No IK**	1.1 (3.2)$_{ab}$	0.6 (3.5)	0.7 (2.7)$_{ab}$	-1.1 (3.3)$_{c}$	-0.4 (2.7)$_{ac}$	1.1 (3.2)$_{b}$
	IK	-8.1 (7.5)	-5.6 (4.8)$_{a}$	-5.4 (4.1)$_{a}$	-10.5 (7.9)$_{b}$	-5.7 (4.0)$_{a}$	-5.9 (3.7)$_{a}$
DK-S	**No IK**	8.8 (4.4)$_{a}$	9.7 (4.4)$_{a}$	11.0 (4.5)$_{b}$	7.9 (4.1)$_{a}$	11.0 (4.4)$_{b}$	13.8 (3.7)$_{c}$
	IK	9.7 (8.1)$_{a}$	7.6 (7.9)$_{ab}$	1.1 (6.3)$_{c}$	9.4 (8.3)$_{a}$	8.1 (5.4)$_{a}$	5.0 (4.7)$_{b}$
PK-S	**No IK**	10.2 (5.2)$_{ab}$	11.4 (5.8)$_{cd}$	12.7 (5.3)$_{c}$	9.1 (4.7)$_{ad}$	12.1 (5.3)$_{bc}$	15.6 (4.7)$_{e}$
	IK	11.6 (9.4)$_{a}$	9.8 (7.6)$_{ab}$	4.2 (7.2)$_{c}$	11.4 (9.9)$_{a}$	10.5 (5.6)$_{ab}$	6.9 (5.8)$_{b}$

1 Significant differences between all tasks with no IK.
2 Significant differences between all tasks with IK.
3 Significant differences between all tasks with IK except for DK-S and PK-S.

Global optimization significantly decreased the peak adduction angle for all marker clusters in HS, for the distal-lateral, mid-anterolateral, and mid-lateral cluster in DK-S, and for the distal-lateral and mid-lateral cluster in PK-S.

Table 5-12: Mean and standard deviation (in brackets) peak adduction moment for each marker cluster and global optimization condition in each task. Numbers indicate significant differences between tasks, described below the table. Values with different letters across a row indicate significant differences between marker clusters.

Task	IK	DA[1,2,3]	DAL[1,2,4]	DL[1]	MA[1,2]	MAL[1,2,4]	ML[1]
HS	No IK	-0.5 (0.9)$_{a}$	0.0 (0.4)$_{bc}$	-0.1 (0.7)$_{b}$	-0.3 (0.7)$_{c}$	-0.1 (0.5)$_{bc}$	-0.2 (0.7)$_{bc}$
	IK	-0.8 (0.6)$_{a}$	-0.6 (0.6)	-0.4 (0.4)$_{c}$	-0.9 (0.6)$_{a}$	-0.7 (0.7)$_{ab}$	-0.5 (0.45)$_{b}$
DK-S	No IK	-1.6 (1.2)$_{a}$	-0.6 (0.5)$_{b}$	-0.9 (1.2)$_{bc}$	-1.3 (1.2)$_{d}$	-0.9 (0.8)$_{cd}$	-1.1 (1.1)$_{bcd}$
	IK	-1.7 (1.4)$_{a}$	-1.3 (1.2)$_{a}$	-0.4 (0.6)$_{b}$	-1.8 (1.3)$_{b}$	-1.3 (1.0)$_{a}$	-0.6 (0.7)$_{b}$
PK-S	No IK	-0.9 (0.9)$_{a}$	-0.3 (0.2)$_{b}$	-0.5 (0.8)$_{bc}$	-0.6 (0.8)$_{bc}$	-0.5 (0.4)$_{c}$	-0.6 (0.6)$_{bc}$
	IK	-1.4 (1.3)$_{a}$	-0.8 (0.9)$_{ab}$	-0.3 (0.2)$_{c}$	-1.4 (1.2)$_{a}$	-0.9 (0.8)$_{a}$	-0.5 (0.6)$_{bc}$

1 Significant differences between all tasks with no IK.
2 Significant difference between DK-S and HS with IK.
3 Significant difference between PK-S and HS with IK.
4 Significant difference between DK-S and PK-S with IK.

Global optimization significantly decreased the peak adduction moment for all clusters in HS, for the distal-anterolateral, mid-anterior, and mid-anterolateral cluster in DK-S, and distal-anterolateral, mid-anterior, mid-anterolateral, and mid-lateral cluster in PK-S but increased the peak adduction moment for the distal-lateral and mid-lateral cluster in DK-S.

Table 5-13: Mean and standard deviation (in brackets) peak external rotation angle for each marker cluster and global optimization condition in each task. Numbers indicate significant differences between tasks, described below the table. Values with different letters across a row indicate significant differences between marker clusters.

Task	IK	DA[1,4]	DAL[2,3,4]	DL[2,3,5]	MA[1,4]	MAL[1,4]	ML[1]
HS	No IK	9.4 (9.3)$_{ac}$	6.3 (7.0)$_{ab}$	4.1 (8.4)$_{b}$	10.4 (9.2)$_{c}$	6.5 (7.3)$_{ab}$	8.6 (10.1)$_{a}$
	IK	15.2 (8.2)$_{a}$	12.8 (7.4)	9.5 (7.8)$_{b}$	13.6 (9.2)$_{a}$	11.5 (7.4)	9.9 (8.3)$_{b}$
DK-S	No IK	11.8 (10.8)$_{a}$	5.8 (8.0)$_{b}$	4.7 (12.2)$_{bc}$	13.3 (12.4)$_{a}$	9.5 (8.5)$_{ac}$	11.8 (11.3)$_{a}$
	IK	19.8 (14.8)$_{a}$	17.0 (11.3)$_{ab}$	6.6 (11.0)$_{c}$	21.4 (13.9)$_{a}$	16.8 (9.5)$_{a}$	11.5 (9.5)$_{b}$
PK-S	No IK	14.6 (11.0)$_{ab}$	12.7 (10.2)$_{bc}$	8.5 (12.5)$_{c}$	16.2 (12.4)$_{ab}$	15.3 (10.2)$_{a}$	15.0 (12.2)$_{ab}$
	IK	22.7 (18.6)$_{a}$	21.2 (13.8)$_{a}$	10.8 (12.5)$_{b}$	24.3 (19.8)$_{a}$	19.2 (12.7)	14.4 (13.9)$_{b}$

1 Significant differences between all tasks with no IK.
2 Significant differences between all tasks with no IK except for HS and DK.
3 Significant difference between HS and DK-S with IK.
4 Significant difference between HS and PK-S with IK.
5 Significant difference between DK-S and PK-S with IK.

Global optimization significantly increased the peak external rotation angle for the distal-anterior, distal-anterolateral, mid-anterior, mid-anterolateral cluster in all movements and the distal-lateral cluster in HS and PK-S.

Table 5-14: Mean and standard deviation (in brackets) peak external rotation moment for each marker cluster and global optimization condition in each task. Numbers indicate significant differences between tasks, described below the table. Values with different letters across a row indicate significant differences between marker clusters.

Task	IK	DA[1,2]	DAL[1,2,4,5]	DL[1,4,5]	MA[1]	MAL[1,2,3,4]	ML[1,4,5]
HS	No IK	0.6 (0.3)	0.7 (0.3)	0.6 (0.3)	0.6 (0.3)	0.7 (0.3)	0.6 (0.3)
	IK	0.6 (0.3)$_{a}$	0.7 (0.3)	0.6 (0.3)	0.5 (0.3)$_{b}$	0.7 (0.3)	0.6 (0.3)
DK-S	No IK	0.5 (0.2)	0.5 (0.2)	0.4 (0.2)	0.4 (0.2)	0.5 (0.2)	0.5 (0.2)
	IK	0.5 (0.3)$_{ab}$	0.5 (0.3)	0.3 (0.3)$_{d}$	0.5 (0.3)$_{a}$	0.5 (0.3)$_{bc}$	0.4 (0.2)$_{c}$
PK-S	No IK	0.5 (0.2)	0.6 0.2)	0.5 (0.2)	0.5 (0.2)	0.6 (0.2)	0.5 (0.2)
	IK	0.6 (0.4)$_{a}$	0.5 (0.3)$_{ab}$	0.2 (0.2)$_{c}$	0.5 (0.4)$_{a}$	0.6 (0.3)$_{a}$	0.3 (0.3)$_{b}$

1 Significant difference between HS and DK-S without IK.
2 Significant differences between DK-S and PK-S without IK.
3 Significant difference between HS and PK-S without IK.
4 Significant difference between HS and DK-S with IK.
5 Significant differences between HS and PK-S with IK.

Global optimization significantly decreased the peak external rotation moment for the distal-lateral and mid-lateral cluster in all tasks, and mid-anterior cluster in HS, and the distal-anterolateral cluster in PK-S.

Table 5-15: Mean and standard deviation (in brackets) peak internal rotation angle for each marker cluster and global optimization condition in each task. Values with different letters across a row indicate significant differences between marker clusters.

Task	IK	DA	DAL	DL	MA	MAL	ML
HS	No IK	-11.1 (6.2)$_{ab}$	-13.0 (7.6)$_{ac}$	-17.8 (6.9)$_{d}$	-9.8 (8.4)$_{a}$	-14.2 (8.2)$_{bcd}$	-14.2 (6.9)$_{c}$
	IK	-13.6 (7.2)	-12.8 (7.6)	-16.9 (9.0)$_{a}$	-15.1 (7.8)	-12.4 (6.9)	-12.8 (6.8)$_{b}$
DK-S	No IK	3.0 (9.3)$_{ab}$	-3.9 (8.2)$_{c}$	-5.7 (10.4)$_{cd}$	4.1 (11.5)$_{a}$	-1.2 (8.8)$_{d}$	0.8 (11.5)$_{b}$
	IK	-1.0 (11.3)$_{a}$	-1.6 (9.3)$_{ab}$	-7.7 (11.8)$_{c}$	0.5 (8.9)$_{a}$	-0.6 (7.6)$_{ab}$	-4.3 (8.9)$_{b}$
PK-S	No IK	2.4 (12.8)$_{a}$	-5.2 (15.2)$_{bc}$	-8.3 (14.7)$_{b}$	2.4 (13.5)$_{a}$	-1.8 (13.3)$_{a}$	0.2 (12.9)$_{ac}$
	IK	0.4 (15.8)$_{a}$	-1.1 (17.2)$_{ab}$	-10.4 (16.9)$_{c}$	1.0 (17.1)$_{a}$	-1.2 (17.4)$_{ab}$	-6.7 (15.1)$_{bc}$

There was a main effect of task in which peak internal rotation angle was significantly greater in HS (-13.6°) compared to both DK-S (1.5°) and PK-S (2.4°) for all clusters and IK conditions ($F = 45.15$, $p < 0.001$, $\eta^2 = 0.54$).

Global optimization significantly decreased the peak internal rotation angle for the mid-anterior cluster in HS, the distal-anterior, mid-anterior, and mid-lateral cluster in DK-S, and mid-lateral cluster in PK-S. IK constraints significantly increased the peak internal rotation angle for the distal-anterolateral cluster in DK-S and PK-S.

Table 5-16: Mean and standard deviation (in brackets) peak internal rotation moment for each marker cluster and global optimization condition in each task. Numbers indicate significant differences between tasks, described below the table. Values with different letters across a row indicate significant differences between marker clusters.

Task	IK	DA[2]	DAL[1]	DL[2,3]	MA[2]	MAL[1]	ML[2,3]
HS	**No IK**	-0.2 (0.2)	-0.2 (0.2)	-0.2 (0.2)	-0.2 (0.2)	-0.1 (0.2)	-0.2 (0.2)
	IK	-0.3 (0.2)$_{ab}$	-0.2 (0.2)$_{ace}$	-0.3 (0.2)$_{cd}$	-0.3 (0.2)$_{ad}$	-0.2 (0.2)$_{bdf}$	-0.3 (0.2)$_{ef}$
DK-S	**No IK**	0.0 (0.2)	0.1 (0.2)	0.0 (0.2)	0.0 (0.3)	0.1 (0.2)	0.0 (0.2)
	IK	-0.3 (0.3)$_{a}$	-0.3 (0.3)	-0.3 (0.2)$_{a}$	-0.4 (0.3)$_{b}$	-0.2 (0.3)	-0.3 (0.2)$_{a}$
PK-S	**No IK**	-0.2 (0.4)	0.0 (0.3)	-0.1 (0.4)	-0.1 (0.4)	0.0 (0.3)	-0.2 (0.3)
	IK	-0.3 (0.3)$_{ab}$	-0.2 (0.3)$_{a}$	-0.4 (0.3)$_{c}$	-0.4 (0.3)$_{cd}$	-0.3 (0.3)$_{bcd}$	-0.4 (0.3)$_{d}$

1 Significant differences between all tasks without IK.
2 Significant differences between all tasks except HS and PK-S without IK.
3 Significant differences between all tasks except HS and DK-S with IK.

Global optimization significantly decreased the peak internal rotation moment for all marker clusters and tasks.